Post-harvest Evaluation of Nitrogen Fertilizer Management in the Palouse Region

A thesis

Submitted in Partial Fulfillment of the Requirements for the

Degree of Master of Science

with a

Major in Water Resources

in the

College of Graduate Studies

University of Idaho

by

Ayana C. Glover

Major Professor: Erin S. Brooks, Ph.D.

Committee Members: David R. Huggins, Ph.D.; Lee Vierling Ph.D.

Department Administrator: Robert Heinse, Ph.D.

August 2018

AUTHORIZATION TO SUBMIT THESIS

This thesis of Ayana C. Glover, submitted for the degree of Master of Science with a Major in Water Resources and titled "Post-harvest Evaluation of Nitrogen Fertilizer Management in the Palouse Region," has been reviewed in final form. Permission, as indicated by the signatures and dates below, is now granted to submit final copies to the College of Graduate Studies for approval.

Major Professor: ________________________________ Date: ______________

Erin S. Brooks, Ph.D.

Committee Members: ________________________________ Date: ______________

David R. Huggins, Ph.D.

________________________________ Date: ______________

Lee Vierling, Ph.D.

Department Administrator: ________________________________ Date: ______________

Robert Heinse, Ph.D.

ABSTRACT

Inefficient use of nitrogen from agricultural systems is a driving factor of chronic and acute environmental degradation (Chen et al., 2006, 2011, 2014, Fuentes et. al., 2003, Brye et. al., 2001, Zhao et. al., 2006) resulting in environmental dilapidation, increased human health risks (Knobeloch et al., 2000) and potential losses in agricultural productivity (Jennings, 1990, Mahler et al., 1985, Bezdicek et al., 2003). Although precision agriculture practices seek to decrease N losses and subsequent costs (Ward et al., 2018, Basso et al. 2010, 2011; Zhang et al. 2010), adoption of precision agriculture is not widespread in the inland Pacific Northwest (Ward et al., 2018). In the Palouse region, four fields were observed (with up to 25 data points at each location) over a five-year period to evaluate and develop integrated post-harvest evaluation strategies to maximize profits and minimize environmental impact of fertilizer management practices. Crop and soil samples were collected at each farm to measure the various factors of nitrogen use efficiency as defined by Huggins et al. (2010). These point data were evaluated for regional and topographic crop performance patterns. The nitrogen balance index (NBI = grain N/ N fertilizer) was directly related to N uptake (Correl = 0.80, R^2= 0.50, RMSE = 0.11) and suggests satellite imagery could efficiently evaluate spatial patterns of crop performance and profitability. Satellite imagery was correlated with crop N content and evaluated for spatial drivers in N variability. The normalized difference red edge index (NDRE) was directly related to grain N content (R^2= 0.59, RMSE = 28.1 kg/ha) by wheat class (hard red and soft white in this study). Crop performance ranged widely and was highly dependent on seasonal weather conditions; however, evidence suggests that stable spatial patterns exist and are correlated to apparent soil electrical conductivity. Grain N content and yield maps successfully demonstrated field scale evaluation of crop performance classification and profitability. The positive relationship between NBI and profitability (field specific R^2 ranging 0.60-0.92) suggests implementing adaptive fertilizer management strategies will result in profitable returns and reduced environmental impact. The pairing of satellite imagery with effective evaluation metrics enables informed sampling by effectively capturing variable crop performance allowing effective evaluation of fertilizer management practices.

ACKNOWLEDGEMENTS

The Philosopher John of Salisbury penned "… we are like dwarfs sitting on the shoulders of giants so that we are able to see more and further than they, not indeed by the sharpness of our own vision or the height of our bodies, but because we are lifted up on high and raised aloft by the greatness of giants."[1]

First and foremost, I am deeply grateful for the unwavering guidance of my advisor Erin Brooks. During the long course of this degree, many life changes and personal growth occurred and he continued to ask questions, offer support and be patient when my progress was slow and many meetings were filled with chaos. I can't thank him enough for continuing to push the research further, maintain a life-view perspective and distill my busy thought process into a tidy finished work.

I am grateful for my committee members who have also stood by my side and provided their expertise and perspective to keep this research purposeful.

This work would not have been possible without the endless hours of the Site-Specific Climate Friendly Farming (SCF) team of grad students, undergraduates, professors and managers at both University of Idaho and Washington State University. Matt Yourek in particular was critical at providing an extensive amount of work with the soil data clean up and processing as well as the orthorectification and processing of the satellite images. Caley Gasch and Matteo Poggio provided soil depth and apparent electrical conductivity maps for my spatial analysis. I am so grateful for the many helping hands to help collect and process the many samples each year. The USDA ARS, Palouse Conservation Field Station team was critical in the processing of the harvest samples providing both manual labor, equipment and assistance for the many hours of grinding, threshing, weighing and measuring of samples.

The generous funding from the SCF and Regional Approaches to Climate Change (REACCH) projects provided critical funds to support this work and the funding from the National Science Foundation made my education possible.

---

[1] METALOGICON, J.B. Hall and J.P. Haseldine (eds.), Turnhout: Brepols, 2013 pg 257

DEDICATION

This dedication is inspired by the many hours my husband read Shel Silverstein and other works to our children while I was completing this degree.

The Finishers

A student's heart and mind
are filled with countless things,
from the worries of the future
to the changes life must bring.
A mother, like a student,
worries much the same,
except her thoughts are selfless
and for another's gain.

When the two are melded
and conflicts do ensue,
forgiveness is required
for all she didn't do.
So, when her doubts get heavy,
her children brave yet small
remind her what's important
and keep her head up tall.

We've pressed on together
and at the journey's end,
patience, love and fortitude
are how this work was penned.
A toast to every person
who helped us make it through,
for the love and sacrifice,
all credit goes to you.

TABLE OF CONTENTS

LIST OF FIGURES

LIST OF TABLES

LIST OF ABBREVIATIONS & FORMULAS

Abbreviation	*Formula*	*Definition [units]*
Available N uptake efficiency	N_t/N_{av}	
Available NUE	$\frac{\left(\frac{G_w}{N_{av}}\right)}{100}$	Available nitrogen use efficiency
BD		Bulk density [g/cm^3]
Garbs		Garbanzo beans
GDD	$GDD = \frac{T_{max} + T_{min}}{2} - T_b \; when \; T_{avg} < T_b$	Growing degree day
GPC	Measured protein	Grain protein concentration [g/kg]
G_w	$\frac{wet\ G_w[g]}{4\ [m^2]} * 10\ \frac{[m^2 * kg]}{[g * ha]}$	Yield [kg/ha]
G_w (dry)	$wet\ G_w * 1 - \frac{moisture[\%]}{100}$	Grain dry yield [g/4 m^2] no moisture content
G_w (wet)	Measured grain weight	Grain wet Yield [g/4 m^2] variable moisture content
G_w relative	$\frac{G_w - \bar{x}_{year}}{\bar{x}_{year}}$	Relative Yield [kg/ha]
GWC		Gravimetric water content
HRSW		Hard red spring wheat
HRWW		Hard red winter wheat
IN		Inorganic nitrogen
N fertilizer utilization efficiency	$\frac{G_w}{N_f}$	
N retention efficiency	(N_{av}/N_s)	
N uptake efficiency	(N_t/N_s)	
N utilization efficiency	$\frac{\left(\frac{G_w}{N_t}\right)}{100}$	
N_{av}	$(N_g + N_{res} + N_h)$	Available nitrogen [kg/ha]
NBI	$\frac{N_g}{N_f}$	Nitrogen balance index
N_f		Fertilized nitrogen [kg/ha]
N_g	$\frac{GPC\ [g/kg]}{5.7} * wet\ G_w\ [\frac{kg}{ha}]$	Grain nitrogen [kg/ha]
N_h	$11.3284 * BD \left[\frac{g}{cm3}\right] * \left(1 + GWC \left[\frac{g}{g}\right]\right) * (NO_3[ppm] + NH_3[ppm]) * 1.1198\ [(kg * ac)/(lb * ha)]$	Post-harvest soil inorganic nitrogen [kg/ha]
NH_3		Ammonia
NHI	$\frac{N_g}{N_t}$	Nitrogen harvest index

N_{loss}	$N_{loss} = (N_f - N_h + N_m - N_t + N_p) = N_s - N_{av}$	Nitrogen losses [kg/ha]
N_m	$BD_{1ft}[g/cm^3] * 3E6\ [cm^3 * kg/ha * g] * TN[g/g] * 0.01[g/g]$	Mineralized nitrogen [kg/ha]
NO_3		Nitrate
N_p	$11.3284 * BD[g/cm3] * \ (1 + GWC[g/g]) * (NO_3[ppm] + NH_3[ppm])$	Pre-plant soil inorganic nitrogen [kg/ha]
N_{res}	$N\ [g/g] * \frac{(biomass[g] - wet\ G_w[g])}{4[m^2]} * 10000[m^2/\text{ha}]$	Residue N content [kg/ha]
NRI	$\frac{N_f}{N_s}$	Nitrogen retention index
N_s	$(N_m + N_f + N_p)$	Nitrogen supply [kg/ha]
N_t	$(N_g\ +\ N_{res})$	N content in the total aboveground biomass [kg/ha]
NUE	$\frac{G_w[kg/ha]}{N_s[kg/ha]}$	Nitrogen use efficiency
PC		Performance class
P_c	5-year average for Palouse Region	Crop price [$/kg]
P_p	5-year average for Palouse Region	Price of Production [$/ha]
P_N	5-year average for Palouse Region	Price of Nitrogen [$/kg]
RR	$RR = (G_w * P_c)\ -\ (P_p\ + (P_N * N_f))$	Returns to risk
SCF		Site Specific Climate Friendly Farming project
Sp Barley		Spring barley
Sp Canola		Spring canola
SWSW		Soft white spring wheat
SWWW		Soft white winter wheat
T_{avg}		Daily average temperature [°C]
T_b	0°C (WW); 2.6°C (SW)	Base temperature for wheat growth[°C]
T_{max}		Daily max temperature [°C]
T_{min}		Daily minimum temperature [°C]
TC		Total soil organic carbon [g/kg]
TN		Total soil organic nitrogen [g/kg]
UNR	$\frac{N_s[lb/ac]}{G_w\ [bu/ac]}$	Unit nitrogen requirement [kg/ha]

CHAPTER 1: AN INTRODUCTION TO FIELD-SCALE NITROGEN USE EFFICIENCY AND POST-HARVEST EVALUATION TECHNIQUES.

INTRODUCTION

Agriculture sits at the center of numerous debates including food security, environmental protection, governmental policy, economic stability, agricultural suitability and many more. Although precision agriculture (PA) has been rated as one of the top 10 advancements in agricultural history, recent research has questioned the stability and resilience of current agricultural lands and practices (Hatfield et al., 2011, 2018, McBratney et al., 2005, Zhang et al., 2002, Johnson et al., 2000). PA has been determined as an effective tool for more efficient agricultural production (Bullock et al., 2009, Fridgen et al., 2004, Huggins et al., 2010, Johnson et al., 2000, Mulla et al., 2013, Peralta et al., 2013, 2015, Taylor, 2016, Yost et al., 2017, Zhang et al., 2002, Zhang et al., 2010). McBratney et al. (2005) suggests future research efforts need to be focused on economic assessment, quantification of temporal variability, whole-farm applications, assessment of crop quality and environmental impact rather than one specific management practice. Evaluation methods integrating biophysical, economic and environmental factors will provide a holistic approach for resilient agricultural practices and adaptive management (Zhang et al., 2002, Johnson et al., 2000).

Inefficient fertilizer management practices can be traced back to the Green Revolution. Although the Haber-Bosch process had been discovered in Germany in 1913, N fertilizers were not domestically mass produced in the US until 1953 (US Commodities Reports 1942-2017). The combination of increased inorganic fertilizer production and advances in cereal genetics spurred the onset of the 1950's Green Revolution (Hedden, 2003, Pinstrup-Andersen et al., 1985, Ribaudo et al., 2011). Cost effective N fertilizers were applied at high rates and record yields were achieved (Jennings, 1990, Alston et al., 2009, Chen et al., 2011, Ribaudo et al., 2011, Fiez et al., 1995). Since the 1980's yield increases have slowed and potentially stagnated (Alston et al., 2009), however, nitrogen practices haven't changed accordingly. Several studies indicate the prosperous fertilizer practices in the mid-20th century are having less or even detrimental effects today (Chen et al., 2011, Chen et al., 2014, Fuentes et. al., 2003, Brye et. al., 2001, Zhao et. al., 2006).

The highest variable production cost annually for the dryland grain producers in the inland Pacific Northwest are nitrogen fertilizers (Painter, 2016). Annual estimates of global nitrogen losses have been valued at $45 billion (Ladha et al., 2005). Inefficient use of nitrogen represents a substantial resource and financial loss at global and local scales (WWC, 2009). Excess agricultural nutrients have also been correlated to chronic and acute environmental degradation (Chen et al., 2011, Chen et al., 2014, Fuentes et. al., 2003, Brye et. al., 2001, Zhao et. al., 2006) including increased human health risks (Knobeloch et al., 2000), environmental dilapidation and losses in agricultural productivity (Jennings, 1990, Mahler et al., 1985, Bezdicek et al., 2003). Precision agriculture seeks to minimize N losses by spatially varying synthetic fertilizer rates (Ward et al., 2018, Basso et al. 2009, 2010; Zhang et al. 2010), yet adaption of precision agriculture is not widespread in the Palouse region (Ward et al., 2018).

Although nitrogen cycling is difficult to effectively measure, track and characterize (Dawson et al., 2008, Ladha et al., 2005, Pan et al., 2006); evaluation metrics have successfully assessed nitrogen efficiency and critical crop performance relationships (Reganold, 2011, Huggins & Pan, 1993, Huggins et al. 2010). Evaluation metrics such as returns to risk (Ward et al., 2018), nitrogen use efficiency (Moll et al., 1982, Huggins et al., 1993, 2003, 2010) and classification using crop quality standards (Taylor, 2016, Huggins et al., 2010, Kaur et al., 2017) have assessed the economic, biophysical and social aspects of successful wheat production. In the Palouse region, Taylor (2016) demonstrated that much of the field scale variability in dryland winter wheat N uptake was captured by variability in the Nitrogen Balance Index (NBI = grain nitrogen (N_g) /applied nitrogen fertilizer (N_f)) (R^2 =0.418, RMSE 0.517) for soft white winter wheat and Huggins et al. (2010) demonstrated similar results for hard red spring wheat. Current evaluation techniques are time and cost intensive and there is a lack of comprehensive techniques that are intuitive to growers. Simplified evaluation metrics integrated with other effective crop performance metrics would evaluate the effectiveness of applied precision agriculture strategies and enable more informed adaptive management decisions.

Remote sensing has the capacity to capture spatially extensive data while minimizing labor costs (Mulla, 2013, Shang 2015). The spectral resolution of multi-spectral, broad-band spectrometer satellites allow for smaller spatial and temporal resolutions (Jensen, 2007). Several vegetative indices have been correlated with cropping patterns (Magney et al., 2015,2016, Mulla et al., 2013, Goetz et al., 1985). Vegetative indices such as normalized difference red-edge index (NDRE) using the red-edge (690-730 nm) and green (520- 590 nm) wavelength reflectance are highly correlated leaf chlorophyll content, leaf area index (Mulla et al., 2013, Shang et al., 2015) and nitrogen content in the total aboveground biomass (Magney et al., 2015, 2016). Many satellites have been launched with various spectral, spatial and temporal resolutions. Multispectral satellite images that have high temporal (~10 days) and spatial resolutions (~5 m), such as RapidEye™, are ideal for agricultural purposes (Mulla, 2013). The increased availability of unmanned aerial vehicles (UAVs) such as drones could economically provide real-time, reliable data (Candiago et al., 2015) and mitigate issues such as cloud cover and atmospheric interference. High spatial resolution allows variable crop response to be explicitly captured and high temporal resolution allows time sensitive crop properties such as peak biomass to be acquired.

Magney et al. (2015, 2016) demonstrated a strong linear relationship (R^2 = 0.8) between the NDRE and N content in the total aboveground biomass of winter wheat crops in the Palouse region using reflectance from the red (630-685nm) and red-edge (690-730nm) bands (Blackbridge, 2016). Since N crop concentration varies with growth stage, Magney et al. (2015, 2016) determined that early June images produced the best relationships correlating peak greenness (i.e. maximum leaf area index) with end of season N crop content. The relationship demonstrates broad regional applications for N efficiency evaluation.

Dryland agriculture in the Palouse faces several unique environmental and financial factors affecting efficient use of fertilizers. High variability dominates dryland agriculture from spatial variability due to soil, topography (Huggins et al., 2010, Fiez et al., 1995, Baker et al., 2004, Fuentes et al., 2003) and erosion patterns (Brooks et al., 2012, Brown et al., 2010, Ebbert, 1998) to temporal variability due to present and past climatic factors effecting crop photosynthesis (Asseng et al., 2015), pollination (Prasad and Djanaguiraman, 2014; Rezaei et al., 2015) and water availability (Hatfield et al., 2018, Brooks et al., 2012). A legacy of historic erosion in the Palouse region has resulted in extreme variability in topsoil. Extensive soil erosion (up to 200–450 tonnes/ha (90–200 tons/ac) annually Brooks et al., 2012) over the last century has virtually eliminated and redistributed topsoil across the complex landscape (USDA, 1978) resulting in highly variable soil fertility and soil water retention characteristics at regional and field scales. Technological advancements and adoption of conservation tillage practices have increased infiltration rates and significantly decreased erosion rates and sediment loads (Brooks et al., 2012, Ebbert, 1998), but crop responses remain highly variable. Integration of effective evaluation metrics, current production technologies and satellite imagery would help assess the factors in crop performance variability and determine how soil texture, past erosional patterns and organic matter composition could be mitigated by adaptive management practices.

This study seeks to improve site-specific nitrogen management and crop performance through post-harvest evaluation strategies which optimize profitability and minimize environmental impact by:

1.) Developing and applying an integrated assessment of field-scale nutrient management strategies through a point-based evaluation approach and
2.) Exploring the use of remote sensing imagery as an integrative tool to evaluate field scale effectiveness of nutrient management strategies.

REFERENCES

Alston, J. M., Beddow, J. M., & Pardey, P. G. (2009). Agricultural research, productivity, and food prices in the long run. *Science*, *325*(5945), 1209-1210.

Asseng, S., Ewert, F., Martre, P., Rötter, R. P., Lobell, D. B., Cammarano, D., ... & Reynolds, M. P. (2015). Rising temperatures reduce global wheat production. Nature Climate Change, 5(2), 143.

Baker, D. A., Young, D. L., Huggins, D. R., & Pan, W. L. (2004). Economically optimal nitrogen fertilization for yield and protein in hard red spring wheat. Agronomy Journal, 96(1), 116-123.

Basso, B., Cammarano, D., Troccoli, A., Chen, D., & Ritchie, J. T. (2010). Long-term wheat response to nitrogen in a rainfed Mediterranean environment: Field data and simulation analysis. European Journal of Agronomy, 33(2), 132-138.

Basso, B., Ritchie, J. T., Cammarano, D., & Sartori, L. (2011). A strategic and tactical management approach to select optimal N fertilizer rates for wheat in a spatially variable field. European Journal of Agronomy, 35(4), 215-222.

Bezdicek, D. F., Beaver, T., & Granatstein, D. (2003). Subsoil ridge tillage and lime effects on soil microbial activity, soil pH, erosion, and wheat and pea yield in the Pacific Northwest, USA. Soil and Tillage Research, 74(1), 55–63.

Brooks, E. S., Boll, J., & McDaniel, P. A. (2012). Hydropedology in seasonally dry landscapes: the Palouse region of the Pacific Northwest USA. Hydropedology: Synergistic Integration of Soil Science and Hydrology, 329.

Brown, D. J., Brooks, E. S., Eitel, J., Huggins, D. R., Painter, K., Rupp, R., ... & Vierling, L. A. (2010). Site-Specific, Climate-Friendly Farming.

Brye, K. R., Norman, J. M., Bundy, L. G., & Gower, S. T. (2001). Nitrogen and carbon leaching in agroecosystems and their role in denitrification potential.Journal of Environmental Quality, 30(1), 58-70.

Bullock, D. S., Ruffo, M. L., Bullock, D. G., & Bollero, G. A. (2009). The value of variable rate technology: an information-theoretic approach. American journal of agricultural economics, 91(1), 209-223.

Candiago, S., Remondino, F., De Giglio, M., Dubbini, M., & Gattelli, M. (2015). Evaluating multispectral images and vegetation indices for precision farming applications from UAV images. Remote Sensing, 7(4), 4026-4047.

Chen, X. P., Cui, Z. L., Vitousek, P. M., Cassman, K. G., Matson, P. A., Bai, J. S., ... & Zhang, F. S. (2011). Integrated soil–crop system management for food security. Proceedings of the National Academy of Sciences, 108(16), 6399-6404.

Chen, X., Cui, Z., Fan, M., Vitousek, P., Zhao, M., Ma, W., ... & Deng, X. (2014). Producing more grain with lower environmental costs. Nature,514(7523), 486-489.

Dawson, J. C., Huggins, D. R., & Jones, S. S. (2008). Characterizing nitrogen use efficiency in natural and agricultural ecosystems to improve the performance of cereal crops in low-input and organic agricultural systems. Field Crops Research, 107(2), 89-101.

Ebbert, J. C. (1998). Soil erosion in the Palouse River basin: indications of improvement. *US Department of Agriculture*, *7*(445,000), 1-700.

Fiez, T. E., Pan, W. L., & Miller, B. C. (1995). Nitrogen use efficiency of winter wheat among landscape positions. Soil Science Society of America Journal,59(6), 1666-1671.

Fridgen, J. J., Kitchen, N. R., Sudduth, K. A., Drummond, S. T., Wiebold, W. J., & Fraisse, C. W. (2004). Management zone analyst (MZA). *Agronomy Journal*, *96*(1), 100-108.

Fuentes, J. P., Flury, M., Huggins, D. R., & Bezdicek, D. F. (2003). Soil water and nitrogen dynamics in dryland cropping systems of Washington State, USA. *Soil and Tillage Research*, *71*(1), 33-47.

Goetz, A. F. H., Vane G., Solomon, J., Rock, B. (1985). Imaging spectrometry for earth remote sensing. Science, 228(4704), 1147-1152.

Hatfield, J. L., Boote, K. J., Kimball, B. A., Ziska, L. H., Izaurralde, R. C., Ort, D., ... & Wolfe, D. (2011). Climate impacts on agriculture: implications for crop production. Agronomy journal, 103(2), 351-370.

Hatfield, J. L., & Dold, C. (2018). Agroclimatology and Wheat Production: Coping with Climate Change. Frontiers in Plant Science, 9, 224.

Hedden, P. (2003). The genes of the Green Revolution. *TRENDS in Genetics*, *19*(1), 5-9.

Huggins, D., Pan, W., & Smith, J. (2010). Yield, protein and nitrogen use efficiency of spring wheat: evaluating field-scale performance. Chapter, 17, 2010-001.

Huggins, D. R., & Pan, W. L. (2003). Key indicators for assessing nitrogen use efficiency in cereal-based agroecosystems. Journal of Crop Production,8(1-2), 157-185.

Huggins, D. R., & Pan, W. L. (1993). Nitrogen efficiency component analysis: an evaluation of cropping system differences in productivity. Agronomy Journal, 85(4), 898-905.

Jensen, John R. Remote Sensing of the Environment: An Earth Resource Perspective. 2nd ed. Upper Saddle River, NJ: Pearson Prentice Hall, 2007. Print.

Jennings, M. D., Miller, B. C., Dezdicek, D. F., & Granatstein, D. (1990). Sustainability of dryland cropping in the Palouse: A historical view. Soil and Water Conservation Society.

Johnson, G., Lamb, J., Rehm, G., Porter, P., Strock, J., Hicks, D., Eash, N., Eidman, V., Potter, B., 2000. An integrated approach to precision farming research. Proceedings of Fifth International Conference on Precision Agriculture (CD), July 16–19, 2000. Bloomington, MN, USA.

Kaur, H., Huggins, D. R., Rupp, R. A., Abatzoglou, J. T., Stöckle, C. O., & Reganold, J. P. (2017). Agro-ecological class stability decreases in response to climate change projections for the Pacific Northwest, USA. Frontiers in Ecology and Evolution, 5, 74.

Knobeloch, L., Salna, B., Hogan, A., Postle, J., & Anderson, H. (2000). Blue babies and nitrate-contaminated well water. Environmental Health Perspectives, 108(7), 675–678.

Ladha, J. K., Pathak, H., Krupnik, T. J., Six, J., & van Kessel, C. (2005). Efficiency of fertilizer nitrogen in cereal production: retrospects and prospects. Advances in agronomy, 87, 85-156.

Mahler, Robert L. "Northern Idaho Fertilizer Guide: Winter Wheat." University of Idaho Extension CIS453 (2007): 1–4. Print.

Magney, T., Yourek, M., Ward, N., Finch, S., Eitel, J., Vierling, L., Brooks, E., Huggins, D., Brown, D. "Determining the controls on nitrogen uptake from space." REACCH Annual Report Year 4 N.p., 2015. Web. 5 Aug. 2015.

Magney, T. S., Eitel, J. U., & Vierling, L. A. (2016). Mapping wheat nitrogen uptake from RapidEye vegetation indices. Precision Agriculture, 1-23.

McBratney, A., Whelan, B., Ancev, T., & Bouma, J. (2005). Future directions of precision agriculture. Precision agriculture, 6(1), 7-23.

Moll, R. H., Kamprath, E. J., & Jackson, W. A. (1982). Analysis and interpretation of factors which contribute to efficiency of nitrogen utilization 1. Agronomy Journal, 74(3), 562-564.

Mulla, D. J. (2013). Twenty five years of remote sensing in precision agriculture: Key advances and remaining knowledge gaps. Biosystems Engineering, 114(4), 358-371.

Painter, Kate (2016). Crop Enterprise Budget Cost Calculators. Retrieved from http://www.webpages.uidaho.edu/~kpainter/

Pan, W., Schillinger, W., Huggins, D., Koenig, R., & Burns, J. (2006, November). Fifty Years of Predicting Wheat Nitrogen Requirements Based on Soil Water, Yield, Protein and Nitrogen Efficiencies. In ASA-CSSA-SSSA Annual Meeting Abstracts. Raun, W.R., and G.V. Johnson. 1999. Improving nitrogen use efficiency for cereal production. Agronomy Journal 91:357-363.

Pinstrup-Andersen, P., & Hazell, P. B. (1985). The impact of the Green Revolution and prospects for the future. Food Reviews International, 1(1), 1-25.

Peralta, N. R., & Costa, J. L. (2013). Delineation of management zones with soil apparent electrical conductivity to improve nutrient management. Computers and Electronics in Agriculture, 99, 218-226.

Peralta, N. R., Costa, J. L., Balzarini, M., Franco, M. C., Córdoba, M., & Bullock, D. (2015). Delineation of management zones to improve nitrogen management of wheat. Computers and Electronics in Agriculture, 110, 103-113.

Prasad, P. V., & Djanaguiraman, M. (2014). Response of floret fertility and individual grain weight of wheat to high temperature stress: sensitive stages and thresholds for temperature and duration. Functional Plant Biology, 41(12), 1261-1269.

Reganold, J. P., Jackson-Smith, D., Batie, S. S., Harwood, R. R., Kornegay, J. L., Bucks, D., ... & Schumacher Jr, A. (2011). Transforming US agriculture. Science, 332(6030), 670-671.

Rezaei, E. E., Siebert, S., & Ewert, F. (2015). Intensity of heat stress in winter wheat—phenology compensates for the adverse effect of global warming. Environmental Research Letters, 10(2), 024012.

Ribaudo, M., Delgado, J., Hansen, L., Livingston, M., Mosheim, R., Williamson, J. (2011). Nitrogen in Agricultural Systems: Implications for Conservation Policy. USDA Economic Research Report 127.

Shang, J., Liu, J., Ma, B., Zhao, T., Jiao, X., Geng, X., ... & Walters, D. (2015). Mapping spatial variability of crop growth conditions using RapidEye data in Northern Ontario, Canada. *Remote Sensing of Environment*, *168*, 113-125.

Taylor, S. E. (2016). Precision Nitrogen Management: Evaluating and Creating Management Zones Using Winter Wheat Performance (Masters thesis, Washington State University).

"Washington Wheat Facts 2008-2009." (2009) *Washington Wheat Commission*. Washington Grain Commission, Web. 28 Oct. 2015.

Ward, N. K., Maureira, F., Stöckle, C. O., Brooks, E. S., Painter, K. M., Yourek, M. A., & Gasch, C. K. (2018). Simulating field-scale variability and precision management with a 3D hydrologic cropping systems model. Precision Agriculture, 19(2), 293-313.

Yost, M. A., Kitchen, N. R., Sudduth, K. A., Sadler, E. J., Drummond, S. T., & Volkmann, M. R. (2017). Long-term impact of a precision agriculture system on grain crop production. Precision Agriculture, 18(5), 823-842.

Zhang, X., Shi, L., Jia, X., Seielstad, G., & Helgason, C. (2010). Zone mapping application for precision-farming: a decision support tool for variable rate application. Precision Agriculture, 11(2), 103-114.

Zhang, N., Wang, M., & Wang, N. (2002). Precision agriculture—a worldwide overview. Computers and electronics in agriculture, 36(2-3), 113-132.

Zhao, R. F., Chen, X. P., Zhang, F. S., Zhang, H., Schroder, J., & Römheld, V. (2006). Fertilization and nitrogen balance in a wheat–maize rotation system in North China. Agronomy Journal, 98(4), 938-945.

CHAPTER 2: REGIONAL NITROGEN USE VARIABILITY IN THE PALOUSE

INTRODUCTION

Nitrogen fertilizers have long been accredited as one of the highest non-point source of pollution to surface waters (Ongley et al., 2010, Quan et al., 2002, Kronvang et al., 1995). However, optimizing input rates to meet the desired outputs (i.e. yields and appropriate protein content) has proven to be difficult due to the inherent heterogeneity and complexity of agricultural systems (Huggins et al., 2010). Comprehensive evaluation techniques which integrate crop quality, environmental standards and suitability will help expose problem areas and practices that result in high levels of non-point source pollution. Variable rate fertilizer management is a form of precision agriculture (PA) which varies fertilizer application over the landscape to minimize subsequent losses. However, adoption of precision agriculture is not widespread in the inland Pacific Northwest (Ward et al., 2018).

High variability dominates dryland agriculture from spatial variability due to soil, topography (Huggins et al., 2010, Fiez et al., 1995, Baker et al., 2004, Fuentes et al., 2003) and erosion patterns (Brooks et al., 2012, Brown et al., 2010, Ebbert, 1998) to temporal variability due to present and past climatic factors effecting crop photosynthesis (Asseng et al., 2015), pollination (Prasad and Djanaguiraman, 2014; Rezaei et al., 2015) and water availability (Hatfield et al., 2018, Brooks et al., 2012). Although nitrogen cycling is difficult to effectively measure, track and characterize (Dawson et al., 2008, Ladha et al., 2005, Pan et al., 2006); evaluation metrics have successfully assessed nitrogen efficiency and critical crop performance relationships (Reganold, 2011, Huggins & Pan, 1993, Huggins et al. 2010b). Evaluation metrics such as returns to risk (Ward et al., 2018), classification techniques using crop quality standards (Taylor, 2016, Huggins et al., 2010, Brown, 2015, Kaur et al., 2017) and nitrogen use (Moll et al., 1982, Huggins et al., 1993, 2004, 2010) have assessed the economic, biophysical and social aspects of successful wheat production. However, current evaluation techniques are time and cost intensive and there is a lack of comprehensive techniques that are intuitive to growers. Huggins et al. (2010) and Taylor (2016) demonstrated in the dryland winter wheat producing region of eastern Washington that much of the field scale variability in N uptake efficiency was captured by variability in the nitrogen balance index (NBI = grain nitrogen (N_g) /applied nitrogen fertilizer (N_f)) (Taylor R^2 =0.418, RMSE 0.517 SWWW; Huggins et al. (2010) R^2=0.87 HRSW). Simplified evaluation metrics integrated with other effective crop performance metrics would provide an ability to evaluate the effectiveness of applied PA strategies and enable more informed adaptive management decisions.

The goal of this study was to develop and evaluate an integrated approach for point based assessments of crop performance and fertilizer management strategies in the high precipitation annual cropping zone of the Palouse region (Kaur et al. 2017).

PROJECT GOALS & OBJECTIVES

1) Investigate spatial and temporal patterns of N uptake between diverse field locations,
2) Evaluate the efficacy of three metrics in evaluating precision agricultural practices namely the nitrogen balance index (Huggins et al., 2010), classification and returns to risk.

SITE DESCRIPTION

The Palouse region (~9000 km^2 (Brooks et al., 2012)) is located in inland Pacific Northwest and are geologically central in the region's paleosol loess deposits (McCool and Busacca, 1999). The fine-grained loess hills (Busacca and McDonald, 1994) were deposited atop Miocene flood basalts during the Pliestocene epoch (Gaylord et al., 2003). The origin of the undulating, silty topography has been highly disputed; however, the characteristically steep northern slopes are believed to be the result of seasonal snow melt and mass wasting patterns (Gaylord et al., 2003, Brooks et al., 2012).

The Palouse region is subject to high variability (McDaniel and Hipple, 2010) in topography, temperature, soils and precipitation. The variable topography of the region characteristically has a steep west to east temperature and precipitation gradient spanning 35mm to 1450mm of annual rainfall (Figure 2.1) (Brooks et al., 2012). The xeric climatic patterns of the region are characterized by winter dominated precipitation with 70% occurring between November and May and intense drought and heat stress during the summer months (Brooks et al., 2012). The soil surveys indicate a clear south-westerly gradient of particle size with the coarsest materials residing in the lower western regions. This gradation of particle sizes and precipitation developed a gradient of soil horizons. Westerly soils with limited precipitation (<400mm) and relatively coarse particle sizes are classified as Haploxerolls due to the limited leaching and absence of restrictive horizons (Donaldson, 1980; Busacca, 1989). In the moderate precipitation range (~450-700mm) the soils are classified as Argixerolls with root restricting layers (1.65 g/cm^3) and argillic (B_t) horizons between 0.2m to 1.3m

(Maaz et al., 2017, “Soil Bulk Density,” n.d.). The wettest regions (>700mm) and finest particle sizes soils are classified as Fragixeralf soils with brittle fragipan horizons due to hydrologically driven movement of clay materials (Donaldson, 1980, Barker, 1981, Busacca, 1989, Soil Survey Staff, 2006).

In general, there are two management systems in the Palouse Region: the annual cropping zone for the wetter and cooler eastern region (450-600mm) and the two-year grain-fallow cropping zone in the warmer western regions (<330mm) (Pan et al., 2016). Cropping rotations in this region vary. The farms in this study had 2 and 3-year rotations all containing winter wheat.

Four growers in the annual cropping region were selected to represent the range in major soils, topographies and climates within the annual cropping zone. The four sites chosen for this analysis were located in Colfax, WA (Figure 2.2), Genesee, ID (Figure 2.3), Leland, ID (Figure 2.4) and Troy, ID (Figure 2.5). Topography ranged greatly at the locations with maximum percent slope (spatial resolution 30 m^2 interpolated to 10 m^2) being 45% at Colfax, 36% at Genesee, 32% at Troy and (spatial resolution 5 m^2 for Tier II site) 18% at Leland. Annual precipitation in the sample locations ranged 379 mm in 2014 at Colfax to 652 mm in 2016 at Troy; see Tables 2.1-2.4 for more detailed management and field summaries for each location.

Two catchments were identified within a field at each farm. One of these catchments was selected for intensive automated and manual monitoring (Brown et al., 2011) and will be referred to as Tier II sites. Each Tier II site was equipped with twelve spatially representative subsites (Figures 2.2-2.5) which served as the primary sampling locations within the catchment. The other catchment and related subsites (Tier III sites) were reserved for crop harvest validation purposes and were monitored over the last two years (2015-2016) of the project.

METHODS

GENERAL

Four locations (Colfax, Genesee, Leland and Troy) in the high rainfall zone of the Palouse region were selected for automated and manual in-situ measurements. Two watersheds (Tier II and Tier III) at each location were chosen for monitoring with spatially representative subsites. The Tier II watersheds were extensively monitored over the 5-year study period. The Tier III watersheds were only monitored the last two years of the study and primarily used for validation purposes. The 12 subsite locations in each watershed were selected as discussed in Ward et al. (2017) using topographic and soil attributes to capture variability in water and crop yield.

REVIEW OF NITROGEN PERFORMANCE METRICS

Based on the theory behind Moll et al. (1982), nitrogen use efficiency has been more specifically defined (Huggins et al., 1993, 2003, 2010) to include inorganic N pathways and to establish N use in relation to crop growth per unit of supplied N by the following equation (Adopted from Pan et al., 1997, Huggins et al., 1993):

$$\mathrm{NUE} = \frac{\mathrm{G_w}}{\mathrm{N_s}} \quad (\text{i.e. available N uptake} \left(\frac{\mathrm{N_t}}{\mathrm{N_{av}}}\right) * \text{N utilization} \left(\frac{\mathrm{G_w}}{\mathrm{N_t}}\right) * \text{Nretention} \left(\frac{\mathrm{N_{av}}}{\mathrm{N_s}}\right)) \tag{2.1}$$

where G_w is the grain weight (i.e. yield [bu/ac]), N_s is the N supply ($N_s = N_f + N_p + N_m$), N_f is the prescribed nitrogen fertilizer, N_p is the pre-plant soil inorganic nitrogen (IN), N_m is the mineralized soil IN, N_t ($N_g + N_{res}$) is the nitrogen content of the total aboveground biomass, N_{res} is the nitrogen content in the straw residue, N_{av} ($N_h + N_t$) is the available soil IN and N_h is the post-harvest soil inorganic nitrogen. All these terms are measured on a per unit area. This definition of NUE directly quantifies the crop yield per unit N which is the inverse of the unit nitrogen requirement (UNR) (i.e. kg yield per kg N). In the current North Idaho and Washington State fertilizer guides, a 50% soil IN uptake efficiency is assumed in calculating the N required for a given field or the UNR as defined by Huggins et al. (1993, 2003, 2010) in the equation below:

$$UNR = \frac{N_s}{G_w} \tag{2.2}$$

The UNR is commonly used to provide N fertilizer recommendations to meet potential crop yield goals in regional fertilizer guides (Mahler et al., 1985) based on the following equation:

$$\mathrm{N_f} = \mathrm{Gw} * \frac{1}{\mathrm{N_t}/\mathrm{N_s} * \mathrm{G_w}/\mathrm{N_t}} - (\mathrm{N_m} + \mathrm{N_p}) \tag{2.3}$$

In this region, recommended UNR are adjusted slightly by precipitation zone (2.3 – 3.7 [lb N/ bu]) depending on wheat class (Mahler et al., 1985, Washington Wheat Commission 2013). The range of UNR for different precipitation zones accounts in part for nitrogen losses, differences in class efficiency for desired protein levels and variable yield potentials.

Nitrogen uptake efficiency is defined by the following equation:

$$N_{uptake} = \frac{N_t}{N_s} \tag{2.4}$$

For decades, N uptake efficiency has been used as an effective way to evaluate crop performance and to calculate N fertilizer requirements (Moll et al., 1982, Huggins et al., 1993, 2003, 2010, Jennings, 1990, Mahler et al., 1985); however, N uptake efficiency is costly and time intensive to calculate especially when attempting to quantify field scale variability. A 50% nitrogen uptake efficiency is assumed in regional N fertilizer guides. Nitrogen loss can be defined by the following equation:

$$N_{loss} = (N_f - N_h + N_m - N_t + N_p) = N_s - N_{av} \tag{2.5}$$

N loss serves as a metric to track N losses outside the crop zone. Conversely the N retention index tracks the amount of N retained by soil and crop during a growing season. This metric indicates how effectively the N supply supports crop growth demands and is retained in the soil. A low N uptake efficiency and high N retention index indicates the crop demand relative to supply is low, however, the excess residual N is still held in the soil which could potentially reduce the N_f requirements the following growing season (Huggins et al., 2010). Nitrogen retention efficiency is defined by the following equation:

$$N_{retention} = \frac{N_{av}}{N_s} \tag{2.6}$$

According to Huggins et al. (2010) and Taylor (2016) the following metrics have been determined as the key metrics for evaluating NUE with respect to IN.

Huggins et al. (2010) suggests N uptake efficiency, although effective at tracking all inorganic pathways of N, can be simplified through the N balance index (Taylor, 2016, Huggins et al., 2010). This metric is advantageous because it simplifies the key factors in N uptake efficiency as well as measures N content related to quality requirements. The nitrogen balance index is defined by the following equation:

$$NBI = \frac{N_g}{N_f} \tag{2.7}$$

Classification combines different metrics into dichotomous keys which evaluate crop performance based on multiple production and environmental goals. Taylor (2016, an adaption from Huggins et al., 2010) suggested a classification scheme that utilizes grain protein concentrations (GPC) and nitrogen balance index as the key metrics. Huggins et al. (2010) suggests for HRSW N utilization efficiency and N harvest indices were very stable and inability to achieve both protein and yield goals was due to N uptake efficiency variability. Classification can be an effective method to compare crop performance areas within and between fields and/or management zones. An adaptation of the HRSW Huggins et al. (2010) and SWWW Taylor (2016) classification schemes was developed for this project due to differences in wheat classes (Figure 2.6).

DATA COLLECTION

Field measurements were made at the 12 subsites in each catchment to track seasonal changes in inorganic forms of soil nitrogen and soil water as well as total above ground crop biomass, total nitrogen in the grain and N content in the total aboveground biomass. Fertilizer application rates were provided by the growers.

During the study period, growers managed the fields with their usual tillage, rotation and fertilizer management practices (Tables 2.1-2.4). Tier II crop sample distribution is as follows: 142 total wheat samples, 59 spring wheat samples (12 SWSW, 47 hard red spring wheat (HRSW)), 83 winter wheat samples (36 soft white winter wheat (SWWW), 47 hard red winter wheat (HRWW)). Tier III samples are as follows: 61 wheat samples, 12 spring wheat samples (0 SWSW, 12 HRSW), 49 winter wheat samples (24SWWW, 25 HRWW). Summaries of management practices for each of the locations can be found in Tables 2.1-2.4.

A 5m digital elevation model (DEM) was created from a real time kinematic (RTK) based GPS survey for the Tier II Leland watershed due to the relatively small variability in the landscape, all other DEMs were sourced from United States Geological Survey (USGS) National Elevation Dataset (NED).

Hourly precipitation was measured using a tipping bucket rain gauge with a siphoning snowfall adapter (Campbell Scientific Inc.) and a windscreen (Sutron Corporation). Gaps in the weather data were filled using other weather sources and interpolated to field site location (Yourek, 2016).

Soil texture was measured every 0.3m (1 foot) to 1.5m (5 ft) in fall 2011. Bulk density (g/cm^3) was calculated from soil cores taken post-harvest using a 2.3cm Giddings probe (Giddings Machine

Company Inc.™) in 2012 and 2013 for each 0.3m (1 ft) segment. There were compaction issues with the first three 0.3m samples at all locations but Colfax, so additional manual soil core (7.62cm, 3 in) samples were taken at the Genesee, Troy and Leland locations (2013, 2014). The depth to a restrictive soil horizon was defined using bulk density based on a critical threshold of 1.65 g/cm^3.

Soil inorganic nitrogen (IN) was determined from composite samples collected twice a year, pre-plant and post-harvest. In 2012 and 2013 a 2.3cm diameter Giddings probe (Giddings Machine Company Inc.™) was used to take soil samples every 0.3m to 1.5m. In 2014 to 2016 hand augers (7.62cm, 3in) were used to collect soil samples. At each subsite a composite sample for each 0.3m depth (up to 1.5m) was comprised of three soil samples. The soil samples were taken approximately 1m away from the stationary monitoring probes in a triangular pattern (Figure 2.7). A sub-sample of the composite was taken and processed for IN. Soil nitrate and ammonia concentrations (mg/L, mg IN per 0.025L of extract) were determined using 0.1M KCl extraction and analyzed using a Lachat flow injection analyzer (Lachat Instruments™). Soil IN content was calculated using:

$$Soil\ IN\ \left[\frac{lb}{ac}\right] = 11.3284\left[\frac{lb*cm^3}{ac*g*ppm}\right]*BD\left[\frac{g}{cm3}\right]*\left(1+GWC\left[\frac{g}{g}\right]\right)*(NO3[ppm]+NH3[ppm])*1.1198\ [(kg*ac)/(ha*lb)] \quad (2.8)$$

where GWC is the gravimetric water content determined by drying soil samples at 105°C for 24 hours and converted to volumetric water content using bulk density measurements. Soil N content was calculated for each 30cm depth then summed for total soil N content for the subsite (150cm) as in Yourek (2016).

Total soil nitrogen (TN) and carbon (TC) concentration samples were collected in fall 2011 and 2012 TruSpec™ analyzer and averaged by depth. Mineralization rates for each subsite were determined from 30 cm total nitrogen soil samples using the following equation, bulk density for the top 30 cm and an assumed 1% turnover rate.

$$N_m\left[\frac{kg}{ha}\right] = BD\ \left[\frac{g}{cm^3}\right]*30\ [cm\ depth]*1000\ \left[\frac{cm^2*kg}{g*ha}\right]*\frac{total\ N\ [\%]}{100}*0.01 \quad (2.9)$$

Each year (2012-2016) four 1 square meter aboveground biomass samples were hand harvested for each Tier II subsite. The total aboveground biomass weight of all four 1 square meter plots was recorded after drying. Total yield (i.e. grain weight G_w) was recorded after the dried biomass samples were threshed using a stationary plot combine. Grain protein concentration (GPC) and moisture content were measured with near infrared reflectance using an Infratec 1241 Grain Analyzer (FOSS™). Grain N was calculated using:

$$N_g[kg/ha] = \frac{GPC\ [\%]}{5.7} * \frac{Wet\ G_w\ [kg/ha]}{100} \quad (2.10)$$

A subsample of the threshed crop residue was ground (0.1mm) and analyzed for N concentration with a TruSpec™ (LECO Corp.) through dry combustion and gas chromatography and N residue content calculated using:

$$N_{res}[kg/ha] = N\ [\%] * \frac{(biomass[g] - grain[g])}{4[m^2]} * 10[\frac{m^2 * kg}{g * ha}] \quad (2.11)$$

Total aboveground N (N_t) was calculated by adding grain N (N_g) to residue N (N_{res}) (2013-2015). If residue N was not available N_t was determined using the following equations:

For spring wheat:

$$N_t = \frac{N_g}{0.81} \quad (2.12)$$

For winter wheat:

$$N_t = \frac{N_g}{0.78} \quad (2.13)$$

These relationships were established based on data collected in Palouse region (Appendix 1.A, full results in Chapter 3).

TOPOGRAPHIC CLASSIFICATION

To investigate regional patterns of nitrogen performance and stability, the subsites were classified into four topographic regions (flat, draw, north facing slope, south facing slope). The extreme topographic variability in the Palouse region results in significant differences in north and south facing slopes regarding water availability and solar radiation. Topographic wetness index, were calculated using the DEMs described previously and using SAGA Inc. open source software (Conrad et al., 2015). The topographic wetness index (TWI) (Beven and Kirkby, 1979) was calculated for each subsite to classify a point as wet (TWI > 6.6), dry (TWI < 4.2) or moderate (4.2 < TWI <6.6). Total solar insolation calculated within ArcGIS 10.4.1 was used to classify each point as north facing (yearly solar radiation < 1080000), south facing (yearly solar radiation > 1175000) or flat (i.e. geographically neutral solar radiation (1080000 <yearly solar radiation < 1175000)). Both the wetness index and solar insolation was used to classify these landscapes. Wet, flat sites were classified as draws and dry and geographically neutral solar radiation points were characterized as flat (characterizing both upland and summit positions). Topographically moderate points were classified by their solar radiation as north or south facing.

FINANCIAL ANALYSIS

The returns to risk (RR) metric was used for the financial analysis with the following equation:

$$RR\ [\$/kg] = G_w\ [kg/ha] * P_c\ [\$/ha] - \left(P_p\ [\$/ha] + \left(P_N\ [\$/kg] *\ N_f\ [kg/ha]\right)\right) \tag{2.13}$$

where P_c is the price of the crop, P_p is the estimated cost of production without nitrogen fertilizer costs, P_N is the price of nitrogen fertilizer and N_f is the amount of nitrogen fertilizer applied (Table 5). Due to the yearly variability of these costs, P_c, P_p and P_N values were estimated using 5-year averages (2011-2016) in the Palouse region (Painter, 2016). A five-year average would be representative of both the study period and dampen any yearly anomalies. The grain yield and fertilizer application rates were based on yield and prescription fertilizer application maps provided by the growers. Protein level premiums and discounts were not included in these calculations.

RESULTS

SPATIAL AND TEMPORAL N UPTAKE PATTERNS AT REGIONAL AND LOCAL SCALES

The regional five-year average N uptake efficiency for all wheat classes was 50% with a standard deviation of 18% which supports the 50% uptake efficiency estimate assumed in the regional fertilizer guides (Table 2.6, full results Appendix 1.B). However, farm-level N uptake efficiencies for a given year ranged from 0.23 to 0.66 (Appendix 1.B). The five-year average N uptake efficiency of the Troy and Genesee fields were both greater than 60% whereas the average N uptake efficiency for Colfax was below 40%.

Protein widely varied over a range of yields in each wheat class with HRWW having the broadest variability. Clear differences in the GPC and yield relationship (Figure 2.8) were seen between spring and winter wheat due to different protein requirements, with spring wheat generally yielding lower than winter wheat. Each farm (identified by color) seemed to have a unique GPC and yield relationship for each class of wheat grown (Figure 2.8). The nitrogen harvest index (R^2 = 0.98), nitrogen utilization efficiency (R^2 = 0.91) and harvest index (R^2 = 0.88) all had very strong relationships across wheat classes, protein concentrations and yields (Figure 2.9). N uptake efficiency was inconsistent within wheat classes (Figure 2.9). This study also supports previous research (Huggins et al., 2010) finding that field scale protein can range 3-4%. The regional data also indicated that a direct relationship exists between NBI and N uptake efficiency. NBI explains 64% of the variance in N uptake efficiency (Figure 2.10). The NBI for spring crops were significantly (p value < 0.05) lower than NBI for winter crops according to the ANOVA statistic (Appendix 1.C).

The spatial variability in crop performance could be generally explained by variability in soil and topographic characteristics (Tables 2.9 & 2.10). At Colfax and Genesee there was a strong site-specific relationship between relative yield and total carbon in the top 30 cm (Figure 2.11). Troy and Leland had much narrower ranges of organic matter and the relationship was not as strong. Hilltops (generally flat upper slope positions) consistently had low NBI. Draw locations characteristically had high yields, high organic matter, low BD (deep soils) and high NBI. Although the absolute magnitude of NBI varied from one year to the next, the areas of the field that had a large NBI often produced the greatest crop yields and were most profitable (Tables 2.9 & 2.10). There were no significant differences between the crop performance between the north and south facing slopes.

A direct relationship exists between NBI and G_w (Figure 2.12). A clear distinction between spring and winter wheat can be seen with winter wheat having a steeper slope than spring wheat. Locations were distinguishable for spring wheat. NBI was also directly related to returns to risk (RR) at three locations (Genesee, Leland and Troy) (Figure 2.13) with the more efficient areas being most profitable.

Based on the classification system described in Figure 2.6, the majority of the evaluation points in this study ranked as performance class (PC) 1 which indicate protein goals and nitrogen efficiency goals were consistently being met. The next most prominent performance class was PC 2 followed by PC 4 and PV 3, respectively (Table 2.6). Spring wheat generally did not profit as well as winter wheat (Table 2.7).Winter wheat had a higher frequency of PC 1 and PC 2 where GPC goals were achieved and were more profitable, however, winter wheat also had a large number of PC 4 where neither goal was achieved. Spring wheat had higher average NBI in PC 1 and 3 than winter wheat and monetarily benefitted from insurance nitrogen in PC 3. Genesee had the least spatial variability in crop performance with the majority (49/59 samples) falling in PC 1 where both NBI and GPC goals were consistently met. Troy had the largest number of PC 4 with nearly half (19/36 samples) not achieving nitrogen or protein goals with very few of the other performance classes. Colfax had the highest number of PC 2 (where protein goals were achieved but NBI goals were not met) compared to other locations. Similarly, over half the Leland samples were PC 1 (23/44) with nearly half of the points (18/44) in PC 2.

DISCUSSION

The spatially and temporally variable crop performance in this study not only confirm the need for site specific nutrient management but also reinforces the need for site-specific crop performance evaluation approaches which encourage adaptive management strategies. On average these farms have achieved a 50% uptake efficiency similar to current fertilizer guide estimates, however there is extreme temporal and spatial variability. In this short 5-year study, we were not able to capture any changes in organic N pools and therefore we do not know if the inorganic N losses represent an off-site loss as opposed to an accumulation of soil organic N. Recent research near Pullman, WA indicates that long term no-tillage field can accumulate as much as 39 [kg/ha/yr] (35 [lbs N/ac/yr]) of total N nitrogen (Unger et al., 2015).

Most of the key components of nitrogen use efficiency (N uptake efficiency, N retention efficiency and N utilization efficiency) have very stable relationships with quality requirements (yield and protein) even with mixed wheat classes. These data support previous class specific work (Huggins et al., 1993, 2004, 2010, Taylor, 2016). The combined classes and broad topographic distribution of sampling sites in this study, demonstrate the extreme stability of these relationships at the field scale and between classes. This suggests that environmental factors and local climate support effective intra-plant translocation of nitrogen into the grain. However, the broad response of N uptake across protein and yield ranges suggest that inability to achieve protein and yield goals is due to localized N uptake inefficiency. Effective post-harvest evaluation of nitrogen efficiency must include N uptake efficiency to capture the source of variability in crop performance.

The direct regional relationship (Figure 2.11) identified in this study between the N uptake efficiency and the NBI confirm recent work (Huggins et al., 2010, Taylor, 2016) suggesting NBI can be an effective surrogate indicator for N uptake efficiency. Rather than costly and time-consuming plot studies to determine N uptake efficiency, nitrogen fertilizer efficiency can be evaluated with an estimate of the grain nitrogen to applied fertilizer. Recent studies have also indicated crop N can be measured with satellite imagery containing red-edge and near-infrared bands using the normalized difference red-edge index (NDRE) (Magney et al., 2015, 2016). Therefore, spatial evaluation of nitrogen will be possible with GPS data such as yield monitors and fertilizer maps. Spatial evaluation would allow for effective evaluation of adaptive management practices. The crop performance classification based on protein and NBI, as well as the returns to risk metric, provides a very comprehensive strategy for evaluating spatial patterns in crop performance and developing adaptive management strategies. The strong relationship between NBI and returns to risk (Figure 2.13) at three of the sites indicates that profitability is closely linked to efficient nitrogen fertilizer management. Although this was a strong relationship in this dataset, there are certainly conditions where the relationship should not be expected. For example, the under-application of nitrogen fertilizer may result in a large NBI but a low RR if the crop yield experiences prolonged nitrogen stress. Therefore, the RR metric nicely complements the NBI and classification metric because it accounts for overall yield as well as fertilizer and commodity pricing. In this study, over half the points evaluated were classified as class 1 or 3 indicating the majority of the fields met nitrogen efficiency goals and were profitable. Specifically, the average NBI of PC 1 and PC 3 was 1.22 and 1.11 respectively and average returns were $585/ha and $786/ha respectively (Table 2.9). In contrast the points rated in PC 2 (i.e. meeting their protein goals but not meeting the NBI goal) had the lowest NBI and the least returns of all the classes. However, since we did not account for price deductions for not meeting protein goals in the RR metric in this study, the RR in the PC 2 and PC 4 regions is likely inflated. As expected the lowest relative crop yields were seen in PC 2 and PC 4 (Table 2.9).

The classification approach allows for adaptive management strategies which target certain classes or regions within a field. Any location which consistently does not achieve protein goals should be evaluated to see if they are meeting N efficiency goals. Troy had the highest percentage of PC 4 samples. Transitioning PC 4 areas to PC 3 by reducing N rates would help reduce unnecessary financial losses and environmental impact. A consistent underperforming PC 4 site, such as site 4 in Colfax (Table 2.11), would likely benefit from reduced nitrogen application fertilizer.

In general, the topographic analysis in this study indicated that the draw locations (having a high topographic wetness index) are consistently more productive, more profitable and more efficiently utilize nitrogen fertilizer than the rest of the field (Tables 2.9 and 2.10). The draws also tended to have the greatest soil organic matter, the lowest bulk density and the lowest clay content. The crop performance on the north slopes, south slopes and flat sites were not significantly different. This demonstrates the inherent challenge in evaluating field scale crop performance at the point scale. Obtaining sufficient samples to capture field scale variability limits the application of these methods in post-harvest evaluation in practice.

MANAGEMENT IMPLICATIONS

In the following section we highlight some of the key findings from the sampling location (Colfax, Genesee and Leland) based on the 5-year crop performance evaluation.

Colfax: Demonstrates a Need for Variable Rate

The crop performance analysis at the Colfax location clearly indicates that profitability would increase if variable rate fertilizer strategies were adopted rather than the uniform application rates strategies applied during this study. Sites 4 and 8, both of which were located on divergent ridge locations consistently had low yields, low NBI and the lowest RR values. Conversely sites 2 and 5 consistently met and achieved yield goals and had the highest relative NBI for winter wheat. Only 3/12 sites made money with spring wheat over the 2-year observation period. One of these years was a drought year (2014) receiving 100mm less precipitation than in 2013. Over the course of the study period 26/61 samples did not reach yields necessary to break even ($0 RR), however, in practice these low returns may be augmented with premiums for high proteins. Colfax also had the second lowest average NBI and the highest standard deviation suggesting N uptake was highly variable across the field as well as the second highest N retention rate (after Genesee). This may suggest there is a correlation between total soil carbon and N retention or that N mineralization rate estimates in fertilizer guides are underestimated and N is effectively held within the soil profile. In this case it may be advantageous to collect pre-plant soil samples in the areas with high OM to ensure N is not being over applied. Spring wheat are highly variable in crop response and struggle to meet yield goals. Since Colfax has the second highest organic matter and institutes no till farming practices, this location would likely benefit from variable rate practices to better match N requirements.

Genesee: Demonstrates Efficiency

The Genesee field site follows variable rate fertilizer application strategies based on zones defined from satellite imagery using high precision fertilizer application technology (Exactrix system). This farm consistently achieved crop performance goals throughout the field Genesee demonstrates the advantages of variable rate fertilizer management strategies in achieving nitrogen efficiency and RR goals. Genesee had a very polarized classification distribution, with exclusively PC 1 and PC 3 sites. Monetarily, the Genesee fields had positive RR at all 12 Tier II and Tier III locations every year of the study. Genesee also had the highest yields and average NBI as well as consistently meeting protein goals. NBI was regularly above 1.0 for spring crops and only 3/24 points had an average NBI below 0.8.

Similar to other farms, higher fertilizer rates were applied to achieve GPC goals in parts of the field in Genesee, however, the crop response consistently achieved yield goals unlike the other farms. Some of the unique characteristics of the management at Genesee are 1) the broad range of fertilizer rates relative to the other farms applied in multiple zones, 2) all nitrogen fertilizer is applied at seeding and 3) it followed a unique diverse crop rotation which included canola and spring barley. The average amount of fertilizer applied to the field is also lower than the other sites, however, the field maintained relatively large crop yields. Genesee has a unique crop rotation that includes both hard red and soft white wheat classes as well as canola and spring barley.

Although the 1-foot total soil carbon concentration did not vary much between locations, the 5-foot average was substantially higher at Genesee (0.95) versus the other locations (Troy: 0.67, Leland: 0.70, Colfax: 0.77). At the Colfax and Genesee (no-till sites) there was a correlation between relative yield and total soil carbon (Figure 2.11). This supports previous research indicating deeper soils with higher organic matter achieve higher yields (Jennings, 1990, Papendick et al., 1985). These data suggest improving soil health (i.e. organic matter, Doran et al. 2000, Morrow et al., 2017) may directly impact the relative crop response and overall profitability. The sites with conventional tillage (Troy and Leland) had much narrower ranges of organic matter and did not exhibit the same strong relationship between TC and relative yields. One limitation to this study was that we used an estimated mineralization rate based on a one percent turnover of TN in the first 30 cm of soil. It is possible that this estimate may be too low at the Genesee or any other sites. More mineralization studies could help indicate whether these estimates are truly representative of the region. The degree to which increasing soil health is an effective tool for growers to help increase soil water holding capacity (Tisdall et al., 1982), mineralization (Unger et al., 2015) and yield responses (Doran et al., 2000, Morrow et al., 2017, Pan et al., 2017) to ensure best management practices for optimum yields is an ongoing active research area.

High Temporal Variability Requires Multiple Observation Years

The extreme variability in crop performance observed from one year to the next during the study emphasizes the need for multiple years of observation to better understand the temporal stability of these patterns to make informed adaptive management decisions. Precipitation during the study period ranged from 379-648 [mm] and temperature fluctuations ranged 4%-170% of average demonstrating highly variable weather conditions for the dryland region over a 5-year period. Abnormally dry summer conditions in 2014 resulted in a catastrophic crop failure at the Leland farm. RR losses were observed in 13/44 samples at the Leland location with the majority (12 of 13 samples) of monetary losses observed in 2014, with 12 of 12 sites receiving negative RR values. However, NBI values indicate this year as the most efficient, with an average NBI of 0.95 compared to an average of 0.80 over the study period. Exclusively using this metric to measure the efficacy of different management strategies may not effectively capture crop performance. In 2014 high protein concentrations combined with low yields (averaging 2.8 Mg/ha(43.8 [bu/ac])) resulted in severe economic losses. An average yield of 3.9 [Mg/ha](54.7 [bu/ac]) would be required to break even using generalized RR costs, however, this was the only year SWSW was observed during this study.

Leland in general did not exhibit any consistent patterns of low and/or high productivity over the study period. This temporal variability could be due to a number of climatic and topographic factors. It is likely one of them may be long periods of saturated conditions in draw locations. The N retention efficiency widely fluctuated. For example, the average N retention rate of 0.90 in 2014 (SWSW) compared to 0.62 in 2013 (SWWW). This variability in N retention may indicate that excess N one year may be used in the following year but may also be due to wheat class differences. The low soil water availability that is characteristic of the shallow Southwick soils in this area likely made the site more vulnerable to precipitation during the growing season. Without any temporally consistent patterns at the Leland farm it is difficult to suggest any major changes to the fertilizer management. More long-term data would be necessary before trying to drastically modify current practices.

Along with drought stress, excess water conditions were also observed during this study period. Although this study did not investigate pulse crops directly, Troy had spring crop failure (crop samples were not obtainable for garbanzos) for 2 out of 3 years. In the third year, the grower opted to chemically fallow into a winter canola due to excessive water conditions (i.e. it was too wet to plant). This same phenomenon was observed at a larger scale in 2018 where over 37,123 acres of cropland could not be planted with spring cultivars due to excessive water (USDA RMA). These data demonstrate that spring crops were consistently less profitable across all performance classes (Tables 2.6 & 2.7). Hatfield (2018) observed that agriculturally suitable areas are shifting in the Great Plains region. Since 2000, yields are declining in previously successful states and traditionally unsuccessful states are seeing record yield increases since 1980. Iterative and interdisciplinary evaluation metrics such as ones utilized in this study can provide critical data concerning the suitability and stability of agricultural lands and management practices.

CONCLUSIONS

Comprehensive evaluation of N efficiency and crop performance requires multiple metrics. The nitrogen balance index (NBI) in this study effectively captures N uptake efficiency patterns explaining 64% of the variability. Returns to risk and classification metrics effectively capture diverse field scale crop responses in yield, protein and UNR. In this study draw locations were generally the most efficient and profitable compared to other topographic locations. The direct relationship between percent total soil carbon and relative yield suggest that draw locations have higher relative yields to their higher total soil carbon and management strategies which can potentially increase soil organic matter and improve overall crop performance. The most prominent performance class in this study was PC 1 suggesting that protein and nitrogen goals are generally being met, however, with a large contingency of PC 2 many of the farms apply insurance nitrogen to obtain the desired protein concentrations. A strong direct relationship between NBI and returns to risk suggest improving N efficiency will generally improve profits. When used together, evaluation metrics like the NBI, classification and RR can accurately capture the relative temporal and spatial stability of crop performance (i.e. NUE) at various field locations and will assist in maintaining resilience to changing climatic patterns.

REFERENCES

Asseng, S., Ewert, F., Martre, P., Rötter, R. P., Lobell, D. B., Cammarano, D., ... & Reynolds, M. P. (2015). Rising temperatures reduce global wheat production. Nature Climate Change, 5(2), 143.

Barker, R. J. (1981). Soil survey of Latah County area, Idaho (No. 37-39). US Department of Agriculture, Soil Conservation Service.

Basso, B., Cammarano, D., Troccoli, A., Chen, D., & Ritchie, J. T. (2010). Long-term wheat response to nitrogen in a rainfed Mediterranean environment: Field data and simulation analysis. European Journal of Agronomy, 33(2), 132-138.

Basso, B., Ritchie, J. T., Cammarano, D., & Sartori, L. (2011). A strategic and tactical management approach to select optimal N fertilizer rates for wheat in a spatially variable field. European Journal of Agronomy, 35(4), 215-222.

Beven, K.J., Kirkby, M.J. (1979) A physically-based variable contributing area model of basin hydrology' Hydrology Science Bulletin 24(1), p.43-69.

Bezdicek, D. F., Beaver, T., & Granatstein, D. (2003). Subsoil ridge tillage and lime effects on soil microbial activity, soil pH, erosion, and wheat and pea yield in the Pacific Northwest, USA. Soil and Tillage Research, 74(1), 55–63.

Brooks, E. S., Boll, J., & McDaniel, P. A. (2012). Hydropedology in seasonally dry landscapes: the Palouse region of the Pacific Northwest USA. Hydropedology: Synergistic Integration of Soil Science and Hydrology, 329.

Brown, D. J., Brooks, E. S., Eitel, J., Huggins, D. R., Painter, K., Rupp, R., ... & Vierling, L. A. (2011, December). Site-Specific, Climate-Friendly Farming. In AGU Fall Meeting Abstracts.

Brye, K. R., Norman, J. M., Bundy, L. G., & Gower, S. T. (2001). Nitrogen and carbon leaching in agroecosystems and their role in denitrification potential. Journal of Environmental Quality, 30(1), 58-70.

Bullock, D. S., Ruffo, M. L., Bullock, D. G., & Bollero, G. A. (2009). The value of variable rate technology: an information-theoretic approach. American journal of agricultural economics, 91(1), 209-223.

Busacca, A. J. (1989). Long Quaternary record in eastern Washington, USA, interpreted from multiple buried paleosols in loess. Geoderma, 45(2), 105-122.

Busacca, A. J., & McDonald, E. V. (1994). Regional sedimentation of late Quaternary loess on the Columbia Plateau: sediment source areas and loess distribution patterns. Washington Division of Geology and Earth Resources Bulletin, 80, 181-190.

Chen, X. P., Cui, Z. L., Vitousek, P. M., Cassman, K. G., Matson, P. A., Bai, J. S., ... & Zhang, F. S. (2011). Integrated soil–crop system management for food security. Proceedings of the National Academy of Sciences, 108(16), 6399-6404.

Chen, X., Cui, Z., Fan, M., Vitousek, P., Zhao, M., Ma, W., ... & Deng, X. (2014). Producing more grain with lower environmental costs. Nature,514(7523), 486-489.

Chen, X., Zhang, F., Römheld, V., Horlacher, D., Schulz, R., Böning-Zilkens, M., ... & Claupein, W. (2006). Synchronizing N supply from soil and fertilizer and N demand of winter wheat by an improved Nmin method. Nutrient Cycling in Agroecosystems, 74(2), 91-98.

Chi, J., Waldo, S., Pressley, S. N., Russell, E. S., O'Keeffe, P. T., Pan, W. L., ... & Lamb, B. K. (2017). Effects of climatic conditions and management practices on agricultural carbon and water budgets in the inland Pacific Northwest USA. Journal of Geophysical Research: Biogeosciences.

Conrad, O., Bechtel, B., Bock, M., Dietrich, H., Fischer, E., Gerlitz, L., Wehberg, J., Wichmann, V., and Böhner, J. (2015): System for Automated Geoscientific Analyses (SAGA) v. 2.1.4, Geosci. Model Dev., 8, 1991-2007, doi:10.5194/gmd-8-1991-2015. Download.

Dawson, J. C., Huggins, D. R., & Jones, S. S. (2008). Characterizing nitrogen use efficiency in natural and agricultural ecosystems to improve the performance of cereal crops in low-input and organic agricultural systems. Field Crops Research, 107(2), 89-101.

Donaldson, N., United States. Soil Conservation Service, & Washington State University. Agricultural Research Center. (1980). Soil survey of Whitman County, Washington. Washington?]: The Service.

Doran, J. W., & Zeiss, M. R. (2000). Soil health and sustainability: managing the biotic component of soil quality. Applied soil ecology, 15(1), 3-11.

Ebbert, J. C. (1998). Soil erosion in the Palouse River basin: indications of improvement. *US Department of Agriculture*, *7*(445,000), 1-700.

Fiez, T. E., Pan, W. L., & Miller, B. C. (1995). Nitrogen use efficiency of winter wheat among landscape positions. Soil Science Society of America Journal,59(6), 1666-1671.

Fridgen, J. J., Kitchen, N. R., Sudduth, K. A., Drummond, S. T., Wiebold, W. J., & Fraisse, C. W. (2004). Management zone analyst (MZA). *Agronomy Journal*, *96*(1), 100-108.

Fuentes, J. P., Flury, M., Huggins, D. R., & Bezdicek, D. F. (2003). Soil water and nitrogen dynamics in dryland cropping systems of Washington State, USA. *Soil and Tillage Research*, *71*(1), 33-47.

Gaylord, D. R., Busacca, A. J., & Sweeney, M. R. (2003). The Palouse loess and the Channeled Scabland: a paired Ice-Age geologic system. Quaternary Geology of the United States, INQUA, 123-134.Hatfield, J. L., Boote, K. J., Kimball, B. A., Ziska, L. H., Izaurralde, R. C., Ort, D., ... & Wolfe, D. (2011). Climate impacts on agriculture: implications for crop production. Agronomy journal, 103(2), 351-370.

Hatfield, J. L., & Dold, C. (2018). Agroclimatology and Wheat Production: Coping with Climate Change. Frontiers in Plant Science, 9, 224.

Huggins, D., Pan, W., & Smith, J. (2010). Yield, protein and nitrogen use efficiency of spring wheat: evaluating field-scale performance. Chapter, 17, 2010-001.

Huggins, D. R., & Pan, W. L. (2003). Key indicators for assessing nitrogen use efficiency in cereal-based agroecosystems. Journal of Crop Production,8(1-2), 157-185.

Huggins, D. R., & Pan, W. L. (1993). Nitrogen efficiency component analysis: an evaluation of cropping system differences in productivity. Agronomy Journal, 85(4), 898-905.

Jennings, M. D., Miller, B. C., Dezdicek, D. F., & Granatstein, D. (1990). Sustainability of dryland cropping in the Palouse: A historical view. Soil and Water Conservation Society.

Johnson, G., Lamb, J., Rehm, G., Porter, P., Strock, J., Hicks, D., Eash, N., Eidman, V., Potter, B., 2000. An integrated approach to precision farming research. Proceedings of Fifth International Conference on Precision Agriculture (CD), July 16–19, 2000. Bloomington, MN, USA.

Kaur, H., Huggins, D. R., Rupp, R. A., Abatzoglou, J. T., Stöckle, C. O., & Reganold, J. P. (2017). Agro-ecological class stability decreases in response to climate change projections for the Pacific Northwest, USA. Frontiers in Ecology and Evolution, 5, 74.

Knobeloch, L., Salna, B., Hogan, A., Postle, J., & Anderson, H. (2000). Blue babies and nitrate-contaminated well water. Environmental Health Perspectives, 108(7), 675–678.

Kotchenova, S. Y., Vermote, E. F., Matarrese, R., & Klemm Jr, F. J. (2006). Validation of a vector version of the 6S radiative transfer code for atmospheric correction of satellite data. Part I: Path radiance. Applied optics, 45(26), 6762-6774.

Kronvang, B., Grant, R., Larsen, S. E., Svendsen, L. M., & Kristensen, P. (1995). Non-point-source nutrient losses to the aquatic environment in Denmark: Impact of agriculture. Marine and Freshwater Research, 46(1), 167-177.

Ladha, J. K., Pathak, H., Krupnik, T. J., Six, J., & van Kessel, C. (2005). Efficiency of fertilizer nitrogen in cereal production: retrospects and prospects. Advances in agronomy, 87, 85-156.

Legg, J.O., and J.J. Meisinger. 1982. Soil Nitrogen Budgets. In F.J. Stevenson, ed., Nitrogen in Agricultural Soils, American Society of Agronomy, Madison, WI. pp. 503-566

Maaz, T. M., Schillinger, W. F., Machado, S., Brooks, E., Johnson-Maynard, J. L., Young, L. E., ... & Esser, A. (2017). Impact of climate change adaptation strategies on winter wheat and cropping system performance across precipitation gradients in the inland Pacific Northwest, USA. Frontiers in Environmental Science, 5, 23.

Magney, T., Yourek, M., Ward, N., Finch, S., Eitel, J., Vierling, L., Brooks, E., Huggins, D., Brown, D. "Determining the controls on nitrogen uptake from space." REACCH Annual Report Year 4 N.p., 2015. Web. 5 Aug. 2015.

Magney, T. S., Eitel, J. U., & Vierling, L. A. (2016). Mapping wheat nitrogen uptake from RapidEye vegetation indices. Precision Agriculture, 1-23.

Mahler, Robert L., Guy, Stephen O. "Northern Idaho Fertilizer Guide: Winter Wheat." University of Idaho Extension CIS453 (2007): 1–4. Print.

Mahler, Robert L.., Guy, Stephen O. "Northern Idaho Fertilizer Guide: Soft White Spring Wheat." University of Idaho Extension CIS1101 (2007): 1–4. Print.McBratney, A., Whelan, B., Ancev, T., & Bouma, J. (2005). Future directions of precision agriculture. Precision agriculture, 6(1), 7-23.

McCool, D. K., Busacca, A. J., & Michalson, E. L. (1999). Measuring and modeling soil erosion and erosion damages. Conservation farming in the United States—The methods and accomplishments of the STEEP Program, 23-56.

McDaniel, P. A., & Hipple, K. W. (2010). Mineralogy of loess and volcanic ash eolian mantles in Pacific Northwest (USA) landscapes. Geoderma, 154(3-4), 438-446.

Moll, R. H., Kamprath, E. J., & Jackson, W. A. (1982). Analysis and interpretation of factors which contribute to efficiency of nitrogen utilization 1. Agronomy Journal, 74(3), 562-564.

Morrow, J. G., Huggins, D. R., & Reganold, J. P. (2017). Climate change predicted to negatively influence surface soil organic matter of dryland cropping systems in the Inland Pacific Northwest, USA. Frontiers in Ecology and Evolution, 5, 10.

Mulla, D. J. (2013). Twenty five years of remote sensing in precision agriculture: Key advances and remaining knowledge gaps. Biosystems Engineering, 114(4), 358-371.

Ongley, E. D., Xiaolan, Z., & Tao, Y. (2010). Current status of agricultural and rural non-point source pollution assessment in China. Environmental Pollution, 158(5), 1159-1168.

Painter, Kate (2016). Crop Enterprise Budget Cost Calculators. Retrieved from http://www.webpages.uidaho.edu/~kpainter/

Pan, W., Schillinger, W., Huggins, D., Koenig, R., & Burns, J. (2006, November). Fifty Years of Predicting Wheat Nitrogen Requirements Based on Soil Water, Yield, Protein and Nitrogen Efficiencies. In ASA-CSSA-SSSA Annual Meeting Abstracts. Raun, W.R., and G.V. Johnson. 1999. Improving nitrogen use efficiency for cereal production. Agronomy Journal 91:357-363.

Pan, W. L., et al. "Soil carbon and nitrogen fraction accumulation with long-term biosolids applications." Soil Science Society of America Journal 81.6 (2017): 1381-1388.

Peralta, N. R., & Costa, J. L. (2013). Delineation of management zones with soil apparent electrical conductivity to improve nutrient management. Computers and Electronics in Agriculture, 99, 218-226.

Peralta, N. R., Costa, J. L., Balzarini, M., Franco, M. C., Córdoba, M., & Bullock, D. (2015). Delineation of management zones to improve nitrogen management of wheat. Computers and Electronics in Agriculture, 110, 103-113.

Prasad, P. V., & Djanaguiraman, M. (2014). Response of floret fertility and individual grain weight of wheat to high temperature stress: sensitive stages and thresholds for temperature and duration. Functional Plant Biology, 41(12), 1261-1269.

Quan, W., & Yan, L. (2002). Effects of agricultural non-point source pollution on eutrophica-tion of water body and its control measure. Acta Ecologica Sinica, 22(3), 291-299.

Reganold, J. P., Jackson-Smith, D., Batie, S. S., Harwood, R. R., Kornegay, J. L., Bucks, D., ... & Schumacher Jr, A. (2011). Transforming US agriculture. Science, 332(6030), 670-671.

Rezaei, E. E., Siebert, S., & Ewert, F. (2015). Intensity of heat stress in winter wheat—phenology compensates for the adverse effect of global warming. Environmental Research Letters, 10(2), 024012.

“Soil Bulk Density, Moisture, Aeration.” (n.d.) Guides for Educators. USDA-NRCS, Web. 6 July 2017.

Taylor, S. E. (2016). Precision Nitrogen Management: Evaluating and Creating Management Zones Using Winter Wheat Performance (Doctoral dissertation, Washington State University).

Tisdall, J. M., & Oades, J. (1982). Organic matter and water-stable aggregates in soils. European Journal of Soil Science, 33(2), 141-163.

Unger, R., D. E. Huggins. 2015. Cropping system nitrogen use efficiency after 10 years of no-tillage. In: Borrelli et al. (eds.), Regional Approaches to Climate Change for Pacific Northwest Agriculture: Climate Science Northwest Farmers Can Use. pp. 62-63

Vermote, E. F., & Kotchenova, S. (2008). Atmospheric correction for the monitoring of land surfaces. Journal of Geophysical Research: Atmospheres, 113(D23).

Ward, N. K., Maureira, F., Stöckle, C. O., Brooks, E. S., Painter, K. M., Yourek, M. A., & Gasch, C. K. (2018). Simulating field-scale variability and precision management with a 3D hydrologic cropping systems model. Precision Agriculture, 19(2), 293-313.

Washington Wheat Commission. (2013). *Hard Red Spring Wheat Nitrogen & Fertilizer Management Guide* [PDF file]. Retrieved from 1

Wolff, E., 1864. Entwurf zur Bodenanalyse. Die Landwirthschaftlichen VersuchsStationen 6, 141–171.

Yost, M. A., Kitchen, N. R., Sudduth, K. A., Sadler, E. J., Drummond, S. T., & Volkmann, M. R. (2017). Long-term impact of a precision agriculture system on grain crop production. Precision Agriculture, 18(5), 823-842.

Yourek, M. A. (2016). An Investigation of Crop Senescence Patterns Observed in Palouse Region Fields Using Satellite Remote Sensing and Hydrologic Modeling (Doctoral dissertation, University of Idaho).

Zhang, X., Shi, L., Jia, X., Seielstad, G., & Helgason, C. (2010). Zone mapping application for precision-farming: a decision support tool for variable rate application. Precision Agriculture, 11(2), 103-114.

Zhang, N., Wang, M., & Wang, N. (2002). Precision agriculture—a worldwide overview. Computers and electronics in agriculture, 36(2-3), 113-132.

Zhao, R. F., Chen, X. P., Zhang, F. S., Zhang, H., Schroder, J., & Römheld, V. (2006). Fertilization and nitrogen balance in a wheat–maize rotation system in North China. Agronomy Journal, 98(4), 938-945.

CHAPTER 2 FIGURES

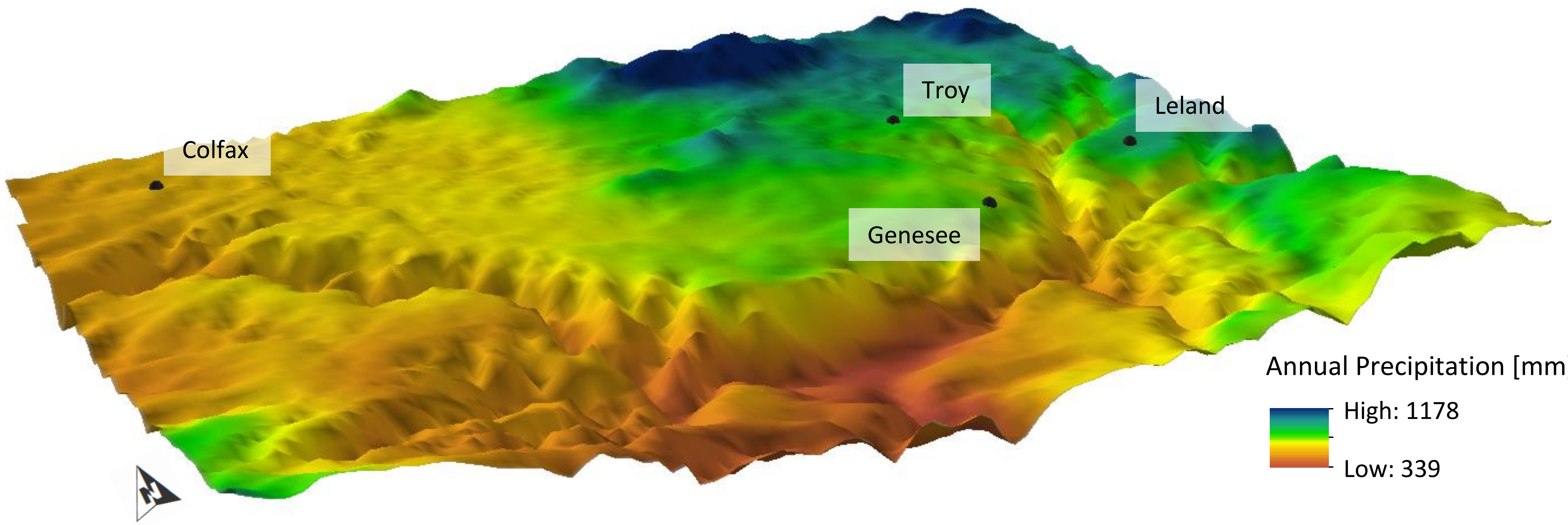

Figure 2.1: Annual precipitation [mm] of the Site-specific Climate Friendly Farming project locations.

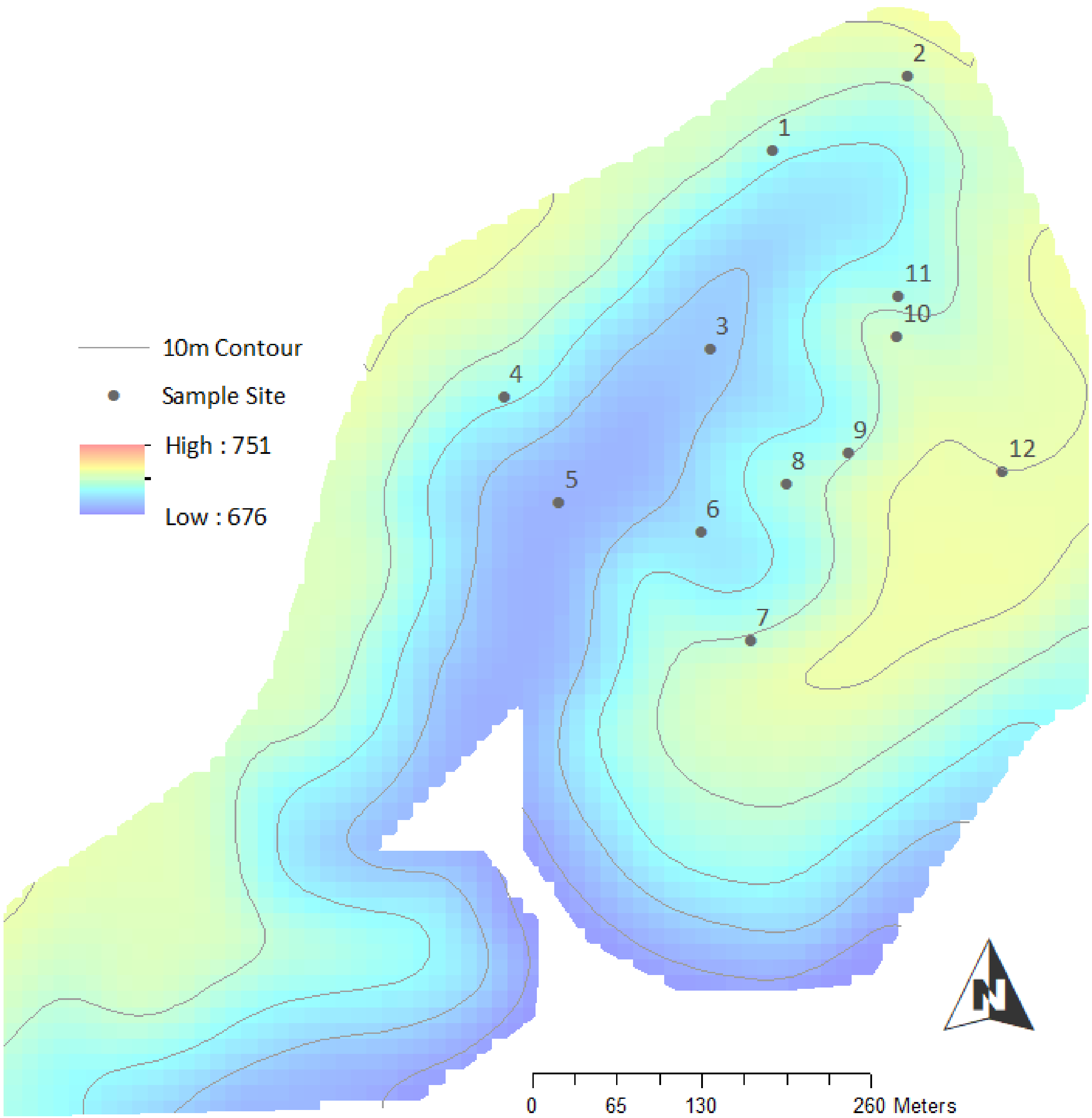

Figure 2.2: Colfax Tier II field sampling locations and digital elevation map [m].

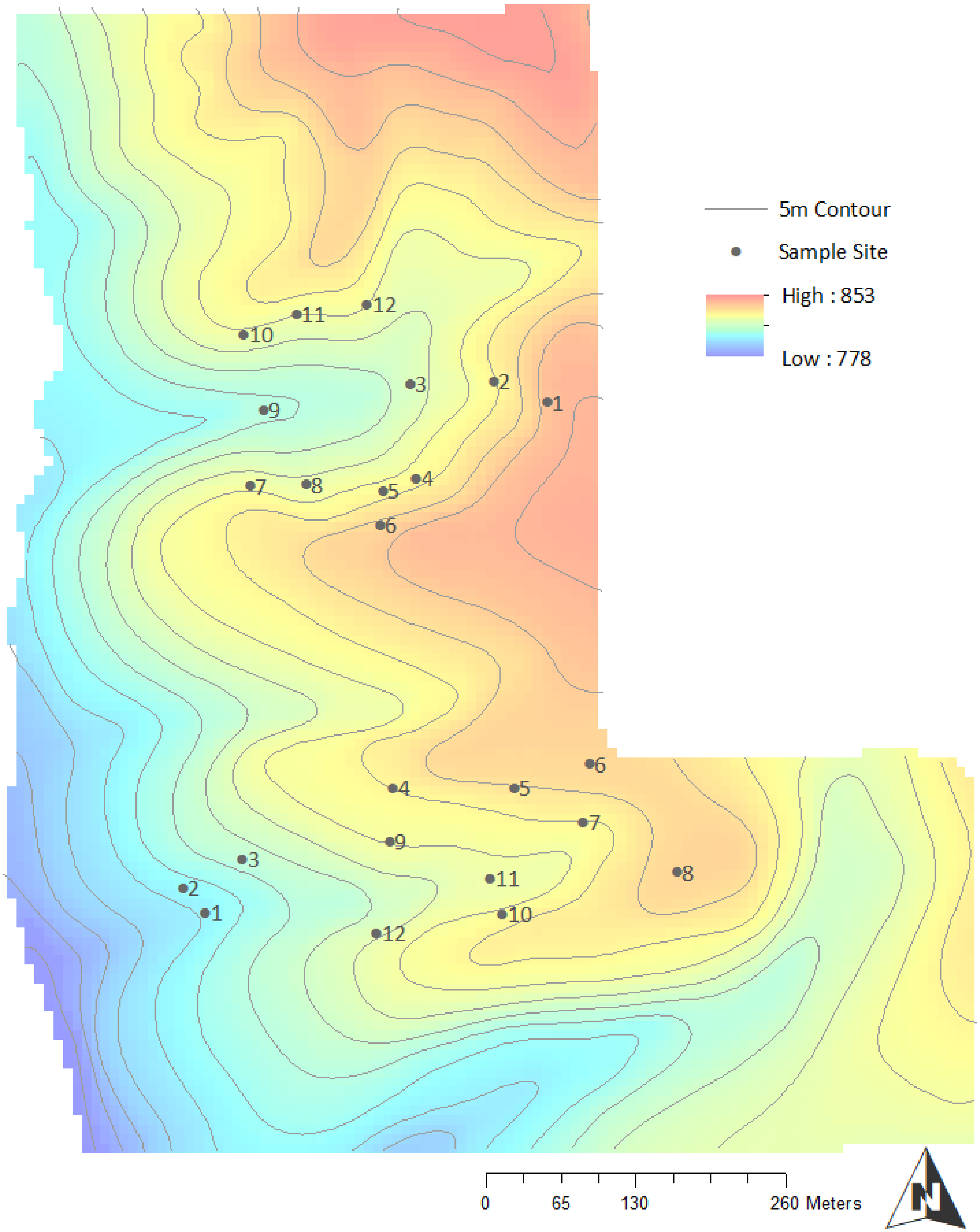

Figure 2.3: Genesee field sampling locations and digital elevation map [m].

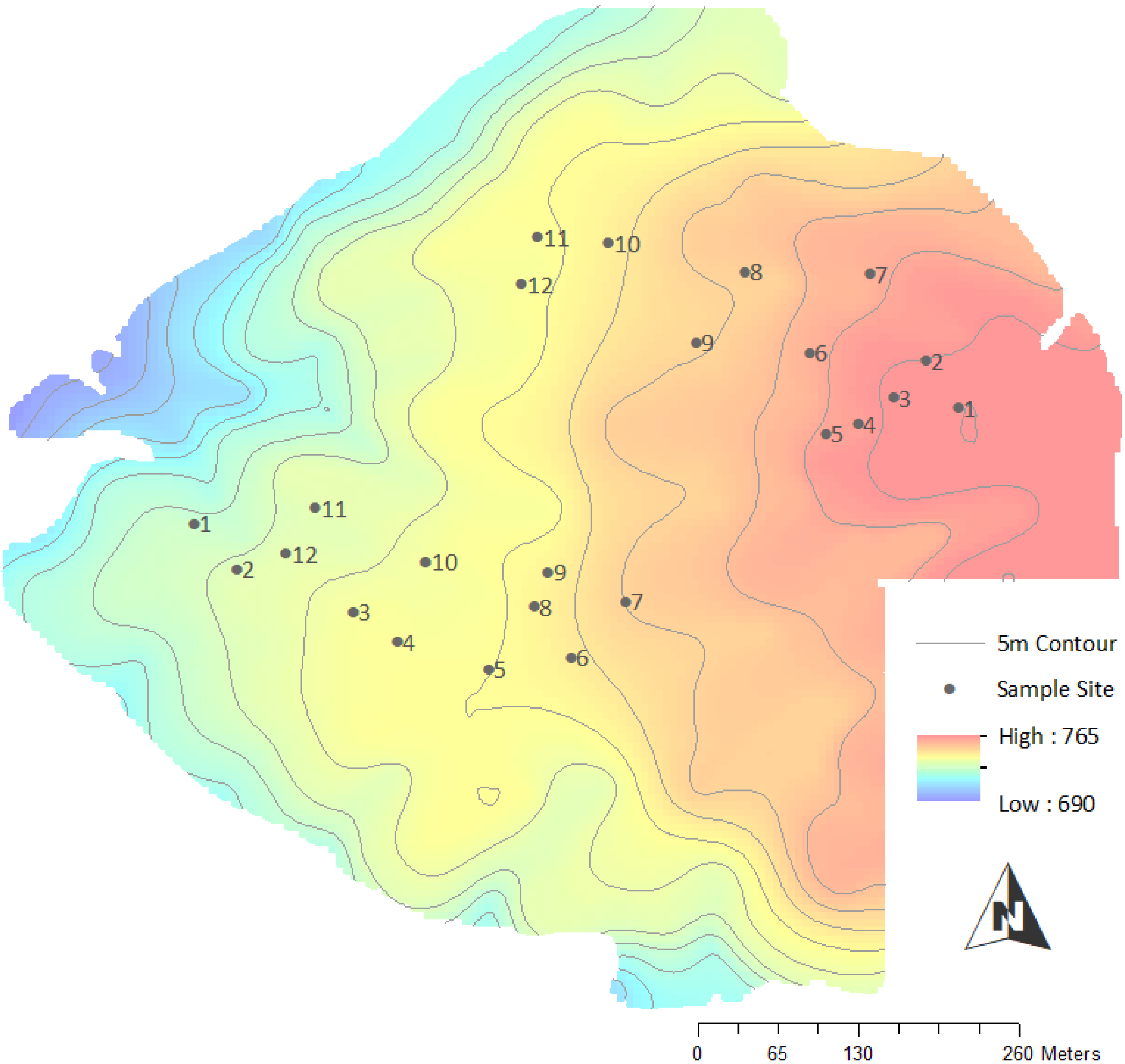

Figure 2.4: Leland field sampling locations and digital elevation map [m].

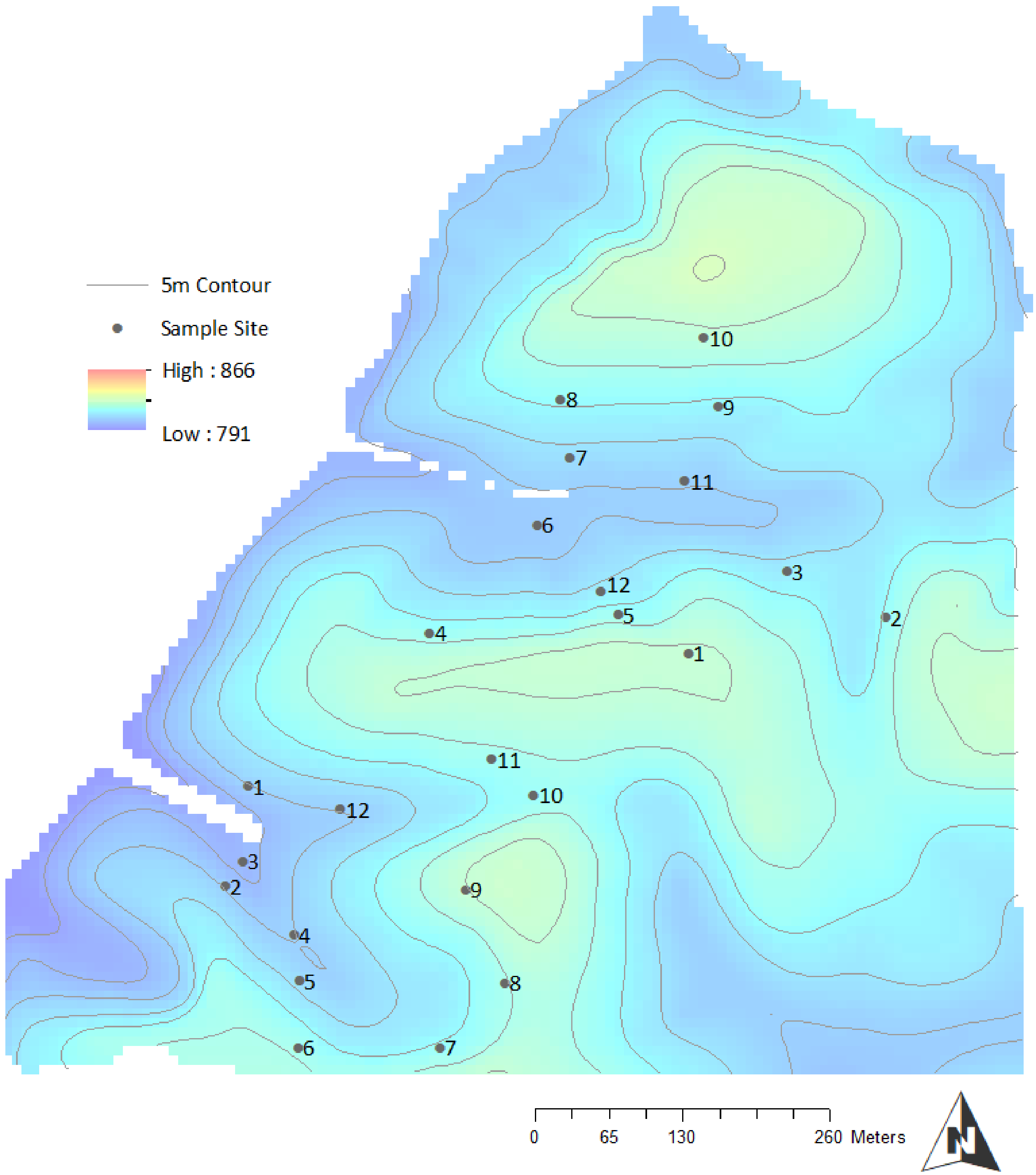

Figure 2.5: Troy field sampling locations and digital elevation map [m].

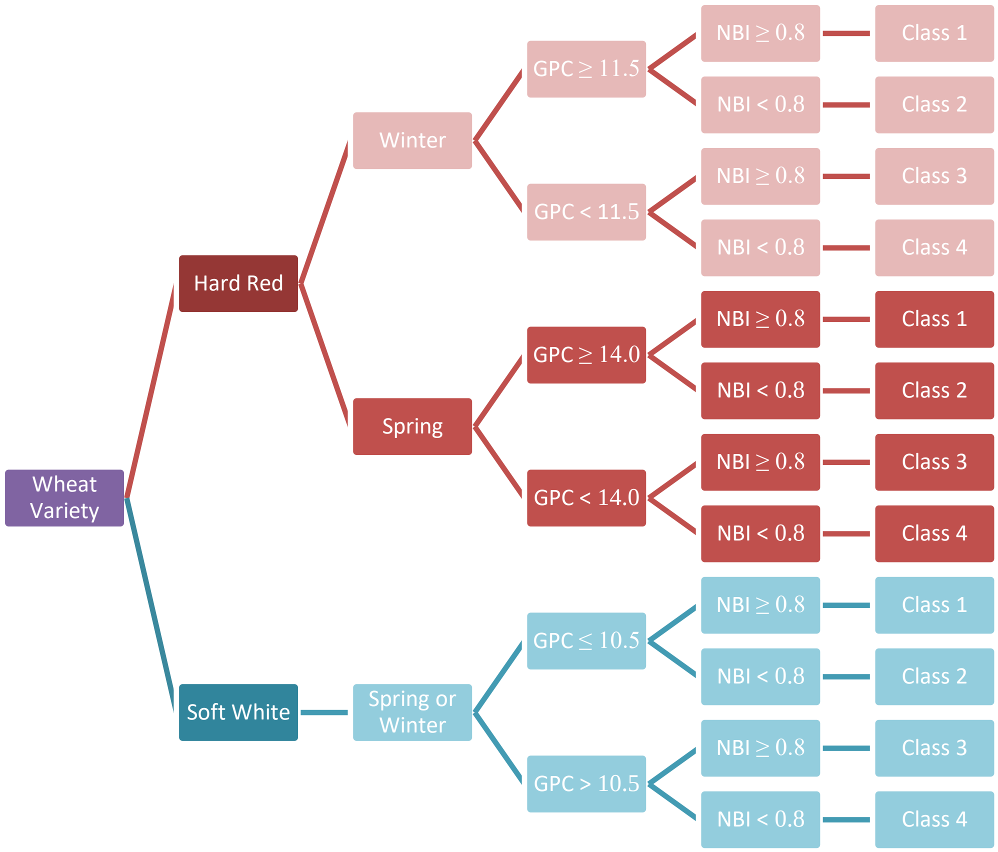

Figure 2.6: Point based evaluation classification scheme. Varied grain protein concentration (GPC) [%] standards were used for different wheat classes.

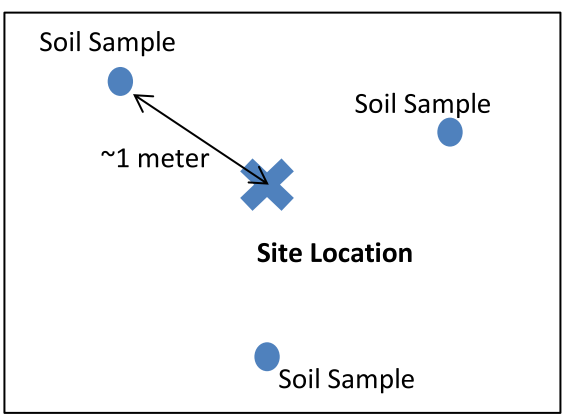

Figure 2.7: Soil sampling design diagram.

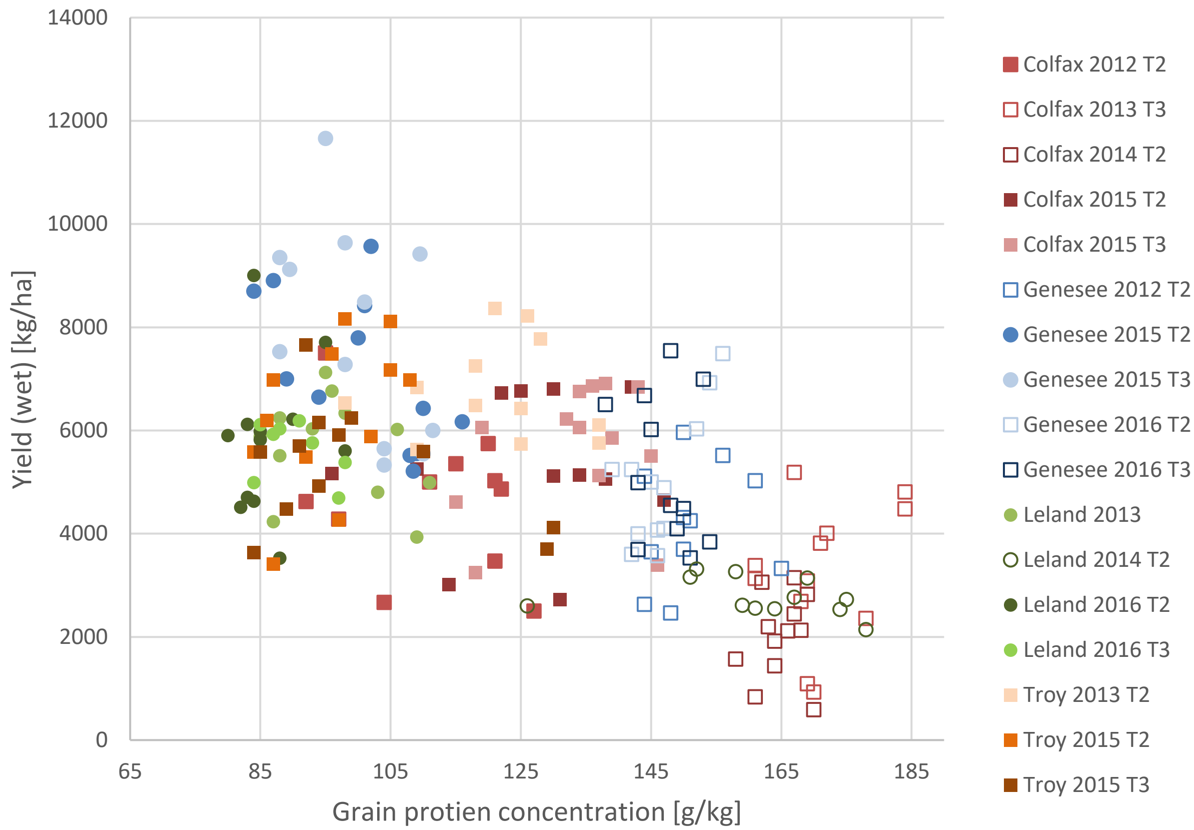

	Key	Example
Hard Red	Square	■
Soft White	Circle	●
Mixed Class	Diamond	◊
Spring Class	Hollow	○
Winter Class	Filled	■
Colfax	Reds	■
Genesee	Blues	●
Leland	Greens	●
Troy	Oranges	■

Figure2.8: Tier II grain protein concentration [g/kg] vs yield [kg/ha] and graphics key.

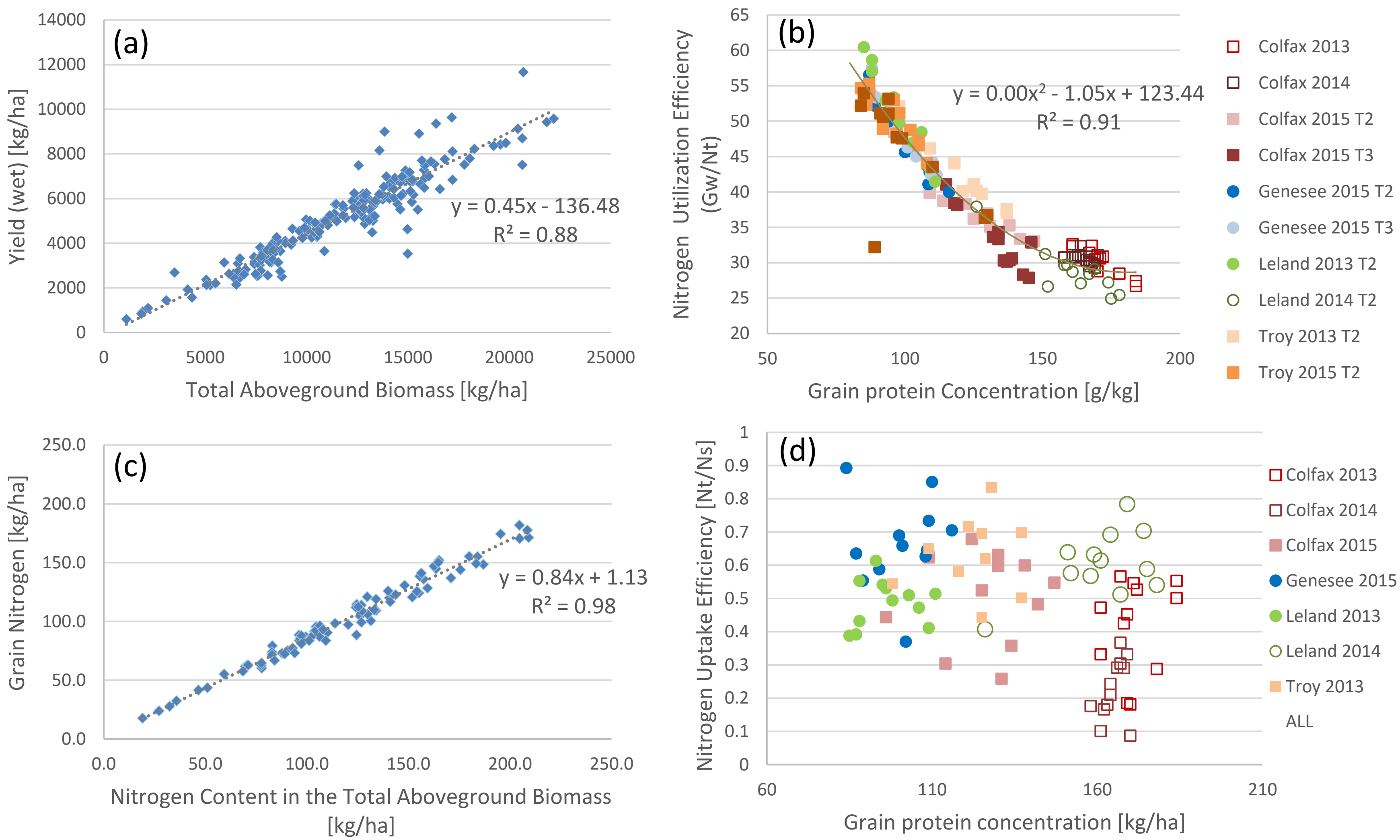

Figure 2.9: Nitrogen use efficiency relationships with mixed classes (a) Harvest Index for all sample sites, (b) N utilization efficiency vs grain protein concentration [g/kg] using key from Figure 2.9, (c) Nitrogen Harvest Index for all sample sites, (d) N uptake efficiency vs grain protein concentration [g/kg]. (T2 = Tier II sites, T3 = Tier III sites).

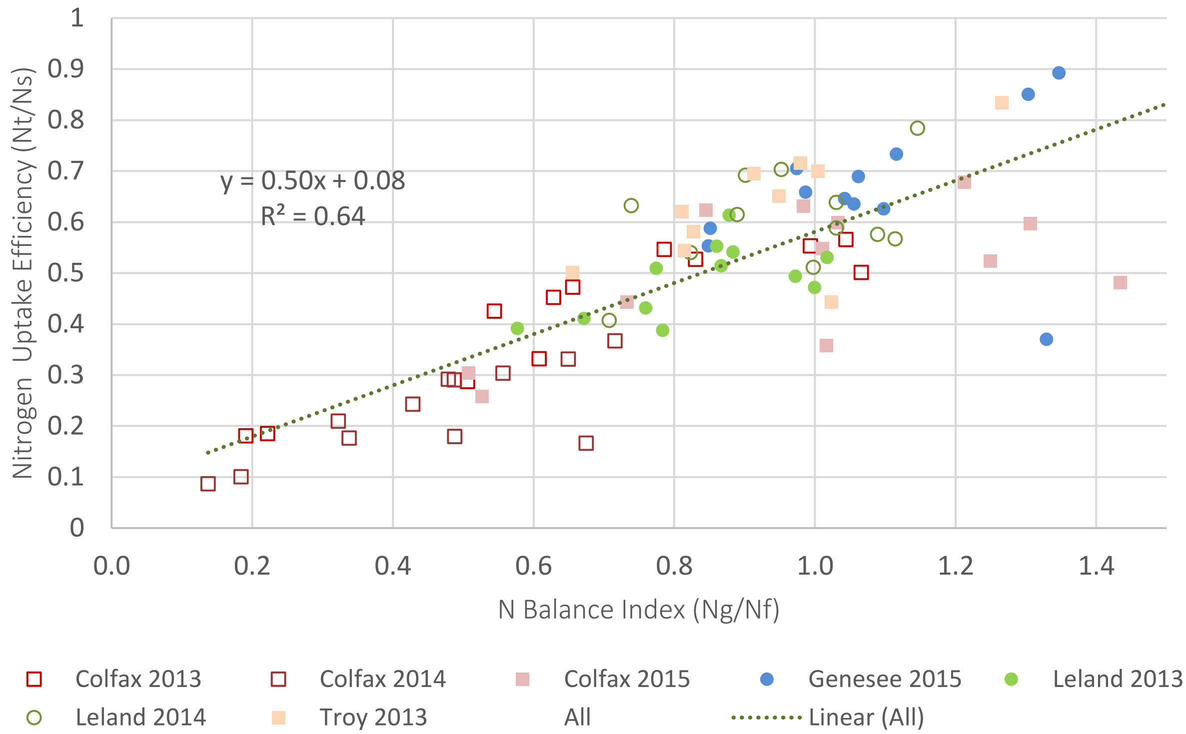

Figure 2.10: Nitrogen balance index vs N uptake efficiency.

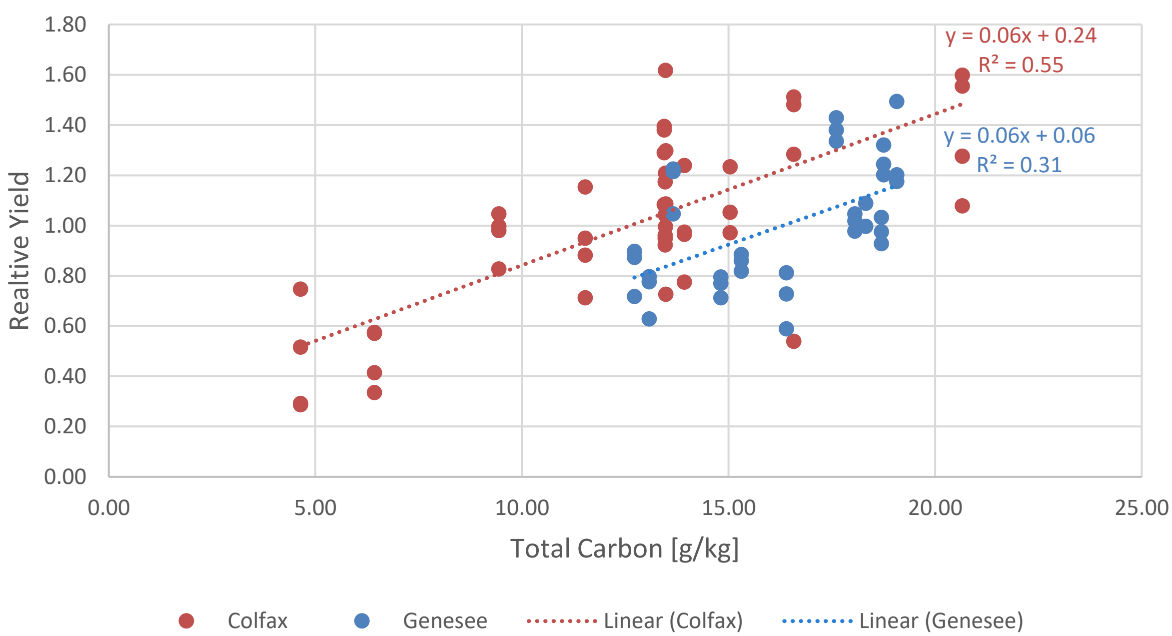

Figure 2.11: Relative yield vs 30 cm total soil carbon concentration [g/kg] at no-till farms.

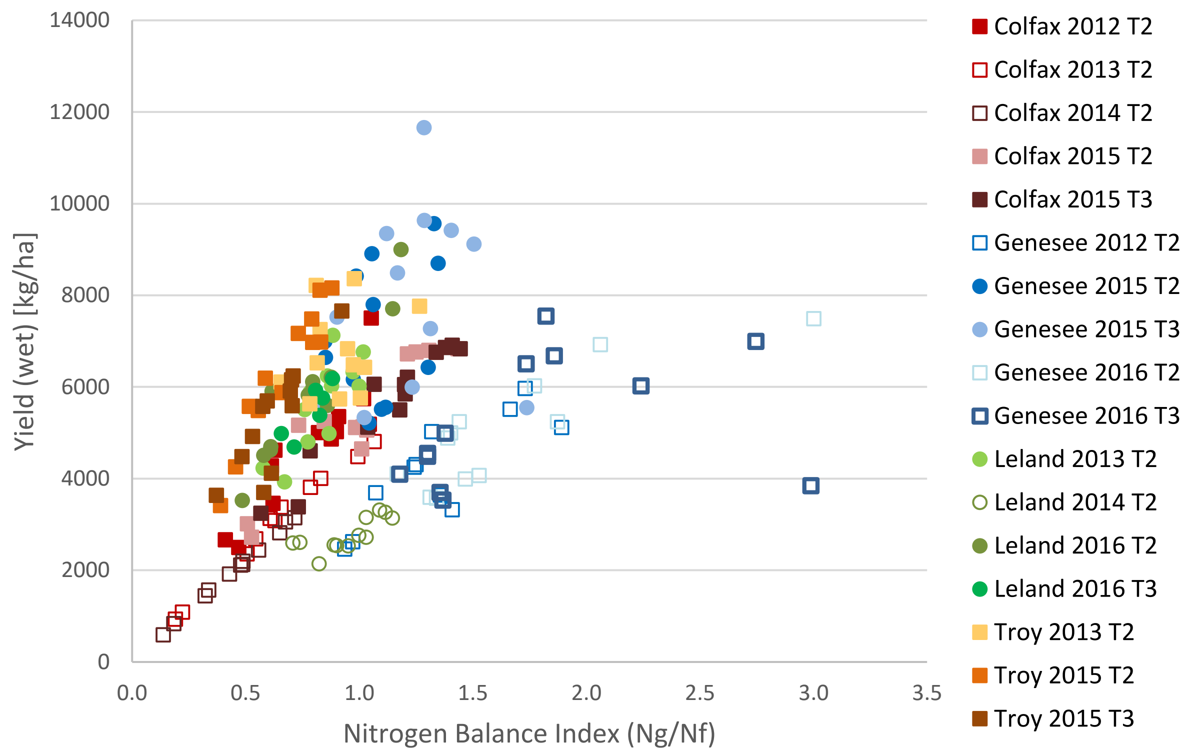

Figure 2.12 Nitrogen Balance Index and yield [kg/ha] relationship.

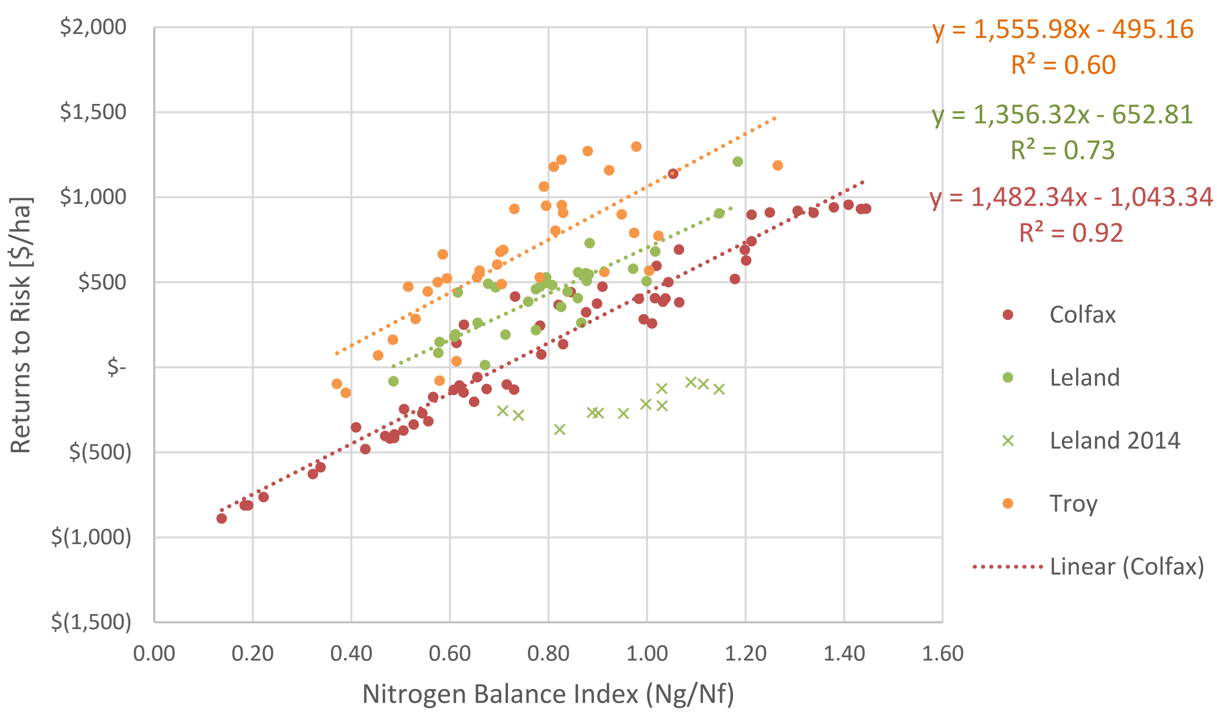

Figure 2.13: Returns to risk and nitrogen balance index at Leland, Colfax and Troy.

CHAPTER 2 TABLES

Table 2.1: Colfax management and rotation summary.

	Annual Prec. [mm]	Tier II Site Size [ha]	Tier III Site Size [ha]	Tillage	Planter	Fertilizer Type	Fertilizer Rate [kg N/ha]	Crop
2012	491	16.0	36.9	No Till	Direct Seed	Uniform: Urea Sp. Foliar: Urea	119	HRWW
2013	475	16.0	36.9	No Till	Direct Seed	Uniform: Urea Sp. Foliar: Urea	146	HRSW
2014	379	16.0	36.9	No Till	Direct Seed	Uniform: Urea Sp. Foliar: Urea	129	HRSW
2015	400	16.0	36.9	No Till	Direct Seed	Uniform: Urea Sp. Foliar: Urea	119	HRWW
2016	486	16.0	36.9	No Till	Direct Seed	Uniform: Urea Sp. Foliar: Urea		Chem. Fallow

Table 2.2: Genesee management and rotation summary.

	Annual Precip. [mm]	Tier II Site Size [ha]	Tier III Site Size [ha]	Tillage	Planter	Fertilizer Type	Fertilizer Rates [kg N/ha]	Crop
2012	587	12.0	20.7	No Till	Direct Seed - Exactrix	NH3 at planting	High: 108 Med2:91 Med:68 Low:35	HRSW
2013	588	12.0	20.7	No Till	Direct Seed - Exactrix	NH3 at planting	High: 108 Med2:91 Med:68 Low:35	SP BARLEY
2014	507	12.0	20.7	No Till	Direct Seed - Exactrix	NH3 at planting		SP CANOLA
2015	600	12.0	20.7	No Till	Direct Seed - Exactrix	NH3 at planting	High: 151 Med2:129 Med:95 Low:62	SWWW
2016	625	12.0	20.7	No Till	Direct Seed - Exactrix	NH3 at planting	High: 108 Med2:91 Med:68 Low:35	HRSW

Table 2.3: Leland management and rotation summary.

	Annual Precip. [mm]	Tier II Site Size [ha]	Tier III Site Size [ha]	Tillage	Fertilizer Type	Fertilizer Rates [kg N/ha]	Crop
2012	624	8.9	18.1	Fall: Heavy Harrow			GARBS
2013	631	8.9	18.1	Conservation Fall: Chisel	Zones: Urea Sp: Topdress Sp: fungicide	High: 134 Med: 112 Low: 90	SWWW
2014	541	8.9	18.1	Conservation Fall: Chisel Spring: Hard Harrow	Zones: Urea Sp: Topdress Sp: fungicide	High: 99 Med: 81 Low: 67	SWSW
2015	608	8.9	18.1	Spring: Heavy Harrow			GARBS
2016	648	8.9	18.1	Conservation Fall: Chisel	Zones: Urea Sp: Topdress Sp: fungicide	High: 134 Med: 112 Low: 80	SWWW

Table 2.4: Troy management and rotation summary.

	Annual Precip. [mm]	Tier II Site Size [ha]	Tier III Site Size [ha]	Tillage	Planter	Fertilizer Type	Fertilizer Rates [kg N/ha]	Crop
2012	596	24.9	17.7		Direct Seed			(DNS 2011) GARBS
2013	580	24.9	17.7	Fall subsoiler @ 14-16" depth on 30" centers	Direct Seed	Fall: aqua Starter: MESZ 12%N Zones: Solution 32 Foliar: Urea	High: 224 Med:181 Med2: 157 Low: 138	HRWW
2014	461	24.9	17.7	Spring: cultivator/ harrow	Direct Seed			GARBS
2015	605	24.9	17.7	Conservation tillage Fall: Chisel	Direct Seed	Fall: aqua Starter: MESZ 12%N Zones: Solution 32 Foliar: Urea	High: 180 Med: 159 Med2: 153 Low: 134	HRWW
2016	652	24.9	17.7	Spring: cultivator/ harrow	Direct Seed			Fallow to W. Canola

Table 2.5: 5-year average returns to risk analysis values (Painter, 2016).

	Crop Price [$/kg]	Cost of Production sans N_f [$/ha]		Fertilizer Type Used	Fertilizer price [$/kg]
HRWW	$ 0.31	$ 975.45	Colfax	Urea	$ 1.69*
HRSW	$ 0.31	$ 854.13	Genesee	Anhydrous	$ 1.39
SWWW	$ 0.24	$ 726.20	Leland	Urea	$ 1.69*
SWSW	$ 0.24	$ 732.11	Troy	30% Solution	$ 1.69

*prices reflective of 30% N solution prices rather than urea since urea 5-year average costs not available.

Table 2.6: Regional N efficiency summary.

	Prec. [mm]	N uptake eff. [kg/ha]		NUE [kg G_W/ kg N]		N retention [N_{av}/N_s]		NBI		N losses [kg/ha]		Class Frequency			
		Avg.	σ	Avg.	σ	Avg.	σ	Avg.	σ	Avg.	σ	1	2	3	4
COLFAX	446	0.38	0.17	12.8	6.4	0.75	0.26	0.80	0.34	65.5	93.0	26	26	3	5
GENESEE	581	0.66	0.14	25.1	8.6	0.84	0.19	1.42	0.47	53.1	89.8	49	0	10	0
LELAND	610	0.55	0.10	21.2	5.4	0.76	0.20	0.84	0.17	53.5	44.4	23	18	2	1
TROY	578	0.63	0.12	26.0	4.4	0.71	0.13	0.74	0.20	83.6	48.5	8	3	6	19
Regional		0.50	0.18	19.6	8.6	0.76	0.22	0.98	0.44	62.4	75.8	106	47	21	25

Table 2.7: Crop performance metrics by class.

Class	Frequency			Returns to Risk [$/ha]			NBI		
	HRWW	SWWW	Totals	HRWW	SWWW	Average	HRWW	SWWW	Average
1	30	29	59	$ 720	$ 847	$ 782	1.11	1.03	1.07
2	9	16	25	$ (48)	$ 308	$ 180	0.62	0.68	0.66
3	9	10	19	$ 911	$ 562	$ 728	0.88	1.18	1.04
4	24	1	25	$ 399	$ 13	$ 383	0.61	0.67	0.61
	HRSW	SWSW		HRSW	SWSW		HRSW	SWSW	
1	37	10	47	$ 484	$ (205)	$ 338	1.52	1.00	1.41
2	20	2	22	$ (394)	$ (269)	$ (382)	0.48	0.72	0.50
3	2	0	2	$ 847		$ 847	1.80		1.80
4	0	0	0						

Table 2.8: Topographic and subsite class averages.

		G_w [Mg/ha]		GPC [g/kg]		UNR [kg Gw/ kg N]		N uptake	
COLFAX		**HRSW**	**HRWW**	**HRSW**	**HRWW**	**HRSW**	**HRWW**	**HRSW**	**HRWW**
	AVG	*2.6*	*5.2*	*168*	*124*	*7.4*	*3.2*	*0.32*	*0.50*
	σ	*1.3*	*1.4*	*77*	*15*	*4.4*	*1.2*	*0.15*	*0.14*
	CV	*47%*	*26%*	*46%*	*12%*	*59%*	*38%*	*46%*	*27%*
	Draw	3.5^{a}	5.7^{a}	172^{a}	127^{a}	6.2^{a}	2.7^{a}	0.37^{a}	0.57^{a}
	Flat	0.8^{b}	4.5^{a}	170^{a}	125^{a}	15.7^{a}	6.0*	0.13^{b}	0.26*
	NFS	2.6^{c}	5.2^{a}	166^{b}	130^{a}	6.1^{a}	3.1^{a}	0.35^{a}	0.53^{a}
	SFS	2.1^{c}	5.0^{a}	165^{b}	111^{b}	8.0^{a}	3.1^{a}	0.30^{a}	0.46^{a}
GENESEE		**HRSW**	**SWWW**	**HRSW**	**SWWW**	**HRSW**	**SWWW**	**HRSW**	**SWWW**
	AVG	*4.8*	*7.5*	*148*	*100*	*3.2*	*2.0*	*0.40*	*0.66*
	σ	*1.3*	*1.8*	*6*	*9*	*0.7*	*0.5*	*0.08*	*0.14*
	CV	*28%*	*24%*	*6%*	*6%*	*16%*	*38%*	*21%*	*20%*
	Draw	6.0^{a}	147.5^{a}	150^{a}	94^{a}	3.6*	1.7^{a}	0.35*	0.66^{a}
	Flat	4.8^{b}	109.1^{a}	146^{a}	94^{a}	2.3^{a}	1.6^{a}	0.52^{a}	0.74^{a}
	NFS	4.5^{b}	110.5^{a}	146^{a}	101^{a}	3.8^{a}	2.0^{a}	0.32^{b}	0.69^{a}
	SFS	4.7^{b}	116.3^{a}	150^{a}	104^{a}	3.2^{b}	2.2^{a}	0.40^{a}	0.63^{a}
LELAND		**SWSW**	**SWWW**	**SWSW**	**SWWW**	**SWSW**	**SWWW**	**SWSW**	**SWWW**
	AVG	*2.8*	*5.7*	*161*	*91*	*3.3*	*2.3*	*0.60*	*0.49*
	σ	*0.4*	*1.1*	*14*	*8*	*0.5*	*0.4*	*0.10*	*0.07*
	CV	*13%*	*19%*	*9%*	*9%*	*15%*	*18%*	*16%*	*14%*
	Draw	3.0^{a}	2.9^{a}	163^{a}	94^{a}	3.6^{a}	2.4^{a}	0.54^{a}	0.48^{a}
	Flat	2.6^{a}	5.7^{a}	162^{a}	88^{b}	3.3^{a}	2.3^{a}	0.63^{a}	0.45^{a}
	NFS	3.0^{a}	5.6^{a}	155^{a}	94^{a}	3.2^{a}	2.1^{a}	0.61^{b}	0.55^{b}
	SFS	2.7^{a}	5.8^{a}	167^{a}	92^{s}	3.4^{a}	2.6^{a}	0.61^{b}	0.48^{a,b}
TROY		**HRWW**		**HRWW**		**HRWW**		**HRWW**	
	AVG	*6.1*		*105*		*2.3*		*0.59*	
	σ	*1.3*		*16*		*0.4*		*0.14*	
	CV	*22%*		*16%*		*19%*		*24%*	
	Draw	6.5^{a}		102^{a}		2.0^{a}		0.64^{a}	
	Flat	6.2^{a}		108^{a}		2.4^{b}		0.48^{a}	
	NFS	5.3^{b}		105^{a}		2.4^{a,b}		0.58^{a}	
	SFS	6.5^{a}		106^{a}		2.4^{b}		0.61^{a}	

Note: population letters (a-d) repeat for each class and location; α=0.1 for topographic analysis

Table 2.9: Crop performance by topographic positions.

	$Yield_{rel}$					NBI					RR				
	1	2	3	4	Avg	1	2	3	4	Avg	1	2	3	4	Avg
Draw	1.20	1.10	1.14	0.97	1.2	1.17	0.60	0.90	0.59	0.98	$692	$(107)	$767	$503	$538
Flat	1.04	0.79	1.05	1.06	0.9	1.08	0.63	1.87	0.75	0.87	$464	$53	$669	$726	$331
NFS	1.01	0.83	0.93	0.88	0.9	1.25	0.56	1.25	0.55	1.02	$494	$(154)	$676	$291	$347
SFS	1.04	0.88	1.06	0.85	1.0	1.32	0.53	1.03	0.58	1.03	$654	$(218)	$785	$219	$459
Avg	1.07	0.87	1.03	0.92		1.22	0.58	1.11	0.61		$585	$56	$768	$438	

Table 2.10: Average soil properties and relative performance by topographic positions.

	$Yield_{rel}$	OM [%]	BD [g/m^3]	Clay [%]	NBI_{rel}	RR_{rel}
Draw	1.08[a]	1.80[a]	1.29[a]	29.1[a]	1.11[a]	1.13[a]
Flat	0.96[b]	1.10[b]	1.35[b]	33.6[b]	0.95[b]	0.96[b]
NFS	0.96[b]	1.160.67[b]	1.36[b]	31.7[a,b]	0.99[a,b]	0.95[b]
SFS	1.01[a,b]	1.270.75[b]	1.33[a,b]	32.7[b]	0.96[b]	0.98[b]

Table 2.11: Colfax Tier II relative crop performance site summary.

Site #	$Yield_{rel}$	$Yield_{rel}$ SD	NBI_{rel}	NBI_{rel} SD	RR_{rel}	RR_{rel} SD
1	0.95	0.09	0.85	0.15	0.51	0.51
2	1.21	0.29	1.10	0.26	1.10	0.72
3	1.03	0.22	1.09	0.25	0.67	0.75
4	0.47	0.11	0.44	0.09	-0.75	1.20
5	1.28	0.14	1.33	0.14	1.34	0.26
6	1.19	0.45	1.22	0.43	1.23	0.83
7	0.99	0.12	0.97	0.15	0.57	0.71
8	0.46	0.22	0.48	0.25	-0.83	1.47
9	0.92	0.19	0.95	0.20	0.31	1.13
10	0.98	0.19	0.99	0.26	0.46	1.09
11	1.07	0.15	1.08	0.15	0.69	0.69
12	1.37	0.25	1.34	0.26	1.60	0.41

	2012	**2013**	**2014**	**2015**	**2016**
T2 Avg G_w	4639	3247	2023	5269	
G_w SD	1423	1341	809	1389	
T2 Avg NBI	0.76	0.67	0.45	0.99	
NBI SD	0.22	0.29	0.18	0.29	
T2 Avg RR	$254	$(100)	$(449)	$448	
RR SD	$439	$414	$250	$428	

rel = relative, SD = standard deviation, T2 = Tier II

Table 2.12: Genesee Tier II relative crop performance site summary.

Site #	$Yield_{rel}$	$Yield_{rel}$ SD	NBI_{rel}	NBI_{rel} SD	RR_{rel}	RR_{rel} SD
1	0.93	0.15	0.87	0.07	1.05	0.09
2	0.83	0.06	0.97	0.18	0.75	0.16
3	1.30	0.11	1.21	0.07	1.60	0.15
4	0.93	0.09	0.83	0.09	1.01	0.05
5	0.77	0.03	0.93	0.13	0.64	0.07
6	1.16	0.06	1.22	0.16	1.28	0.17
7	1.36	0.35	1.20	0.49	1.44	0.31
8	0.91	0.11	0.82	0.10	0.96	0.08
9	0.79	0.10	0.77	0.08	0.76	0.05
10	0.72	0.15	0.83	0.12	0.55	0.23
11	1.18	0.14	1.06	0.16	1.40	0.14
12	0.74	0.11	0.85	0.12	0.59	0.20
		2012	**2013**	**2014**	**2015**	**2016**
T2 Avg G_w		4176			7159	5013
G_w SD		1149			1525	1280
T2 Avg NBI		1.35			1.08	1.65
NBI SD		0.31			0.17	
T2 Avg RR		$320			$803	$582
RR SD		$343			$335	$387

rel = relative, SD = standard deviation, T2 = Tier II

Table 2.13: Leland Tier II relative crop performance site summary.

Site #	$Yield_{rel}$	$Yield_{rel}$ SD	NBI_{rel}	NBI_{rel} SD	RR_{rel}	RR_{rel} SD
1	0.90	0.28	0.94	0.27	0.96	0.68
2	1.27	0.19	1.26	0.21	1.45	0.11
3	0.82	0.08	0.83	0.16	0.66	0.06
4	1.14	0.03	1.16	0.02	1.32	0.28
5	1.15	0.34	1.06	0.42	1.21	0.59
6	1.00	0.07	0.97	0.05	0.94	0.20
7	0.80	0.04	0.86	0.07	0.55	0.31
8	1.06	0.06	1.12	0.07	1.02	0.08
9	1.08	0.07	1.08	0.11	1.22	0.24
10	1.00	0.24	0.88	0.16	1.00	0.37
11	0.90	0.18	0.97	0.15	0.85	0.30
12	0.91	0.16	0.91	0.15	0.83	0.25

	2012	**2013**	**2014**	**2015**	**2016**
T2 Avg G_w		5654	2779		5809
G_w SD		986	361		1467
T2 Avg NBI		0.84	0.95		0.78
NBI SD		0.13	0.14		0.22
T2 Avg RR		$416	$(216)		$453
RR SD		$228	$87		$346

rel = relative, SD = standard deviation, T2 = Tier II

Table 2.14: Troy Tier II relative crop performance site summary.

Site #	$Yield_{rel}$	$Yield_{rel}$ SD	NBI_{rel}	NBI_{rel} SD	RR_{rel}	RR_{rel} SD
1	1.21	0.01	1.06	0.25	1.25	0.03
2	1.06	0.32	1.04	0.26	1.04	0.41
3	1.04	0.04	0.97	0.09	1.01	0.06
4	0.75	0.22	0.66	0.08	0.49	0.37
5	0.79	0.08	0.85	0.21	0.60	0.25
6	1.08	0.17	1.17	0.16	1.07	0.16
7	1.13	0.39	1.23	0.19	1.15	0.52
8	1.15	0.11	1.02	0.16	1.15	0.08
9	0.95	0.00	0.99	0.18	0.86	0.13
10	1.32	0.11	1.17	0.15	1.42	0.07
11	1.08	0.10	1.20	0.25	1.08	0.28
12	0.96	0.00	0.84	0.06	0.88	0.13

	2012	**2013**	**2014**	**2015**	**2016**
T2 Avg G_w		6759		6307	
G_w SD		951		1468	
T2 Avg NBI		0.92		0.67	
NBI SD		0.16		0.16	
T2 Avg RR		$808		$737	
RR SD		$275		$478	

rel = relative, SD = standard deviation, T2 = Tier II

CHAPTER 3: POST HARVEST SPATIAL EVALUATION OF NITROGEN USE VARIABILITY

INTRODUCTION

Field scale optimization of fertilizer rates to meet the desired outputs (i.e. yields and appropriate protein content) has proven to be difficult due to the inherent heterogeneity and complexity of agricultural systems (Huggins et al., 2010) and has resulted in equally heterogeneous fertilizer management practices. Current regional fertilizer management guides are based on point scale management and sampling (Mahler et al., 1985) and do not integrate economic metrics with minimal post-harvest evaluation techniques. Global agricultural assessments suggest integrated and multi-disciplinary approaches to management and evaluation will be critical for future agriculture (McBratney et al., 2005, Zhang et al.,.2002, Johnson et al., 2000). Precision agriculture and global positioning system (GPS) has the capacity to integrate field scale data with economic and environmental factors to assess current agriculture practices.

As the highest variable rate cost per season for dryland agriculture (Painter,2016), management strategies for nitrogen fertilizers necessitate integrated approaches for field-scale evaluation. Several studies have indicated that surfeit nutrients from agricultural systems are a driving factor of chronic and acute environmental degradation (Chen et al., 2011, 2014, 2015, Fuentes et. al., 2003, Brye et. al., 2001, Zhao et. al., 2006) resulting in environmental dilapidation, increased human health risks (Knobeloch et al., 2000) and losses in agricultural productivity (Jennings, 1990, Legg & Meisinger, 1982, Mahler et al., 1985, Bezdicek et al., 2003). Studies have demonstrated meaningful evaluation of crop performance through metrics such as the nitrogen balance index (Taylor, 2016, Glover, 2018), classification schemes (Brown, 2015, Huggins et al., 1993, 2003, 2010b, Kaur et al., 2017) and economic analysis through returns to risk (Ward, 2018) metrics. These metrics applied at various scales have been highly effective at evaluating management zones and assessing nitrogen use efficiency. The integration of agricultural systems with global positioning systems (GPS) technology provides readily available data for spatially explicit nitrogen evaluation at larger spatial scales. Combines, seeders and other managerial implements guided through GPS reduce labor costs, provide greater control over management and minimize costly overlap during pesticide and fertilizer applications. The pairing of satellite data with crop performance metrics into spatially explicit maps could provide site-specific and spatially explicit evaluation strategies for fertilizer management.

Vegetative indices using spectral reflectance of light has been correlated with spatial patterns in cropping patterns (Magney et al., 2015, Mulla et al., 2013, Goez et al., 1985). Vegetative indices such as normalized difference red-edge index (NDRE) using the red-edge (690-730 nm) and green (520-590 nm) wavelength reflectance are highly correlated leaf chlorophyll content estimations (Mulla et al., 2013, Magney et al., 2015, 2016, Shang et al., 2015, Carter, 1994). Many satellite constellations have been launched with various spectral, spatial and temporal resolutions. Multispectral satellite imagery which captures light reflectance from red edge wavelengths and has high temporal (~10 days) and spatial resolutions (~5 m), such as RapidEye™, is ideal for agricultural purposes (Mulla, 2013). High spatial resolution allows crop response variability to be explicitly captured and high temporal resolution allows captured data to represent time sensitive crop properties such as peak biomass. Magney et al. (2015, 2016) demonstrated a strong linear relationship ($R^2 = 0.8$) between the NDRE vegetation index and N content in the total aboveground biomass of winter wheat crops in the Palouse region using reflectance from the red (630-685nm) and red-edge (690-730nm) bands (Blackbridge, 2016) from the RapidEye™ constellation. Since N crop concentration varies with growth stage, Magney et al. (2015, 2016) determined that early June images produced the best relationships correlating peak greenness (i.e. maximum leaf area index) with end of season N crop content. The relationship demonstrates broad regional applications for N efficiency evaluation through to the regionally stable NHI (Glover, 2018). Satellite imagery provides a useful platform for integrated approaches to evaluating economic and biological impacts of nitrogen application.

Dryland agriculture faces several unique environmental and financial factors affecting efficient use of fertilizers. In the Palouse region, yield can exhibit extreme spatial variability due to differences in climate, soil characteristics and topography (Huggins et al., 2010b, Fiez et al., 1995, Baker et al., 2004, Fuentes et al., 2003). Nitrogen management practices are further complicated due to the existence of high temporal variability in crop productivity. Although precision agriculture practices seek to mitigate N losses (Ward et al., 2017, Basso et al. 2010, 2011; Peng et al. 2010), adoption of precision agriculture is not widespread in the inland Pacific Northwest (Ward et al., 2017). Integration of effective evaluation metrics, current production technologies and satellite imagery would demonstrate the value of adapting PA and enable more informed crop sampling and adaptive management decisions.

The goal of this study was to develop and assess an integrated, regional, field-scale spatial mapping approach for evaluating crop performance and nitrogen fertilizer management strategies in the wheat-based cropping systems of the Palouse region.

OBJECTIVES

1. Assess the relationships between satellite derived NDRE, N_t and N_g in wheat crops across the region
2. Classify crop performance using nitrogen balance index (NBI) and profitability maps over multiple year and wheat classes.
3. Interpret the spatial variability in crop performance by identifying the key soil, topographic and climatic factors driving these spatial patterns

SITE DESCRIPTION

The Palouse region (~9000 km^2 (Brooks et al., 2012)) is located in inland Pacific Northwest and are geologically central in the region's paleosol loess deposits (McCool and Busacca, 1999). The fine-grained loess hills (Busacca and McDonald, 1994) were deposited atop Miocene flood basalts during the Pliestocene epoch (Gaylord et al., 2003). The origin of the undulating, silty topography has been highly disputed; however, the characteristically steep northern slopes are believed to be the result of seasonal snow melt and mass wasting patterns (Gaylord et al., 2003, Brooks et al., 2012).

The Palouse region is subject to high variability (McDaniel and Hipple, 2010) in topography, temperature, soils and precipitation. The variable topography of the region characteristically has a steep west to east temperature and precipitation gradient spanning 35mm to 1450mm of annual rainfall (Figure 3.1) (Brooks et al., 2012). The xeric climatic patterns of the region are characterized by winter dominated precipitation with 70% occurring between November and May and intense drought and heat stress during the summer months (Brooks et al., 2012). The soil surveys indicate a clear south-westerly gradient of particle size with the coarsest materials residing in the lower western regions. This gradation of particle sizes and precipitation developed a gradient of soil horizons. Westerly soils with limited precipitation (<400mm) and relatively coarse particle sizes are classified as Haploxerolls due to the limited leaching and absence of restrictive horizons (Donaldson, 1980; Busacca, 1989). In the moderate precipitation range (~450-700mm) the soils are classified as

Argixerolls with root restricting layers (1.65 g/cm^3) and argillic (B_t) horizons between 0.2m to 1.3m (Maaz et al., 2017, “Soil Bulk Density,” n.d.). The wettest regions (>700mm) and finest particle sizes soils are classified as Fragixeralf soils with brittle fragipan horizons due to hydrologically driven movement of clay materials (Donaldson, 1980, Barker, 1981, Busacca, 1989, Soil Survey Staff, 2006).

In general, there are two management systems in the Palouse Region: the annual cropping zone for the wetter and cooler eastern region (450-600mm) and the two-year grain-fallow cropping zone in the warmer western regions (<330mm) (Pan et al., 2016). Cropping rotations in this region vary. The farms in this study had 2 and 3-year rotations all containing winter wheat.

Four growers in the annual cropping region were selected to represent the range in major soils, topographies and climates within the annual cropping zone. The four sites chosen for this analysis were located in Colfax, WA (Figure 3.2), Genesee, ID (Figure 3.3), Leland, ID (Figure 3.4) and Troy, ID (Figure 3.5). Topography ranged greatly at the locations with maximum percent slope (spatial resolution 30 m^2 interpolated to 10 m^2) being 45% at Colfax, 36% at Genesee, 32% at Troy and (spatial resolution 5 m^2 for Tier II site) 18% at Leland. Annual precipitation in the sample locations ranged 379 mm in 2014 at Colfax to 652 mm in 2016 at Troy; see Tables 3.1-3.4 for more detailed management and field summaries for each location.

Two catchments were identified within a field at each farm. One of these catchments was selected for intensive automated and manual monitoring (Brown et al., 2011) and will be referred to as Tier II sites. Each Tier II site was equipped with twelve spatially representative subsites (Figures 3.2-3.5) which served as the primary sampling locations within the catchment. The other catchment and related subsites (Tier III sites) were reserved for crop harvest validation purposes and were monitored over the last two years (2015-2016) of the project.

METHODS

GENERAL

Four locations (Colfax, Genesee, Leland and Troy) in the high rainfall zone of the Palouse region were selected for automated and manual in-situ measurements. Two watersheds (Tier II and Tier III) at each location were chosen for monitoring with spatially representative subsites. The Tier II watersheds were extensively monitored over the 5-year study period. The Tier III watersheds were only monitored the last two years of the study and primarily used for validation purposes. The 12 subsite locations in each watershed were selected as discussed in Ward et al. (2017) using topographic and soil attributes to capture variability in water and crop yield. At each location, hourly precipitation was measured using a tipping bucket rain gauge with a siphoning snowfall adapter (Campbell Scientific Inc.) and a windscreen (Sutron Corporation). Gaps in the weather data were filled using other weather sources and interpolated to field site location (Yourek, 2016).

The analysis included the four major tasks. First, evaluating regional and crop specific relationships between RapidEye^{TM} satellite imagery based NDRE and crop N content [kg/ha] (i.e. grain N (N_g) and N content in the total aboveground biomass (N_t = (N_g + N_{res}), N_{res} = nitrogen content of aboveground residue) using hand-harvested plot data. A temporal analysis using accumulated growing degree days (GDD) was conducted to identify the optimal time to acquire field-based imagery which best describes field scale variability in N_t.

Secondly, an analysis of the relationship between N content in the total aboveground biomass and grain for multiple crops across the region was performed. Specifically, the nitrogen harvest index (N_g/ N_t) (Huggins et al. 2010b) was evaluated at 6 locations within the Palouse region to investigate how well grain N content could be estimated using N_t derived from relationships with NDRE in satellite imagery.

Third, conduct a field-scale post-harvest evaluation of crop performance by using satellite imagery and nitrogen uptake maps through three diverse metrics namely 1) the nitrogen balance index (NBI), returns to risk (RR) [$/ha] an economic metric and 3) a classification metric weighing quality requirements. The evaluation was performed on multiple wheat classes and multiple locations within the annual cropping region of the Palouse.

Fourth, a synthesis of field and regional scale patterns of temporal and spatial persistence in crop performance was conducted. An exploratory spatial analysis relating NDRE with soil, topographic and climatic factors (e.g. apparent soil electrical conductivity, equivalent precipitation, topographic wetness index) was conducted to provide insight on the challenges of maintaining optimal crop performance throughout complex fields.

NDRE AND CROP N CONTENT RELATIONSHIP EVALUATION

The relationship between NDRE imagery and N_t was established using hand-harvested plot data from each field site during 2012-2016. Each year, four 1 square meter aboveground biomass samples were hand harvested for each Tier II subsite. The total aboveground biomass weight of all four 1 square meter plots was recorded after drying. Total yield (i.e. grain weight G_w) was recorded after the dried biomass samples were threshed using a stationary plot combine. Grain protein concentration (GPC) and moisture content were measured with near infrared reflectance using an Infratec 1241 Grain Analyzer (FOSS™). Grain N (N_g) [kg/ha] was calculated using:

$$N_g[kg/ha] = \frac{GPC\ [\%]}{5.7} * \frac{Wet\ G_w\ [kg/ha]}{100} \tag{3.1}$$

A subsample of threshed crop residue was ground (0.1mm) and analyzed for N concentration with a TruSpec™ (LECO Corp.) through dry combustion and gas chromatography and calculated using:

$$N_{res}[kg/ha\ ] = N\ [\%] * \frac{(biomass[g]-grain[g])}{4[m^2]} * 10\frac{[m^2*kg]}{[g*ha]} \tag{3.2}$$

Three to five RapidEye™ summer images for each growing season (2012-2016) were obtained Blackbridge™ and were atmospherically corrected using a 6S radiative transfer model (Kotchenova et al., 2006, Vermote & Kotchenova, 2007) and run as a module within GRASS v6.3 (GRASS Development Team), as in Yourek (2016). These images were orthorectified with sensor calibration, geometric and terrain corrections.

The RapidEye™ constellation by BlackBridge™ has a spatial resolution sample size at a 6.5m resolution (orthorectification 5m pixels) with a temporal return interval of ~5.5 days and therefore is optimally suited for precision agricultural inquiry. The RapidEye™ constellation collects data in five spectral bands: blue (440-510 nm), green (520- 590 nm), red (630-685 nm), red-edge (690-730 nm) and near-infrared (760-850 nm). These wavelengths were used to calculate the normalized difference red edge (NDRE) vegetation index.

$$NDRE = \frac{NearIR-Red\ Edge}{NearIR+\ Red\ Edge} \tag{3.3}$$

The NDRE value for each Tier II subsite was extracted from 3 to 5 summer images acquired between May and August depending on availability and cloud cover (Appendix 2.A). The root-mean squared error (RMSE) and R-squared (R^2) between the NDRE at each subsite and the hand-harvested plot N_t

for the specific year were used to indicate overall explanatory power of each specific image. For each image the ratio of R^2/RMSE was determined by field and plotted versus growing degree day (GDD).

$$GDD = \frac{T_{max} - T_{min}}{2} - T_b \tag{3.4}$$

where T_{max} and T_{min} represent the maximum and minimum daily temperatures (°C) derived from average hourly temperatures. T_b represents the base temperature (0°C for winter wheat (Baker et al. 1986) and 2.6°C for spring wheat (Campbell et al., 2012)) (Appendix 2.B). Days with T_{min} below T_b and T_{max} exceeding 37°C (98.6°F) (Porter & Gawith, 1999) were set equal to 0. The temporal trend was evaluated by crop type to identify the crop growth stage in terms of an optimal degree day range where NDRE images have the greatest correlation to N_t.

The relationships between NDRE and crop N content (N_t and N_g) were determined using linear regression in the R v3.3.1 using the ggplot2 package. The optimal relationships between NDRE and N_g was based on the minimum root mean squared error (RMSE). Tier II data was used to construct the linear model and the Tier III data was used to validate model accuracy. Additional factors such as season (winter vs spring), class (hard red vs soft white), year and precipitation (surrogate for location) were also evaluated in R to determine if they provide additional explanatory power.

N HARVEST INDEX EVALUATION

The relationship between N_t and N_g was evaluated in terms of the NHI (N_g/N_t). The stability of the NHI for both spring and winter wheat was determined from hand harvested data collected 6 diverse locations (Colfax, WA; Davenport, WA; Genesee, ID; Leland, ID, Pullman, WA; Troy, ID) across the Palouse. These data include the hand harvested plots in the four field sites in this study as well as two others described by Maaz et al. (2017). ANOVA, f-test, t-test and z-test statistics were used to determine whether there is a significant difference in the NHI for spring wheat and winter wheat.

FIELD-SCALE POST-HARVEST EVALUATION OF THREE CROP PERFORMANCE METRICS

N Efficiency Metric – N Balance Index

Although there are numerous approaches to quantify nitrogen use efficiency (see Huggins et al. (2010); Huggins et al. (1993)) in this study we use the nitrogen uptake efficiency and the nitrogen balance index as metrics to quantify how efficiently applied nitrogen fertilizer is being used and assimilated by the crop following the approach of Taylor (2016).

Total soil nitrogen (TN) and carbon (TC) concentration samples were collected in fall 2011 and 2012 TruSpec™ analyzer and averaged by depth. Nitrogen mineralization (N_m) rates [kg/ha] for each subsite were determined from 30 cm total nitrogen soil samples using the following equation, bulk density for the top 30 cm and an assumed 1% turnover rate.

$$N_m \left[\frac{kg}{ha}\right] = BD \left[\frac{g}{cm^3}\right] * 30\ [cm\ depth] * 1000 \left[\frac{cm^2 * kg}{g * ha}\right] * \frac{total\ N\ [\%]}{100} * 0.01 \tag{3.5}$$

Nitrogen uptake efficiency is defined by the following equation:

$$N_{uptake}\ efficiency = \frac{N_t}{N_s} \tag{3.6}$$

where N_s is the nitrogen supply ($N_f + N_p + N_m$) [kg/ha] where N_f is the prescribed nitrogen fertilizer [kg/ha], N_p is the pre-plant soil inorganic nitrogen [kg/ha]. N uptake efficiency quantifies the amount of N is allocated to the total aboveground biomass relative to the total applied and available N over the growing season. The mass balance approach requires extensive and expensive soil and crop sampling, making this method costly although effective. However, the NBI has been suggested as a simplification (Huggins et al., 2010; Taylor, 2016, Glover, 2018) and approximation for N uptake efficiency. The approximation assumes the main drivers influencing spatial variability in crop N uptake are the grain N content and the amount of applied fertilizer. The nitrogen balance index is defined by the following equation:

$$NBI = \frac{N_g}{N_f} \tag{3.7}$$

where N_f is the total seasonal applied nitrogen fertilizer [kg/ha]. If grain N can be effectively determined through satellite imagery, the NBI would serve as a powerful tool in spatial evaluation of field-scale N efficiency.

Crop Performance Classification

Each field was classified using a dichotomous key into distinct performance classes (PC) based on NBI and yield (Figure 3.6). The NBI was calculated using the N_g maps determined from the RapidEye™ satellite imagery and fertilizer maps. We defined an acceptable NBI to be any value greater than 0.8. A NBI value of 0.8 has been shown to correspond to a nitrogen uptake efficiency of 50% (see Chapter 2). Obtaining 50% nitrogen uptake efficiency is critical as it is often inherently assumed in regional fertilizer guides when calculating fertilizer application rates. County wide 10-year average crop yield was used as the yield threshold for classifying the field into low yielding and high yielding regions (WW = 5375 [kg/ha] (80 [bu/ac]), SW = 4031 [kg/ha] (60 [bu/ac])).

Economic Metric – Returns to Risk

Spatially explicit returns to risk maps were created using crop yield and nitrogen fertilizer maps along with crop and fertilizer prices and operating expenses for each grower. The returns to risk was calculated using the following equation:

$$RR\ [\$/kg] = G_w\ [kg/ha] * P_c\ [\$/ha] - \left(P_p\ [\$/ha] + \left(P_N\ [\$/kg] *\ N_f\ [kg/ha]\right)\right) \tag{3.8}$$

where G_w is the grain yield, P_c is the price of the crop, P_p is the estimated cost of production without nitrogen fertilizer costs, P_N is the price of nitrogen fertilizer (Table 3.5) and N_f is the amount of nitrogen fertilizer applied. Due to the yearly variability of these costs, $P_{c,}$ P_p and P_N values were estimated using 5-year averages (2011-2016) in the Palouse region (Kate Painter 5-year summary releases). Protein level premiums and discounts were not included. A five-year average would be representative of both the study period and dampen any yearly anomalies. The grain yield and fertilizer application rates were based on yield and prescription fertilizer application maps provided by the growers.

Economic Metric: A Sensitivity Test

A case study of the yield data at Troy in 2015 was conducted to determine the sensitivity of the returns to risk metric to different data sources. Yield was calculated from NDRE (Appendix 2.D), noninterpolated combine yield point data and interpolated yield combine point data kriged (spherical model) at a maximum distance of 30m using ArcMap (10.4.1). These yield data were used along with spatially explicit prescription fertilizer maps to calculate RR.

SPATIAL TRENDS IN CROP PERFORMANCE

A spatial analysis was performed for the Tier II watersheds using linear regression to identify the primary factors driving field-scale variability in crop N uptake. The three to four most correlated and resulting in the highest R squared were identified for each year. NDRE was used as a surrogate of N_g and was correlated and evaluated against soil, topographic and climatic maps including: soil depth, effective precipitation (Peq), evapotranspiration (ET), ET/Peq ratio, apparent soil electrical conductivity (fall and spring), percent rise (slope), cross sectional curvature, longitudinal curvature, relative elevation, aspect, topographic wetness index (TWI), percent clay (where available, average of first 1.5m), solar radiation and average bulk density (average of first 1.5m). Linear modeling and correlation was conducted using R v3.3.1 using the following packages: geoR, rgdal, nlme, raster, stats and corrplot.

A 5m digital elevation model (DEM) was created from a real time kinematic (RTK) based GPS survey for the Tier II Leland watershed due to the relatively small topographic variability in the landscape; all other DEMs were sourced from United States Geological Survey (USGS) National Elevation Dataset (NED) (30 m^2 resolution extrapolated to 10 m^2). Calculations pertaining to elevation were farm specific. The following topographic parameters were calculated based on the DEMs described above using ESRI™ ArcMap software: aspect, slope (percent rise) and annual solar radiation. Topographic wetness index (Beven and Kirkby, 1979), longitudinal curvature and cross-sectional curvature were calculated using the DEMs described previously and using SAGA Inc. open source software (Conrad et al., 2015). Tier II maps of equivalent precipitation (P_{eq}), evapotranspiration (ET) and P_{eq}/ET ratio were all created as using the modified Soil Moisture Routing model (Yourek, 2016). See Yourek (2016) for a full assessment of this spatially hydrology model at each of these field locations. Tier II soil depth and apparent electrical conductivity (EC_a) maps were created as described in Poggio et al. (2015) and Gasch et al. (2015).

RESULTS

NDRE AND CROP PERFORMANCE RELATIONSHIP EVALUATION

A regression analysis between NDRE (calculated from satellite imagery acquired on optimal acquisition dates) and N_g (determined from hand plots at each field) resulted in the following regional relationship (R^2=0.59):

$$N_{g_{kg/\mathrm{ha}}} = 312.9 * NDRE - 35.0 * Variety{:}SoftWhite - 51.4 \qquad (3.9)$$

RMSE = 28.1 [kg/ha]

A statistical analysis was also performed to determine whether adding additional factors such as year, season (winter vs spring) and precipitation would improve the predictive power of this regional relationship. Class and year proved to be the only significant factors compared to NDRE (Table 3.7).

Since the additional predictive power from having unique relationships for each individual year was minimal compared to general regional models for soft white and hard red wheat for all years (R^2 dropping from 0.61 to 0.59 and RMSE dropping from 28.3.3 to 28.1 [kg/ha] for the general model in Equation 3.9,) a generalized regional model rather than a year-specific model was used for this analysis (Appendix 2.C, Table A2.C-1, A2.C-2).

The correlation between NDRE and N_g and N_t varied with crop growth stage and acquisition time of the imagery (Appendix 2.A). The analysis suggested that N_g may have a stronger relationship to NDRE than N_t (Appendix 2.C, Table A2.C-1, A2.C-2). These relationships were somewhat class and location specific. The optimal number of growing degree days required to ensure maximum correlation with grain nitrogen content was relatively consistent at each farm site but regionally there was a broader range of GDD (see Figure 3.7 and Appendix 2.A).

Regional scale peak greenness (i.e. highest NDRE) for spring wheat was found to occur between 1300-1500 GDD and between ~800-1000 GDD for winter wheat. In general, images with the highest NDRE correlated best with N_g or N_t. In some cases, the best acquisition date for the farm N_g model was a week or two different from the optimum date for a consistent regional N_g model. Final dates chosen for all subsequent analysis can be found in Appendix 2.B (Table A2.B-1).

The relationship between NDRE and other crop performance metrics (grain protein concentration & crop yield) was also evaluated. The relationship between NDRE and G_w was stronger than that (R^2 = 0.63) of N_g or N_t (Appendix 2.D). Although there is a great need for spatially explicit GPC maps to better classification schemes and quality requirements, no relationship existed between NDRE and GPC (Appendix 2E).

N HARVEST INDEX EVALUATION

Harvest data were gathered from around the region (the four study sites in this study as well as Davenport and Pullman locations as discussed in Maaz et al., 2017) to evaluate regional NHI.

The data indicate that the N_g and N_t relationship is regionally stable but significantly different between spring and winter wheat (Appendix 2.C, Table A2.C-1). Wheat class was only statistically significant within spring and winter wheat groupings (Appendix 2.C, Tables A2.C-3, A2.C-4). The NHI for spring wheat averaged 0.81 and winter wheat averaged 0.78 (Table 3.6, Equations 3.10 & 3.11) with very small standard deviations.

For spring wheat:

$$N_t = \frac{N_g}{0.81} \tag{3.10}$$

For winter wheat:

$$N_t = \frac{N_g}{0.78} \tag{3.11}$$

FIELD-SCALE POST-HARVEST EVALUATION OF THREE CROP PERFORMANCE METRICS

The overall performance of the crop as indicated by the NBI, returns to risk mapping and performance class analysis varied widely within each field and between each grower. Mapped NBI derived from the modeled N_g and fertilizer maps ranged between 0.1 – 4.8 indicating a broad range of NBI response spatially (Table 3.9). Spring wheat generally did not perform well over the study period. The majority of the Colfax field consistently did not achieve nitrogen uptake efficiency of 50% (NBI < 0.8) when growing spring wheat (Appendix 2.G, Figure A2.G-1). Over 45% of the Troy field did not achieve NBI of 0.8 in 2013, however, in 2015 the grower managing the Troy field modified his fertilizer management strategy where over 75% of the field achieved and/or exceeded NBI of 0.8 (Table 3.9). Zones were redrawn (more zones added) with reduced fertilizer rates as well as reductions in foliar and starter applications. Some areas were reduced by as much as 44.8 [kg/ha] (40 [lb/ac]). Low rate zones (22.4 [kg/ha], 20 [lb/ac]) were eliminated and replaced with mid-range zones. Despite the majority of the field (54%) being Class 1, a large section of the field (19%) was still rated as Class 4, the poorest performance class (Table 3.10, Figure 3.8). Class 4 areas tended to be located in the draws and in a specific fertilizer zone. The largest percentage of the field was netting >$300/ac (Table 3.11) and the largest financial losses tended to be located in the same areas that were classified as performance class (PC) 4.

The overall field average crop performance at the Leland field varied widely from one year to the next over the three cropping seasons evaluated. The majority of the field was rated as PC 1 or PC 2 during the soft white winter wheat cropping years, however, in 2014 (SWSW) crop performance was particularly poor with 80% of the field rated as PC 3 or 4 (Table 3.9, Appendix 2.G, Figure A2.G-3). The returns to risk indicated negative returns (i.e. overall loss of money) in more than 60% of the field area. This is in stark contrast to the two years with winter wheat where over 90% of the field showed positive economic returns (Table 3.11, Appendix 2.H).

Similar to the Leland field site, spring crops performed poorly at the Colfax fields sites. In 2013 and 2014 over 74% of the field had a NBI less than 0.8 and 13% had a NBI less than 0.4 (N uptake efficiency <25%). Although the NBI improved for the winter wheat crops, the NBI for 19-28% of the field remained below 0.8 in these years (Table 3.9). Although yield maps were not available for this field, hand harvested yield measurements at the 12 locations in the field indicated the grower lost an average of $851/ha in the north facing slopes of the spring wheat field (Table 3.12).

The spring wheat at Genesee had the most efficient use of nitrogen, according to the NBI, compared to other locations. Over 80% of the field had a NBI over 1.2 in 2016 with less than 3% of the field not meeting the NBI goal of 0.8. Unlike the HRSW, 39% of the field for the 2015 SWWW did not meet the 0.8 NBI goal. (Table 3.9, Appendix 2.G, Figure A2.G-1). In 2012 nitrogen uptake goals at Genesee were consistently met at all evaluation points but not necessarily crop yield goals (yield ≥ [90 kg/ha]). Over 60% of the Genesee field in 2012 showed profits of $300/ha or greater.

SPATIAL PATTERNS IN CROP PERFORMANCE

Linear regression and correlation analysis was conducted to evaluate the factors associated with N_g variability at the field scale. Since NDRE and N_g are directly related (Equations 3.9, Appendix 2.C) the analysis essentially examined factors driving spatial variability in NDRE. Table 3.8 indicate the primary factors which best describe spatial variability in NDRE (i.e. N_g) at each of the field sites as determined by linear regression analysis (Appendix 2.F). Although the top explanatory factors varied across the field sites, there were a few consistent predominant factors across each of the field sites. Apart from Leland, fall soil apparent EC (largely representing spatial variability in soil texture) was consistently one of the top driving factors (Appendix 2.F, Figure A2.F-3). There were no clear explanatory factors at the Leland field with regression R^2 values all less than 0.28. For all sites, the relationships with the most explanatory power generally included a topographic attribute such as longitudinal curvature or topographic wetness index in addition to fall apparent soil EC. The analysis indicated that both fall and spring apparent soil EC provided unique and significant predictive power particularly for the Genesee and Colfax field sites. The data suggest that the primary explanatory factors are consistent across years for the same crops. For example, fall and spring apparent EC were primary explanatory factors for all spring wheat crops at Genesee and Colfax but not necessarily for the winter wheat.

At all field sites the spatial NDRE pattern was relatively consistent across all years. The correlation between NDRE maps for the same location ranged from 0.25 to 0.81 (Appendix 2.F). When incorporated into the linear regression analysis the NDRE patterns from prior years were the best predictors for NDRE variability for the current year. Statistical tests (t-test) indicate that the NDRE patterns of the same wheat crop (e.g. SWWW year 1 to SWWW year 4) were more correlated to each other than to patterns of other wheat crops (e.g. SWSW year 2 to SWWW year 4) (P(T<=t) one-tail = 97%). In some cases, adding prior year NDRE map doubled the prediction power of the regression model. For example, when evaluating the 2016 Genesee model (NDRE~ Spring EC_a + Fall EC_a + solar radiation), the addition of the 2012 NDRE values (HRSW) increased the R^2 to 0.78, whereas the 2015 NDRE values (SWWW) only increased the R^2 to 0.60. Adding both years to the model resulted in the best model with an R^2 of 0.79. It is evident the majority of the prediction power stemmed from the 2012 NDRE values with the same crop rather than the 2015 SWWW. However, where prediction power was low, such as the Leland farm, the differences in crop type were minimal. NDRE patterns from the previous years had more predictive power than any other factor evaluated at the Leland farm.

DISCUSSION

NDRE AND CROP N CONTENT RELATIONSHIP EVALUATION

Crop Class NHI Implications

The stability of nitrogen harvest index in this region allows satellite imagery to effectively measure crop nitrogen uptake later in the season. The direct relationship of N_t to N_g allows early summer images of crop biomass to directly relate to end of season nitrogen content when reflectance variability is low. The higher N_t of winter wheat relative to spring wheat may be due to longer growth periods allowing for more total N uptake and more non-grain biomass production resulting in a lower NHI than their spring counterparts. Additionally, generally higher yields in winter wheat would result in lower relative values. The higher NHI of spring wheat may suggest that spring wheat are more efficient at allocating N to the grain, less N is needed in biomass production (e.g. tillering) compared to winter wheat and/or phenological differences in winter and spring wheat allow for timely uptake of N for protein rather than carbohydrate synthesis. Remotely measuring N content enables post-harvest evaluation to be conducted on N efficiency through metrics such as the nitrogen balance index (NBI).

Date Selection

Seasonally dynamic crop performance patterns make date selection for satellite imagery difficult. Choosing satellite images solely based on correlation with N_g or N_t was inconsistent at producing representative data for measuring peak biomass. Some dates with the highest correlation to N_g were during early senescence where NDRE variability was low and therefore, not providing a useful image for evaluation purposes. Some years peak biomass was not totally captured due to cloud cover and/or satellite return periods (Appendix 2.A, Figure A2.A-3). Additionally, various areas of the fields reached peak biomass at different time periods therefore, a given image did not capture peak biomass for the entire field. Evaluating farm specific curves weighing NDRE and GDD over several summer images will produce the best results in choosing an appropriate image for evaluation (Appendix 2.A, Figures A2.A-1 to A2.A-6). Since there are consistencies at the farm scale, a date chosen by peak NDRE and/or a given GDD still produced good local results. The rule of thumb estimates (spring wheat ~1300-1500 GDD; winter wheat ~800-1000 GDD) are viable estimates for peak biomass in the Palouse region. The discrepancies in these various methods for date selection demonstrate some of the limitations of satellite-based evaluation. Evaluation should be based on multiple years of data to compensate for inherent errors and seasonally dynamic crop patterns.

FIELD-SCALE POST-HARVEST EVALUATION OF CROP PERFORMANCE

Using satellite images to identify temporal persistence of crop performance patterns provides an opportunity to evaluate management strategies on a yearly basis using integrative evaluation metrics such as the nitrogen balance index (Chapter 2), classification schemes and returns to risk financial analysis. In the following section we provide an evaluation of the management strategies employed at each of the field sites using these integrative spatial metrics.

Colfax: Demonstrates Inefficiency

The 4-year crop performance analysis of the Colfax field site suggests that there would be clear benefits for adopting variable rate fertilizer strategies. The NBI mapping indicates there is a clear temporally stable pattern with the spring wheat crops whereas winter wheat crops do not exhibit as consistent or extreme variability (Appendix 2.G). The spatial variability in NBI in the Colfax field is closely related to topographic position and water availability. The draws and summits were the most productive while clay knobs and slopes were less productive. These spatial patterns were relatively stable during the study period; however, additional crop years would help determine the relative temporal stability in crop performance particularly for winter crops. The wide variability in NBI and profitability is likely due to the currently employed uniform fertilizer application strategy. The relative success of the winter crops seems to compensate for the inefficiencies and economic losses recorded with the spring crops. A longer assessment may provide greater insight into whether spring wheat is an appropriate crop for this arid region. The grower has historically employed summer fallow strategies on his farm. Spring wheat would benefit from lower N rates and more targeted rates on the slopes and clay knobs (Huggins et al., 2010 A). Winter wheat would benefit from lower N rates on the hillsides and draw locations could potentially benefit from higher N rates depending on water availability. Colfax is an example of a farm that would greatly benefit from implementing these metrics and using the spatial data to delineate stable management zones.

Genesee: Demonstrates an Upper Limit

The crop efficiency metrics at Genesee indicate N uptake requirements have been fitted well for spring cultivars and are achieving high yields with minimal N application; however, winter cultivars may have room for adjustment. The extreme differences in nitrogen balance index between spring and winter wheat may be due to class or environmental factors. The NHI suggests that more N is allocated to biomass growth for winter wheat having a lower N_g to N_t ratio and consequently an inherently lower NBI. One year of winter wheat analysis limits the findings of this field. However, inefficiencies can be seen consistently in the same N fertilizer rate zones which may suggest lowering rates would be advantageous. A multiple year analysis for each class would better indicate stable temporal patterns for nitrogen efficiency. The findings from this study may be favorable to this field because the fertilizer zones are already based on satellite imagery patterns. Therefore, the zone correlation and efficiency analysis may be favorable to this field because similar data sources are used in both cases. Genesee demonstrates that these metrics can be used for even the most efficient of locations to better improve site specific management strategies.

Leland: Demonstrates the Need for Multiple Metrics

The Leland field site represents a site where the spatial variability may be too small and temporal variability too great to confidently alter current fertilizer management strategies. The Leland field was hard hit from the 2014 drought. Although the nitrogen efficiency was high in 2014 (Figure 3.1, Table 3.9, Appendix 2.G), it was largely due to the high protein concentrations found in the crop and the entire field lost money in 2014 year. The subsequent inefficiency (80% of the field with NBI < 0.8) the following year suggests that perhaps some management practices should have been adjusted to account for the low yields resulting in 2014 and therefore, a fair amount of unutilized N in the soil. Leland demonstrates the limitations of the evaluating crop performance based on the nitrogen balance index alone because the nitrogen efficiency map is misleading without availability of profitability and/or yield maps (Figure 3.9). Comparing the nitrogen balance index and the returns to risk maps in Figure 3.9 (Appendix 2.H) demonstrates the power of using multiple applications of production metrics to make informed management decisions. It is evident that the current fertilizer zones may be too complex for the crop response. The extreme crop loss seen in 2014 may serve as a general guideline for the most extreme responses in crop performance and help delineate simpler zones that may streamline management. In general, the crops are responding well to current nitrogen practices. The Leland field demonstrates the need for multiple metrics when assessing N efficiency and that some climates and landscapes may be too homogenous for satellite imagery to be an effective post-harvest evaluation technique.

Troy: Demonstrates Improvement

The crop efficiency metrics indicate that the Troy location responded well to adjustments in N fertilizer rates and subsequently more efficient N use. Management adjustments seen between 2013 and 2015 had drastic effects on the NBI at the Troy field. In 2013, NBI zones coincided with fertilizer zones and lower rates in 2015 resulted in a higher NBI while yields were relatively similar (Table 3.9). These patterns may also suggest lowering the fall nitrogen application due to the high water movement during the winter months would improve NBI. The draw regions also had the greatest standing water throughout the growing season and subsequently could be subject to anoxic growing conditions. Expansion of the current buffer strip (currently located in the main draw) or integration of a tile line may be useful to make the draws more productive and/or manage anoxic growing conditions. Fertilizer zones could be improved with more precise fertilizer applicators; however, there are currently there are not substantial economic incentives since the majority of the field makes well over $600/ha according to the RR metric (Figure 3.10). A long-term analysis determining how stable the resultant PC 4 and low economic zones are, may provide insight into whether investment in more precise fertilizer applicator technologies would be profitable. The crop performance metrics at this location demonstrate that changes in management practices are able to be detected by this methodology and could be used to evaluate management efficacy.

Returns to Risk Error Case Study

Using exclusively satellite image data in calculating metrics such as returns to risk on spatial maps skews the data to not effectively represent poor production areas (Figure 3.11). When yield maps are not available due to equipment malfunctions or lack of sufficient equipment, it may be useful to calculate economics metrics using NDRE derived G_w. Using satellite based G_w data reduces the RR variability whereas, the combine point data had the highest variability (Figure 3.12). Using exclusively satellite derived data eliminates the low productivity areas and has less conservative estimates of losses. Use of satellite imagery as a G_w data source will need further research and potentially location specific models for areas with low productivity. Similar limitations on low productive areas may be seen in the grain N models. This case study demonstrates some of the limitations to using satellite data, namely that it simplifies the actual field variability. The most effective evaluation metrics at capturing field variability will use an amalgamation of satellite and combine based data to capture field-scale patterns. Calculating these metrics over several years will minimize year to year errors.

SPATIAL PATTERNS IN CROP PERFORMANCE

The most compelling evidence for substantiating the presence of consistent crop growth patterns is the high correlation between NDRE of a prior year to the current year. These data suggest that the previous year NDRE of the same crop (e.g. HRWW to HRWW) were better correlated than NDRE from other crops (e.g. HRSW to HRWW) implying that crop patterns are generally stable. Although NDRE is effective at capturing crop performance patterns, it does not explain the variability. The most consistent drivers of crop N variability in these data were soil texture (i.e. fall apparent electrical conductivity) and soil wetness patterns (i.e. spring apparent electrical conductivity). The Palouse region has a long history of extensive soil erosion (Brooks et al., 2012, Busacca et al., 1989, 1994, Gaylord et al., 2003) understanding the distribution of soil texture at a given field could have significant management implications. For example, if high clay content shoulder soils have been redistributed by soil erosion to rich draws, reducing tillage would prevent further soil texture alterations. Other studies have also found that soil depth and type are highly correlated with effective management zones (Peralta et al., 2015, Zhang et al., 2010). Additionally, other crop indices have correlated crop canopy to soil organic matter concentration (Wetterlind et al. 2008). Therefore, increasing organic matter to increase water holding capacity would be another method of increasing crop responses (Young et al, 2014). Persistent crop performance patterns captured by satellite imagery suggest variable rate and adaptive management practices have reliable economic and environmental benefits.

CONCLUSIONS

Evaluation of management strategies using high resolution satellite images can be a powerful and useful tool for growers to manage field-scale variability. Multi-year evaluation provides insight in the temporal stability of spatial patterns. Year to year and inter-farm variability eliminates a one size fits all answer for management practices, but these evaluation methodologies can help identify site-specific strategies. A regionally stable NHI grain N and yield can be accurately measured from satellite imagery during summer months. The best relationships were found for spring wheat between 1300-1500 GDD and winter wheat between ~800-1000 GDD. Grain protein concentration was too small to detect using satellite imagery. Inherent model error suggests that all mapping applications should be conducted over multiple years to establish the stability of the crop performance metrics. Using satellite derived grain N, the nitrogen balance index (NBI [N_g/N_f]) metric demonstrated that on average 47% of the fields were not achieving 50% N uptake efficiency and spring wheat tended not to perform well over the study period. The zones tended to be relatively stable between the years investigated and nitrogen content variability generally correlated well with fall apparent electrical conductivity (EC_a). Classification metrics indicated that on average only half of the fields are achieving both yield and 50% N uptake efficiency. Current classification schemes are limited to NBI and yields rather than including protein levels due to the limited availability of spatially explicit protein concentration data. Progress in combine mounted protein sensors and/or drone based technologies could provide the necessary imagery (Candiago et al., 2015) for classification schemes to include quality standards such as protein content. Financial metrics indicated that on average over 40% of fields are financially neutral or detrimental. These tend to be in areas of either very high or very low water availability. These metrics indicate there is a continued need for evaluation techniques that provide enough data to better understand field scale variability and decision responses. Satellite imagery may be difficult to adopt due to availability and processing requirements, however, effective evaluation techniques such as the NBI and classification schemes could be used with other remote sensing technologies such as drone or other combine mounted equipment.

REFERENCES

Baker, D. A., Young, D. L., Huggins, D. R., & Pan, W. L. (2004). Economically optimal nitrogen fertilization for yield and protein in hard red spring wheat. Agronomy Journal, 96(1), 116-123.

Barker, R. J. (1981). Soil survey of Latah County area, Idaho (No. 37-39). US Department of Agriculture, Soil Conservation Service.

Basso, B., Cammarano, D., Troccoli, A., Chen, D., & Ritchie, J. T. (2010). Long-term wheat response to nitrogen in a rainfed Mediterranean environment: Field data and simulation analysis. European Journal of Agronomy, 33(2), 132-138.

Basso, B., Ritchie, J. T., Cammarano, D., & Sartori, L. (2011). A strategic and tactical management approach to select optimal N fertilizer rates for wheat in a spatially variable field. European Journal of Agronomy, 35(4), 215-222.

Beven, K.J., Kirkby, M.J. (1979) A physically-based variable contributing area model of basin hydrology' Hydrology Science Bulletin 24(1), p.43-69.

Bezdicek, D. F., Beaver, T., & Granatstein, D. (2003). Subsoil ridge tillage and lime effects on soil microbial activity, soil pH, erosion, and wheat and pea yield in the Pacific Northwest, USA. Soil and Tillage Research, 74(1), 55–63.

Brooks, E. S., Boll, J., & McDaniel, P. A. (2012). Hydropedology in seasonally dry landscapes: the Palouse region of the Pacific Northwest USA. Hydropedology: Synergistic Integration of Soil Science and Hydrology, 329.

Brown, D. J., Brooks, E. S., Eitel, J., Huggins, D. R., Painter, K., Rupp, R., ... & Vierling, L. A. (2010). Site-Specific, Climate-Friendly Farming.

Brown, T., Huggins, David R., Keller, Chester, Kruger, Chad, & Reganold, John. (2015). Variable Rate Nitrogen and Seeding to Improve Nitrogen Use Efficiency, ProQuest Dissertations and Theses.

Brye, K. R., Norman, J. M., Bundy, L. G., & Gower, S. T. (2001). Nitrogen and carbon leaching in agroecosystems and their role in denitrification potential.Journal of Environmental Quality, 30(1), 58-70.

Bullock, D. S., Ruffo, M. L., Bullock, D. G., & Bollero, G. A. (2009). The value of variable rate technology: an information-theoretic approach. American journal of agricultural economics, 91(1), 209-223.

Busacca, A. J. (1989). Long Quaternary record in eastern Washington, USA, interpreted from multiple buried paleosols in loess. Geoderma, 45(2), 105-122.

Busacca, A. J., & McDonald, E. V. (1994). Regional sedimentation of late Quaternary loess on the Columbia Plateau: sediment source areas and loess distribution patterns. Washington Division of Geology and Earth Resources Bulletin, 80, 181-190.

Campbell, G. S., & Norman, J. M. (2012). An introduction to environmental biophysics. Springer Science & Business Media.

Carter, L. M., Rhoades, J. D., & Chesson, J. H. (1993). Mechanization of soil salinity assessment for mapping. ASAE Paper, 931557.

Chen, X. P., Cui, Z. L., Vitousek, P. M., Cassman, K. G., Matson, P. A., Bai, J. S., ... & Zhang, F. S. (2011). Integrated soil–crop system management for food security. Proceedings of the National Academy of Sciences, 108(16), 6399-6404.

Chen, X., Cui, Z., Fan, M., Vitousek, P., Zhao, M., Ma, W., ... & Deng, X. (2014). Producing more grain with lower environmental costs. Nature,514(7523), 486-489.

Chen, X., Zhang, F., Römheld, V., Horlacher, D., Schulz, R., Böning-Zilkens, M., ... & Claupein, W. (2006). Synchronizing N supply from soil and fertilizer and N demand of winter wheat by an improved Nmin method. Nutrient Cycling in Agroecosystems, 74(2), 91-98.

Conrad, O., Bechtel, B., Bock, M., Dietrich, H., Fischer, E., Gerlitz, L., Wehberg, J., Wichmann, V., and Böhner, J. (2015): System for Automated Geoscientific Analyses (SAGA) v. 2.1.4, Geosci. Model Dev., 8, 1991-2007, doi:10.5194/gmd-8-1991-2015. Download.

Crookston, R. K. (2006). A top 10 list of developments and issues impacting crop management and ecology during the past 50 years. Crop science, 46(5), 2253-2262.

Donaldson, N., United States. Soil Conservation Service, & Washington State University. Agricultural Research Center. (1980). Soil survey of Whitman County, Washington. Washington?]: The Service.

Fiez, T. E., Pan, W. L., & Miller, B. C. (1995). Nitrogen use efficiency of winter wheat among landscape positions. Soil Science Society of America Journal,59(6), 1666-1671.

Fridgen, J. J., Kitchen, N. R., Sudduth, K. A., Drummond, S. T., Wiebold, W. J., & Fraisse, C. W. (2004). Management zone analyst (MZA). *Agronomy Journal*, *96*(1), 100-108.

Fuentes, J. P., Flury, M., Huggins, D. R., & Bezdicek, D. F. (2003). Soil water and nitrogen dynamics in dryland cropping systems of Washington State, USA. Soil and Tillage Research, 71(1), 33-47.

Gasch, C. K., Hengl, T., Gräler, B., Meyer, H., Magney, T. S., & Brown, D. J. (2015). Spatio-temporal interpolation of soil water, temperature, and electrical conductivity in 3D+ T: The Cook Agronomy Farm data set. Spatial Statistics, 14, 70-90.

Gaylord, D. R., Busacca, A. J., & Sweeney, M. R. (2003). The Palouse loess and the Channeled Scabland: a paired Ice-Age geologic system. Quaternary Geology of the United States, INQUA, 123-134.

Goetz, A. F. H., Vane G., Solomon, J., Rock, B. (1985). Imaging spectrometry for earth remote sensing. Science, 228(4704), 1147-1152.

Fuentes, J. P., Flury, M., Huggins, D. R., & Bezdicek, D. F. (2003). Soil water and nitrogen dynamics in dryland cropping systems of Washington State, USA. Soil and Tillage Research, 71(1), 33-47.

Huggins, D., Pan, W., & Smith, J. (2010a). Site-Specific N Management for Direct-Seed Cropping Systems. Chapter, 16, 2010-001.

Huggins, D., Pan, W., & Smith, J. (2010b). Yield, protein and nitrogen use efficiency of spring wheat: evaluating field-scale performance. Chapter, 17, 2010-001.

Huggins, D. R., & Pan, W. L. (2003). Key indicators for assessing nitrogen use efficiency in cereal-based agroecosystems. Journal of Crop Production,8(1-2), 157-185.

Huggins, D. R., & Pan, W. L. (1993). Nitrogen efficiency component analysis: an evaluation of cropping system differences in productivity. Agronomy Journal, 85(4), 898-905.

Jennings, M. D., Miller, B. C., Dezdicek, D. F., & Granatstein, D. (1990). Sustainability of dryland cropping in the Palouse: A historical view. Soil and Water Conservation Society.

Johnson, G., Lamb, J., Rehm, G., Porter, P., Strock, J., Hicks, D., Eash, N., Eidman, V., Potter, B., 2000. An integrated approach to precision farming research. Proceedings of Fifth International Conference on Precision Agriculture (CD), July 16–19, 2000. Bloomington, MN, USA.

Kaur, H., Huggins, D. R., Rupp, R. A., Abatzoglou, J. T., Stöckle, C. O., & Reganold, J. P. (2017). Agro-ecological class stability decreases in response to climate change projections for the Pacific Northwest, USA. Frontiers in Ecology and Evolution, 5, 74.

Knobeloch, L., Salna, B., Hogan, A., Postle, J., & Anderson, H. (2000). Blue babies and nitrate-contaminated well water. Environmental Health Perspectives, 108(7), 675–678.

Kotchenova, S. Y., Vermote, E. F., Matarrese, R., & Klemm Jr, F. J. (2006). Validation of a vector version of the 6S radiative transfer code for atmospheric correction of satellite data. Part I: Path radiance. Applied optics, 45(26), 6762-6774.

Legg, J.O., and J.J. Meisinger. 1982. Soil Nitrogen Budgets. In F.J. Stevenson, ed., Nitrogen in Agricultural Soils, American Society of Agronomy, Madison, WI. pp. 503-566

Maaz, T. M., Schillinger, W. F., Machado, S., Brooks, E., Johnson-Maynard, J. L., Young, L. E., ... & Esser, A. (2017). Impact of climate change adaptation strategies on winter wheat and cropping system performance across precipitation gradients in the inland Pacific Northwest, USA. Frontiers in Environmental Science, 5, 23.

Magney, T., Yourek, M., Ward, N., Finch, S., Eitel, J., Vierling, L., Brooks, E., Huggins, D., Brown, D. "Determining the controls on nitrogen uptake from space." REACCH Annual Report Year 4 N.p., 2015. Web. 5 Aug. 2015.

Magney, T. S., Eitel, J. U., & Vierling, L. A. (2016). Mapping wheat nitrogen uptake from RapidEye vegetation indices. Precision Agriculture, 1-23.

Mahler, Robert L. "Northern Idaho Fertilizer Guide: Winter Wheat." University of Idaho Extension CIS453 (2007): 1–4. Print.

McBratney, A., Whelan, B., Ancev, T., & Bouma, J. (2005). Future directions of precision agriculture. Precision agriculture, 6(1), 7-23.

McCool, D. K., Busacca, A. J., & Michalson, E. L. (1999). Measuring and modeling soil erosion and erosion damages. Conservation farming in the United States—The methods and accomplishments of the STEEP Program, 23-56.

McDaniel, P. A., & Hipple, K. W. (2010). Mineralogy of loess and volcanic ash eolian mantles in Pacific Northwest (USA) landscapes. Geoderma, 154(3-4), 438-446.

Mulla, D. J. (2013). Twenty five years of remote sensing in precision agriculture: Key advances and remaining knowledge gaps. Biosystems Engineering, 114(4), 358-371.

Nehring, Richard. "Table 7—Average U.S. Farm Prices of Selected Fertilizers, 1960-2013." USDA ERS – Fertilizer Use and Price. USDA - ERS, 12 July 2013. Web. 11 Apr. 2016.

Painter, Kate (2016). Crop Enterprise Budget Cost Calculators. Retrieved from http://www.webpages.uidaho.edu/~kpainter/

Pan, W., Schillinger, W., Huggins, D., Koenig, R., & Burns, J. (2006, November). Fifty Years of Predicting Wheat Nitrogen Requirements Based on Soil Water, Yield, Protein and Nitrogen Efficiencies. In ASA-CSSA-SSSA Annual Meeting Abstracts. Raun, W.R., and G.V. Johnson. 1999. Improving nitrogen use efficiency for cereal production. Agronomy Journal 91:357-363.

Pan, W. L., Young, F. L., Maaz, T. M., & Huggins, D. R. (2016). Canola integration into semi-arid wheat cropping systems of the inland Pacific Northwestern USA. Crop and Pasture Science, 67(4), 253-265.

Peng, S., Buresh, R. J., Huang, J., Zhong, X., Zou, Y., Yang, J., ... & Cui, K. (2010). Improving nitrogen fertilization in rice by site-specific N management. A review. Agronomy for Sustainable Development, 30(3), 649-656.

Peralta, N. R., & Costa, J. L. (2013). Delineation of management zones with soil apparent electrical conductivity to improve nutrient management. Computers and Electronics in Agriculture, 99, 218-226.

Peralta, N. R., Costa, J. L., Balzarini, M., Franco, M. C., Córdoba, M., & Bullock, D. (2015). Delineation of management zones to improve nitrogen management of wheat. Computers and Electronics in Agriculture, 110, 103-113.

Poggio, M., Brown, D. J., & Bricklemyer, R. S. (2015). Laboratory-based evaluation of optical performance for a new soil penetrometer visible and near-infrared (VisNIR) foreoptic. Computers and Electronics in Agriculture, 115, 12-20.

Porter, J. R., & Gawith, M. (1999). Temperatures and the growth and development of wheat: a review. European Journal of Agronomy, 10(1), 23-36.

R Development Core Team, 2013. R: A Language and Environment for Statistical Computing. R Foundation for Statistical Computing, Vienna, Austria. ISBN 3-900051-07-0, URL <http://www.R-project.org>.

Shang, J., Liu, J., Ma, B., Zhao, T., Jiao, X., Geng, X., ... & Walters, D. (2015). Mapping spatial variability of crop growth conditions using RapidEye data in Northern Ontario, Canada. Remote Sensing of Environment, 168, 113-125.

“Soil Bulk Density, Moisture, Aeration.” (n.d.) Guides for Educators. USDA-NRCS, Web. 6 July 2017.

Taylor, S. E. (2016). Precision Nitrogen Management: Evaluating and Creating Management Zones Using Winter Wheat Performance (Doctoral dissertation, Washington State University).

Vermote, E. F., & Kotchenova, S. (2008). Atmospheric correction for the monitoring of land surfaces. Journal of Geophysical Research: Atmospheres, 113(D23).

Ward, N. K., Maureira, F., Stöckle, C. O., Brooks, E. S., Painter, K. M., Yourek, M. A., & Gasch, C. K. (2018). Simulating field-scale variability and precision management with a 3D hydrologic cropping systems model. Precision Agriculture, 19(2), 293-313.

Wetterlind, J., Stenberg, B., & Söderström, M. (2008). The use of near infrared (NIR) spectroscopy to improve soil mapping at the farm scale. Precision Agriculture, 9(1-2), 57-69.

Yost, M. A., Kitchen, N. R., Sudduth, K. A., Sadler, E. J., Drummond, S. T., & Volkmann, M. R. (2017). Long-term impact of a precision agriculture system on grain crop production. Precision Agriculture, 18(5), 823-842.

Yourek, M. A. (2016). An Investigation of Crop Senescence Patterns Observed in Palouse Region Fields Using Satellite Remote Sensing and Hydrologic Modeling (Doctoral dissertation, University of Idaho).

Zhang, N., Wang, M., & Wang, N. (2002). Precision agriculture—a worldwide overview. Computers and electronics in agriculture, 36(2-3), 113-132.

Zhang, X., Shi, L., Jia, X., Seielstad, G., & Helgason, C. (2010). Zone mapping application for precision-farming: a decision support tool for variable rate application. Precision Agriculture, 11(2), 103-114.

Zhao, R. F., Chen, X. P., Zhang, F. S., Zhang, H., Schroder, J., & Römheld, V. (2006). Fertilization and nitrogen balance in a wheat–maize rotation system in North China. Agronomy Journal, 98(4), 938-945.

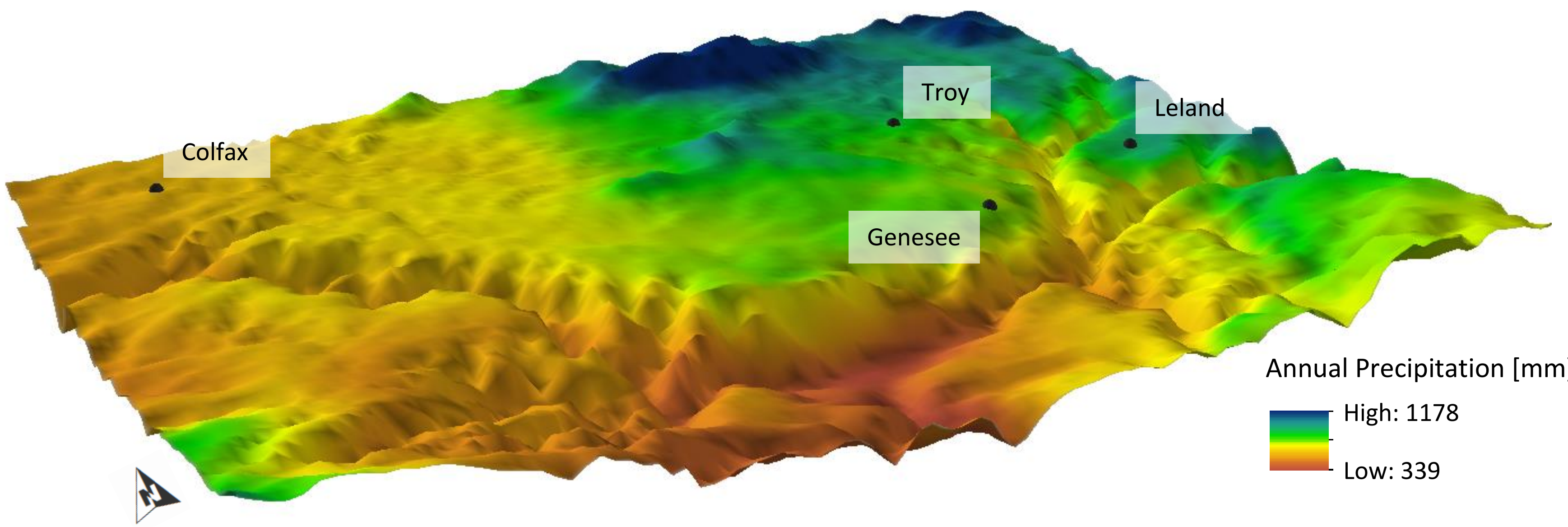

Figure 3.1: Annual precipitation [mm] of the Site-specific Climate Friendly Farming project locations.

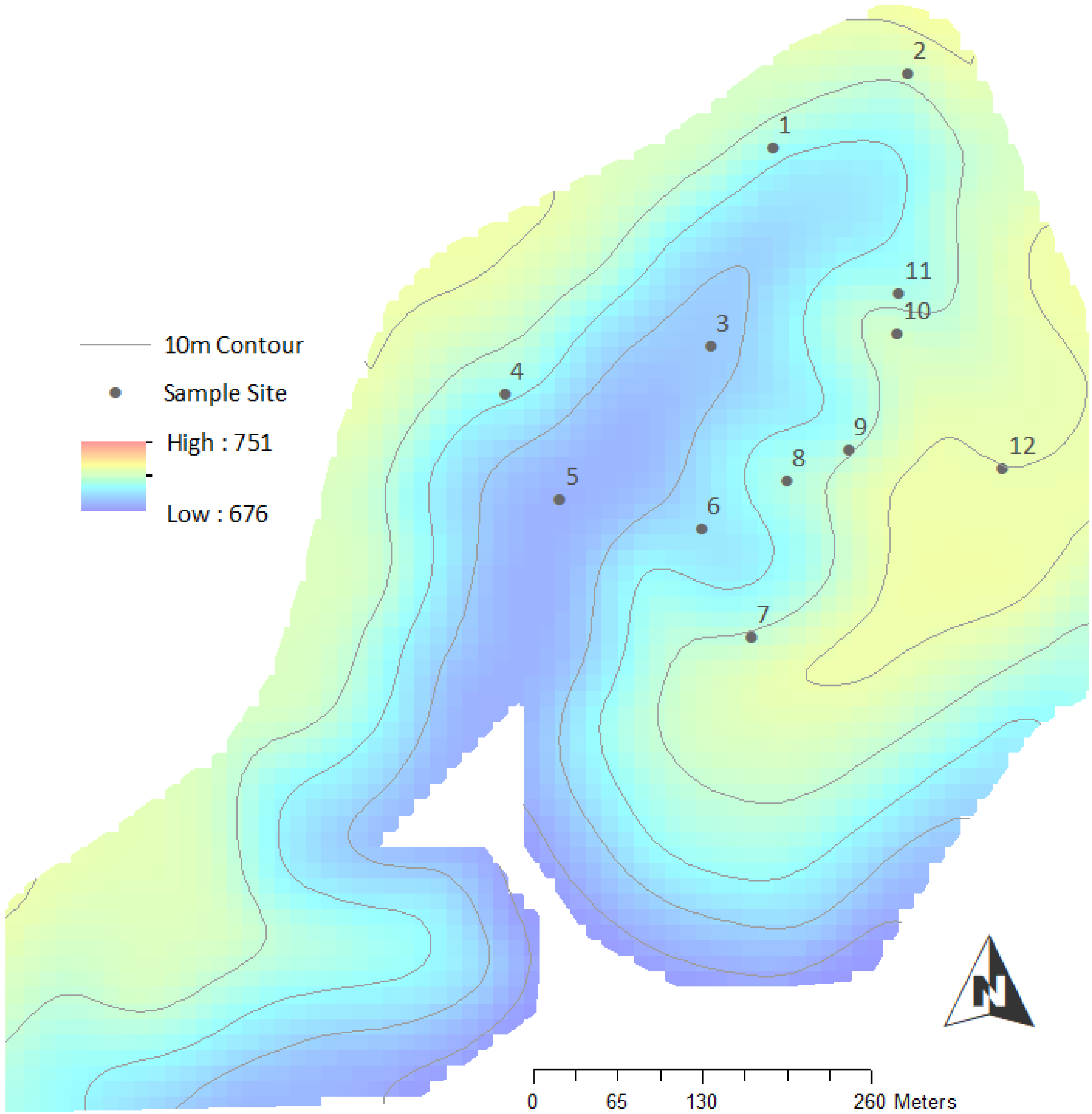

Figure 3.2: Colfax Tier II field sampling locations and digital elevation map [m].

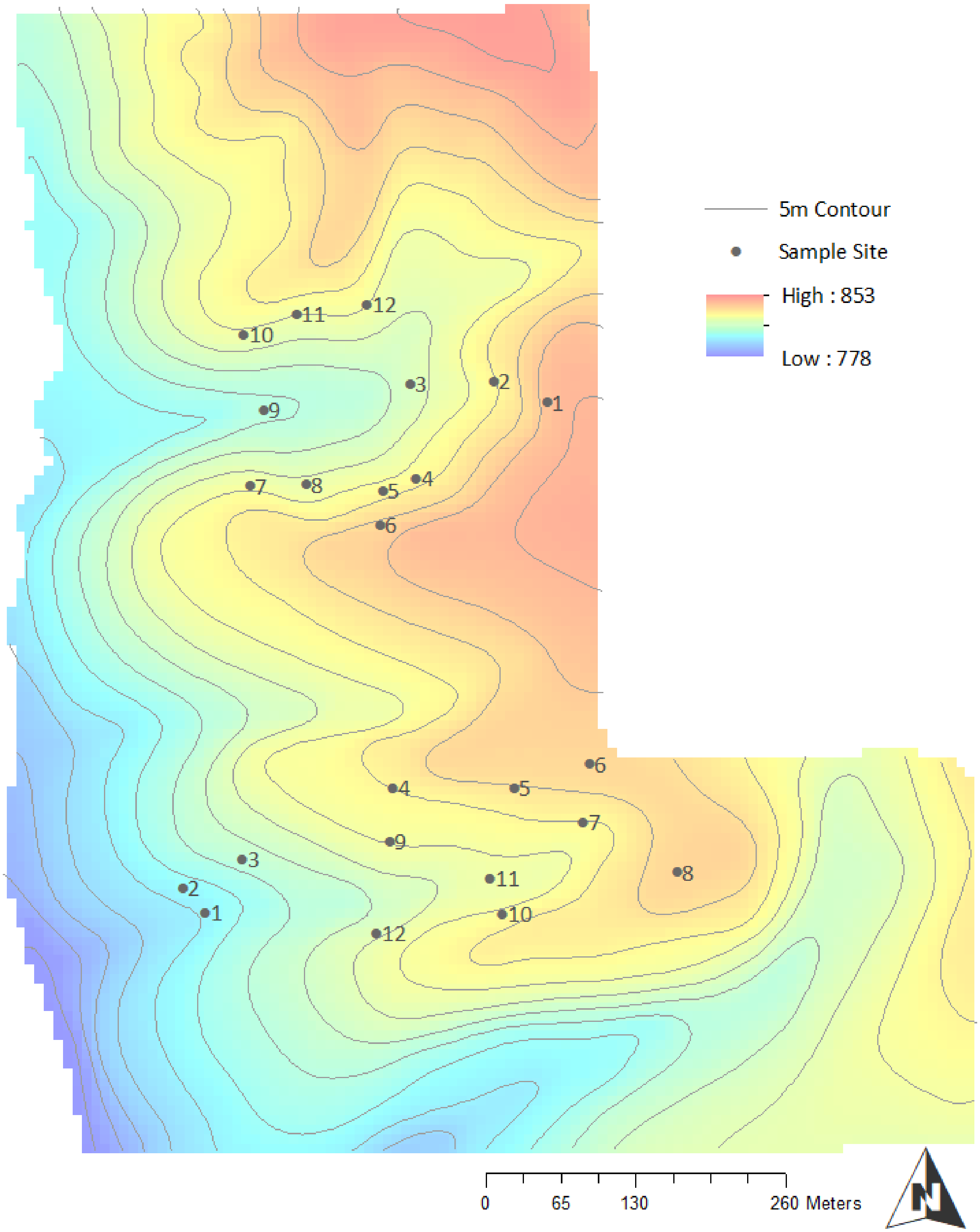

Figure 3.3: Genesee field sampling locations and digital elevation map [m].

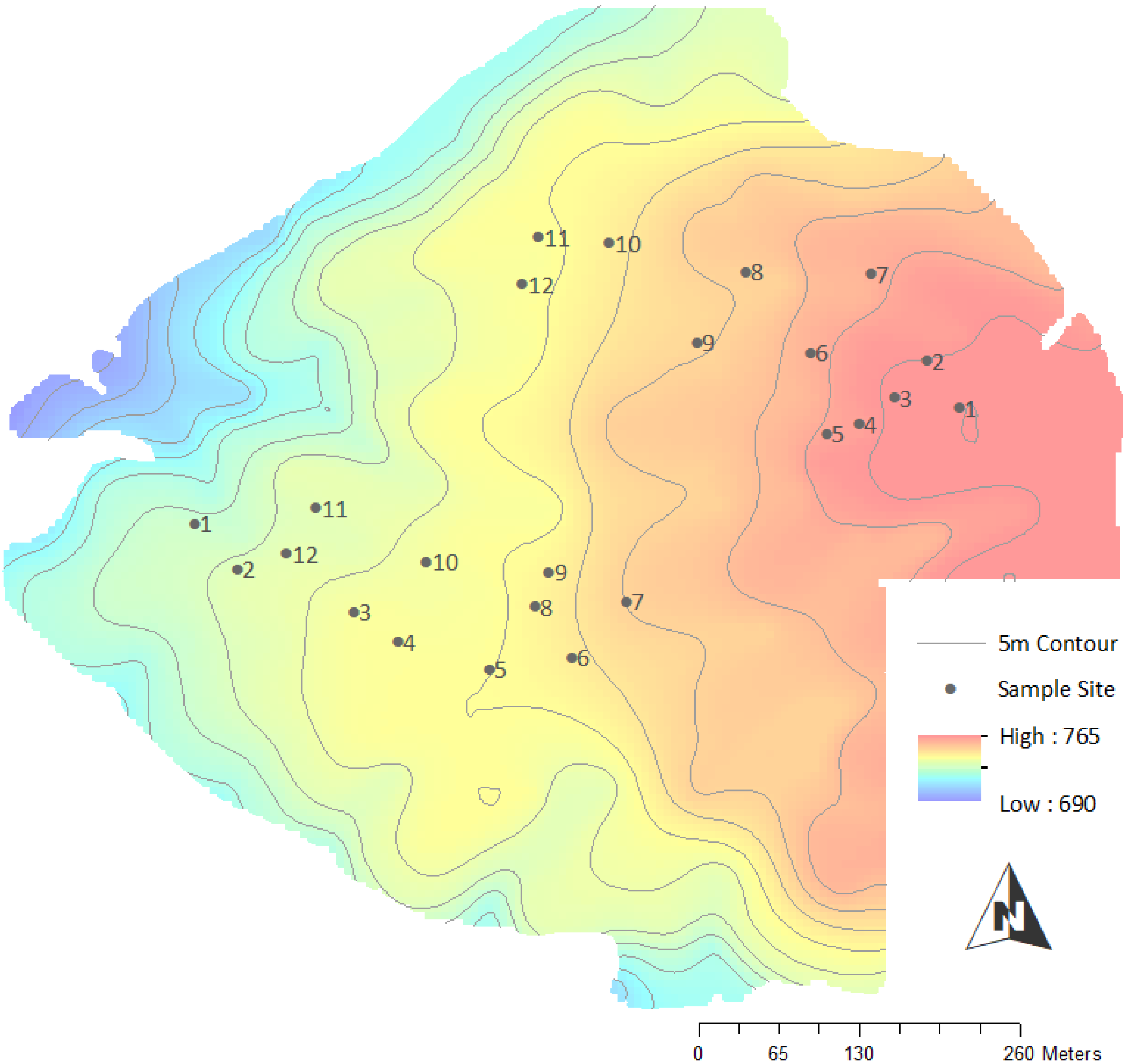

Figure 3.4: Leland field sampling locations and digital elevation map [m].

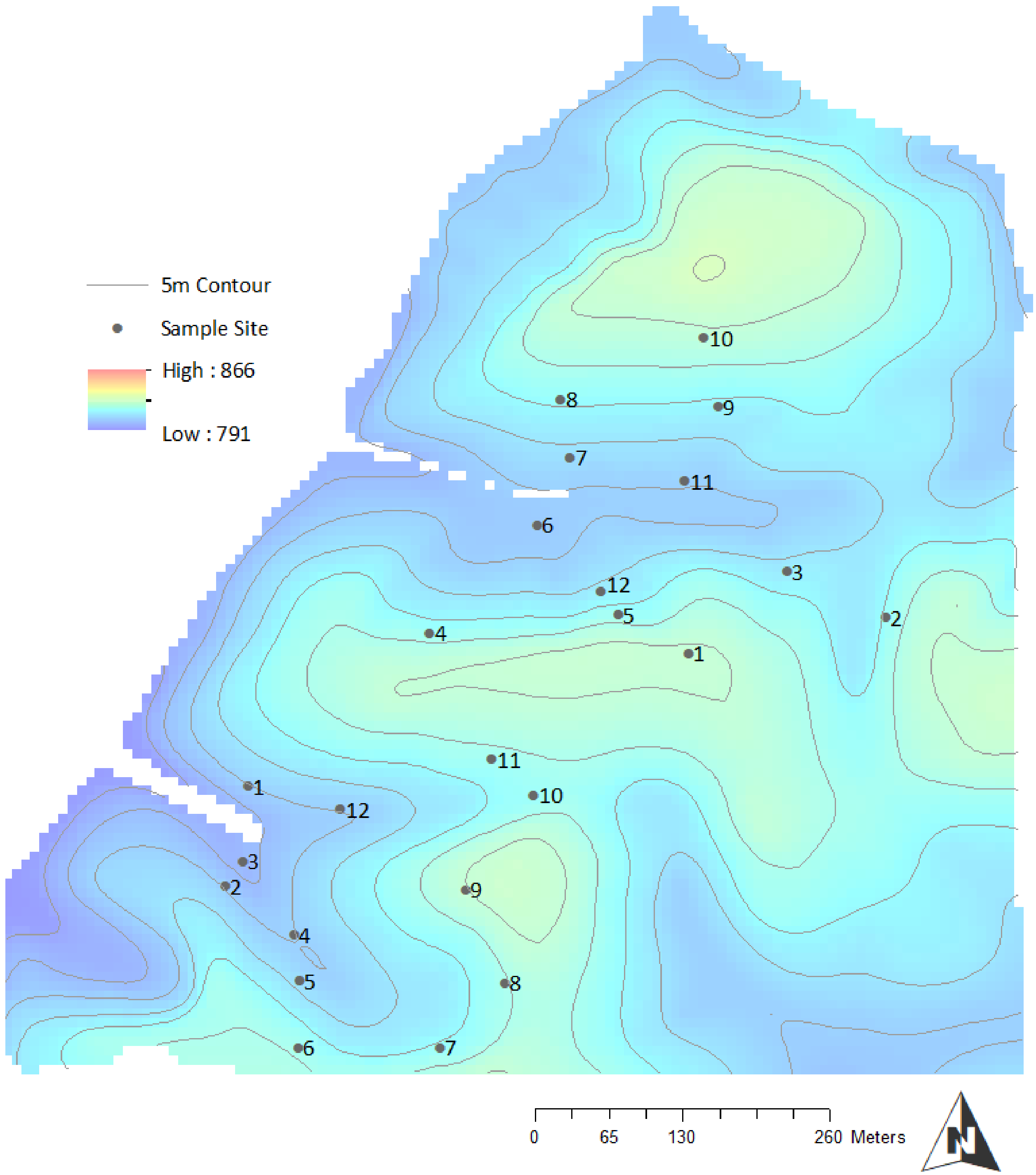

Figure 3.5: Troy field sampling locations and digital elevation map [m].

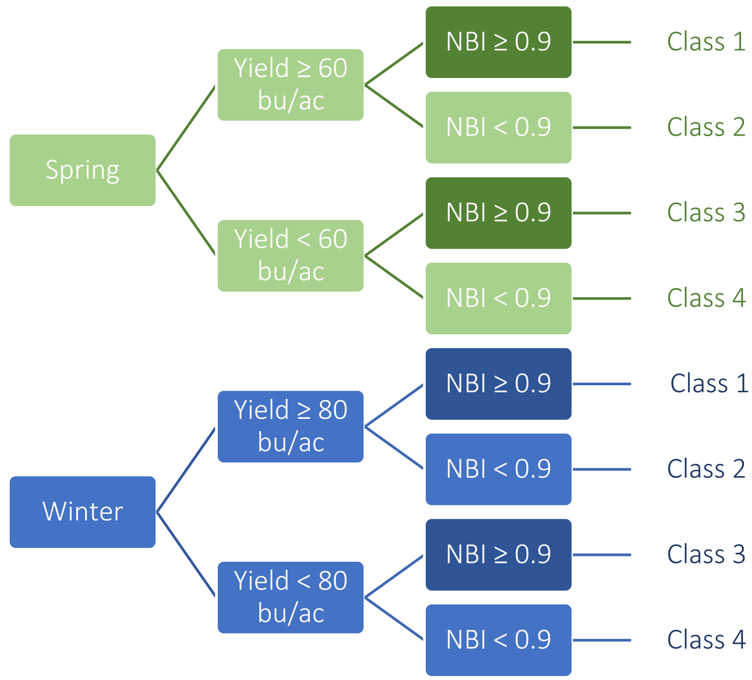

Figure 3.6: Field-based evaluation classification scheme.

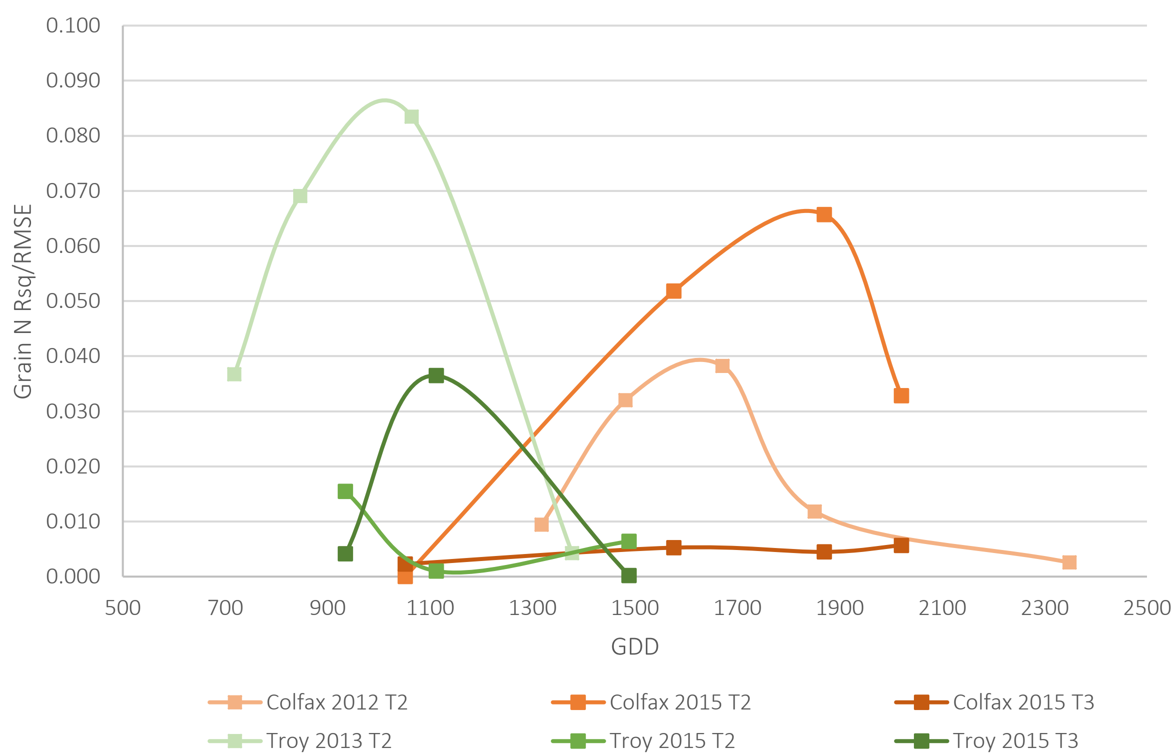

Figure 3.7: Growing degree day vs. grain N content prediction power (R^2/RMSE).

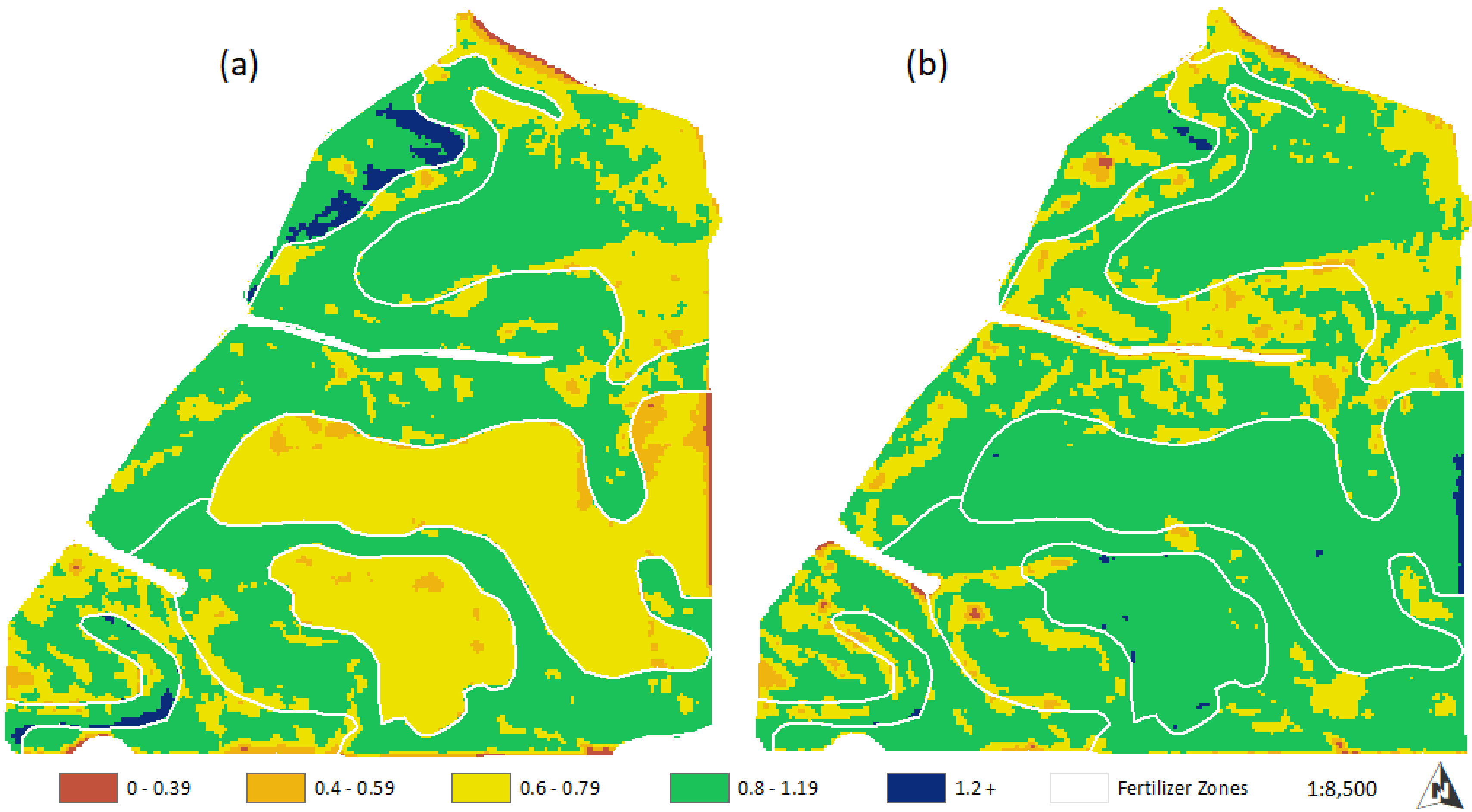

Figure 3.8: Troy nitrogen balance index comparative maps. 2013 (a) and 2015 (b) growing HRWW. Adjustment in N fertilizer application rates drastically shifted N uptake efficiency. 2015 has less distinct lines in conjunction with fertilizer zones compared to the 2013 map.

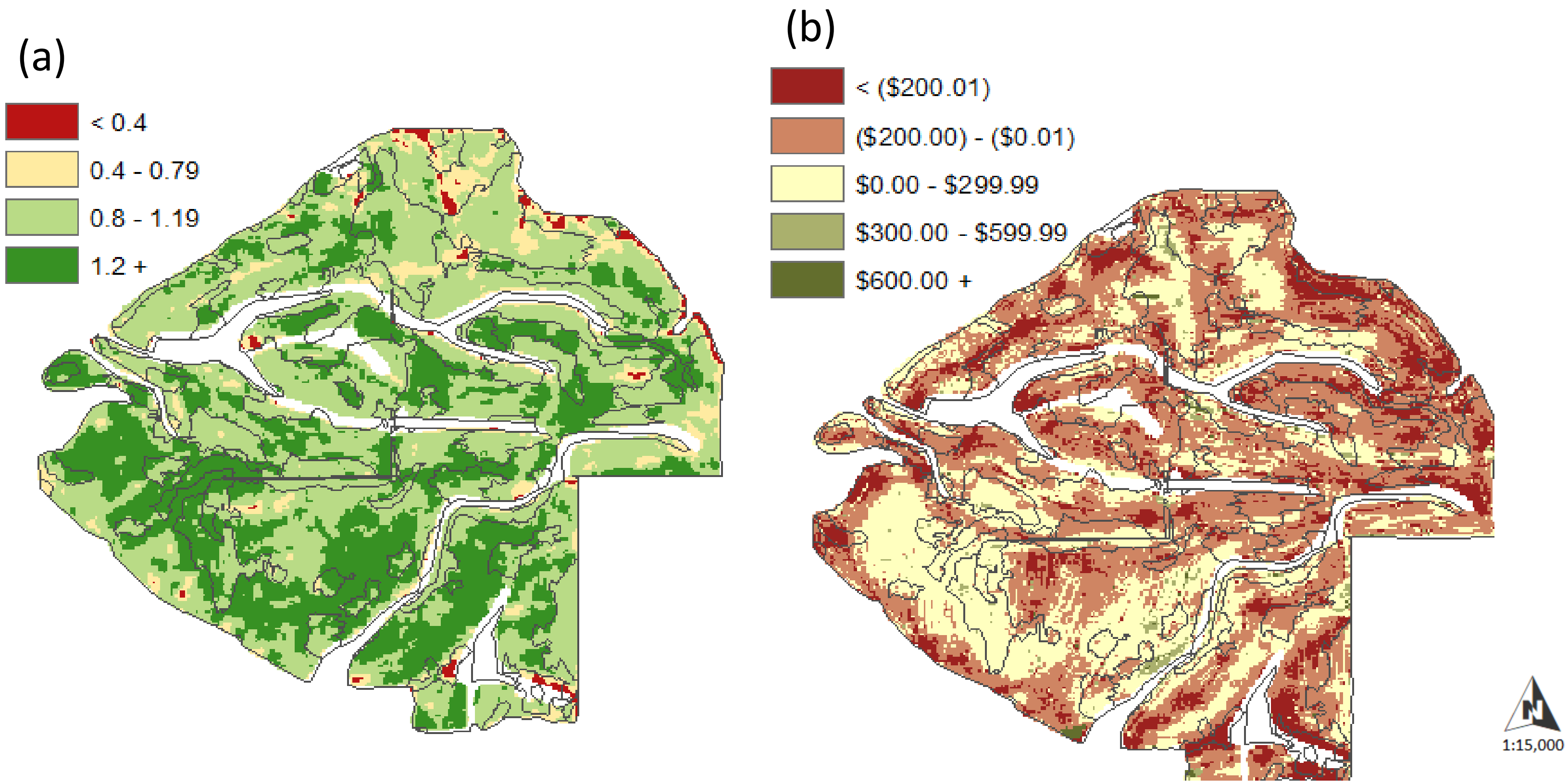

Figure 3.9: Leland 2014 metric comparison maps. (a) nitrogen balance index vs (b) returns to risk [$/ha] for SWSW.

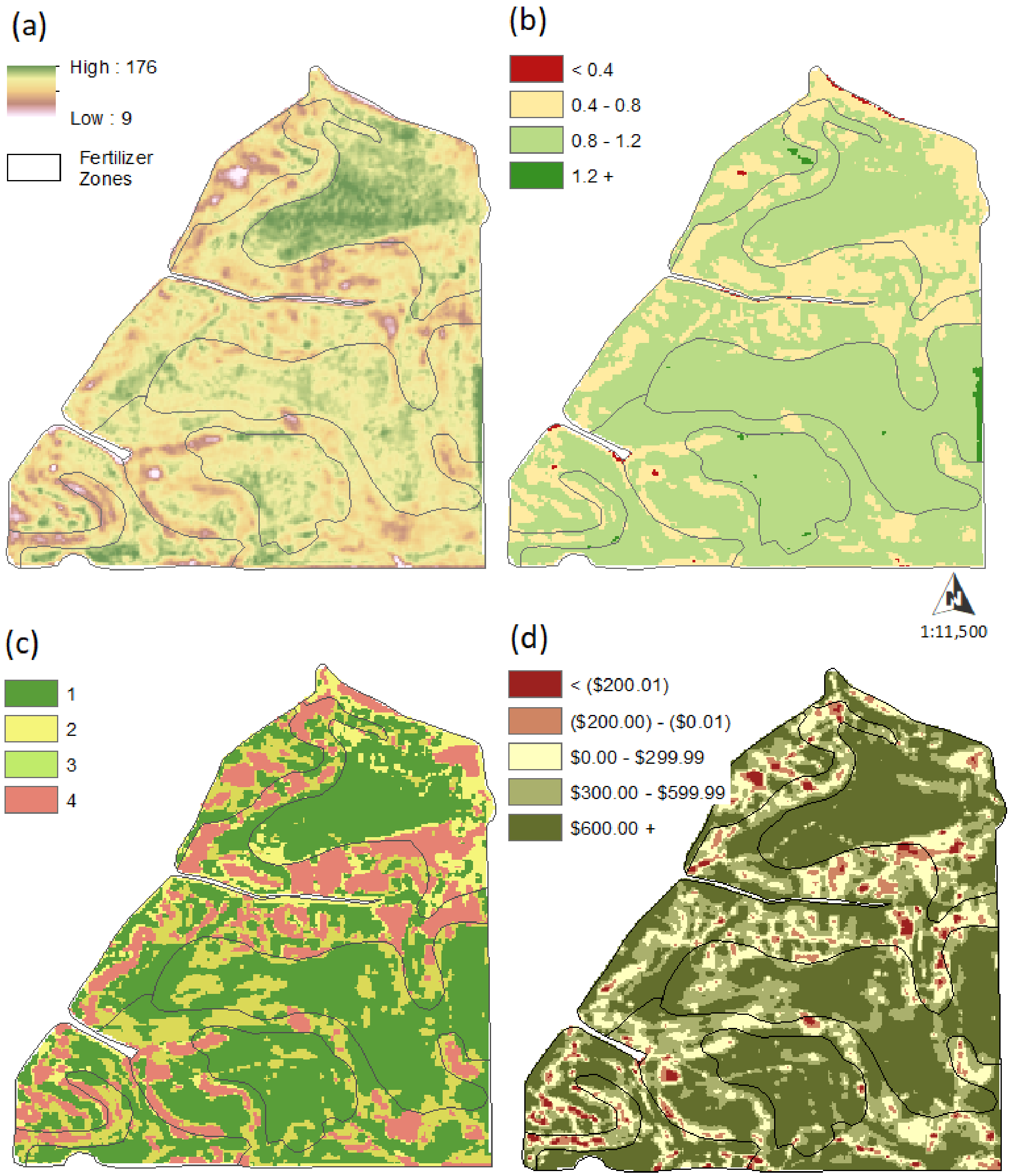

Figure 3.10: Mapping analysis comparison for Troy 2015. (a) Grain N [kg/ha] (b) nitrogen balance index (c) classification (d) returns to risk [$/ha]. Similar patterns can be seen in maps the highest N content areas also produced the best yields. The most efficient areas also tended to be the most profitable in this year.

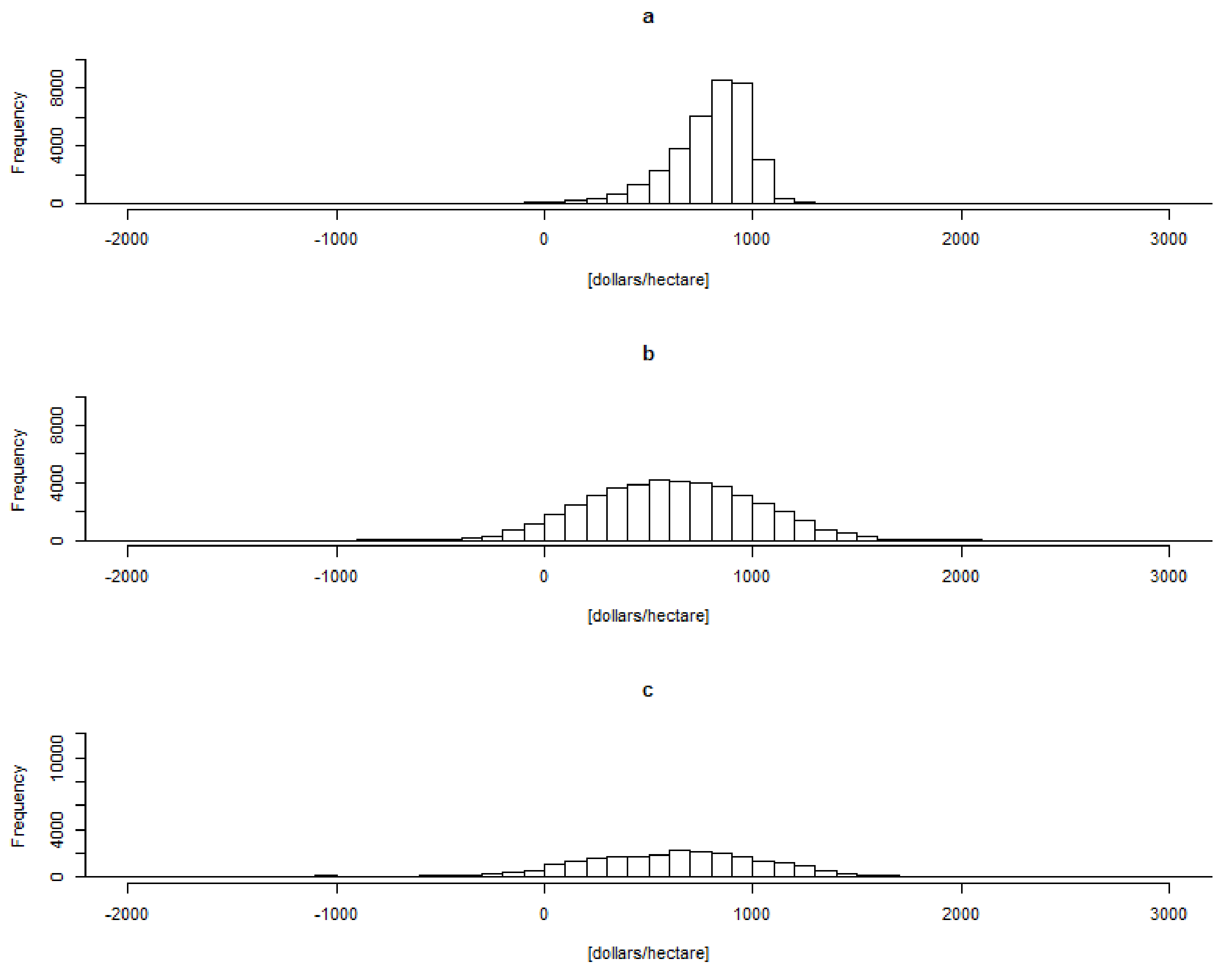

Figure 3.11: Returns to risk frequency distribution for Troy 2015. (a)G_w [kg/ha] calculated from NDRE linear model (Appendix 2.D) (b)G_w [kg/ha] derived from yield map kriging at 30m maximum distance (c) G_w [kg/ha] derived from yield map point data. It is clear NDRE based G_w values are skewed and the resultant economic analysis, no longer describes areas with low profitability.

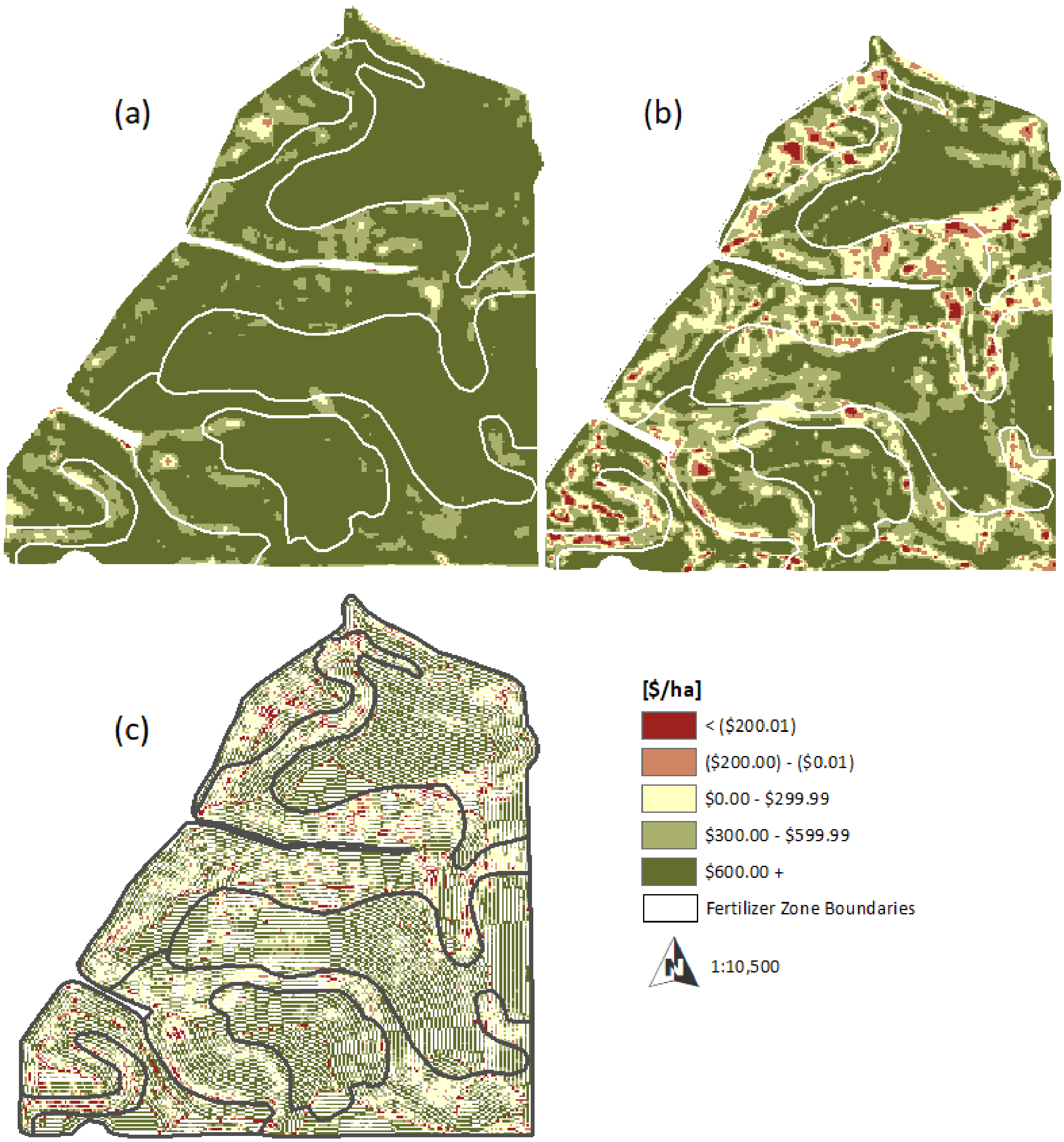

Figure 3.12: Returns to risk map comparative for Troy 2015. (a) Yield calculated from NDRE linear model (Appendix 2.D) (b) Yield derived from yield map kriging at 30m maximum distance (c) Yield derived from yield map point data. It is clear NDRE based G_w values are skewed and the resultant economic maps resulting in minimal patterning seen.

CHAPTER 3 TABLES

Table 3.1: Colfax management and rotation summary.

	Annual Prec. [mm]	Tier II Site Size [ha]	Tier III Site Size [ha]	Tillage	Planter	Fertilizer Type	Fertilizer Rate [kg N/ha]	Crop
2012	491	16.0	36.9	No Till	Direct Seed	Uniform: Urea Sp. Foliar: Urea	119	HRWW
2013	475	16.0	36.9	No Till	Direct Seed	Uniform: Urea Sp. Foliar: Urea	146	HRSW
2014	379	16.0	36.9	No Till	Direct Seed	Uniform: Urea Sp. Foliar: Urea	129	HRSW
2015	400	16.0	36.9	No Till	Direct Seed	Uniform: Urea Sp. Foliar: Urea	119	HRWW
2016	486	16.0	36.9	No Till	Direct Seed	Uniform: Urea Sp. Foliar: Urea		Chem Fallow

Table 3.2: Genesee management and rotation summary.

	Annual Precip. [mm]	Tier II Site Size [ha]	Tier III Site Size [ha]	Tillage	Planter	Fertilizer Type	Fertilizer Rates [kg N/ha]	Crop
2012	587	12.0	20.7	No Till	Direct Seed - Exactrix	NH3 at planting	High: 108 Med2:91 Med:68 Low:35	HRSW
2013	588	12.0	20.7	No Till	Direct Seed - Exactrix	NH3 at planting	High: 108 Med2:91 Med:68 Low:35	SP BARLEY
2014	507	12.0	20.7	No Till	Direct Seed - Exactrix	NH3 at planting		SP CANOLA
2015	600	12.0	20.7	No Till	Direct Seed - Exactrix	NH3 at planting	High: 151 Med2:129 Med:95 Low:62	SWWW
2016	625	12.0	20.7	No Till	Direct Seed - Exactrix	NH3 at planting	High: 108 Med2:91 Med:68 Low:35	HRSW

Table 3.3: Leland management and rotation summary.

	Annual Precip. [mm]	Tier II Site Size [ha]	Tier III Site Size [ha]	Tillage	Fertilizer Type	Fertilizer Rates [kg N/ha]	Crop
2012	624	8.9	18.1	Fall: Heavy Harrow			GARBS
2013	631	8.9	18.1	Conservation Fall: Chisel	Zones: Urea Sp: Topdress Sp: fungicide	High: 134 Med: 112 Low: 90	SWWW
2014	541	8.9	18.1	Conservation Fall: Chisel Spring: Hard Harrow	Zones: Urea Sp: Topdress Sp: fungicide	High: 99 Med: 81 Low: 67	SWSW
2015	608	8.9	18.1	Spring: Heavy Harrow			GARBS
2016	648	8.9	18.1	Conservation Fall: Chisel	Zones: Urea Sp: Topdress Sp: fungicide	High: 134 Med: 112 Low: 80	SWWW

Table 3.4: Troy management and rotation summary.

	Annual Precip. [mm]	Tier II Site Size [ha]	Tier III Site Size [ha]	Tillage	Planter	Fertilizer Type	Fertilizer Rates [kg N/ha]	Crop
2012	596	24.9	17.7		Direct Seed			(DNS 2011) GARBS
2013	580	24.9	17.7	Fall subsoiler @ 14-16" depth on 30" centers	Direct Seed	Fall: aqua Starter: MESZ 12%N Zones: Solution 32 Foliar: Urea	High: 224 Med:181 Med2: 157 Low: 138	HRWW
2014	461	24.9	17.7	Spring: cultivator/ harrow	Direct Seed			GARBS
2015	605	24.9	17.7	Conservation tillage Fall: Chisel	Direct Seed	Fall: aqua Starter: MESZ 12%N Zones: Solution 32 Foliar: Urea	High: 180 Med: 159 Med2: 153 Low: 134	HRWW
2016	652	24.9	17.7	Spring: cultivator/ harrow	Direct Seed			Fallow to W. Canola

Table 3.5: 5-year average returns to risk values [$/unit] (Painter, 2016).

	Crop Price [$/kg]	Cost of Production w/o Nf [$/ha]		Fertilizer Type Used	Fertilizer price [$/kg]
HRWW	$ 0.31	$ 975.45	Colfax	Urea	$ 1.69*
HRSW	$ 0.31	$ 854.13	Genesee	Anhydrous	$ 1.39
SWWW	$ 0.24	$ 726.20	Leland	Urea	$ 1.69*
SWSW	$ 0.24	$ 732.11	Troy	30% Solution	$ 1.69

*prices reflective of 30% N solution prices rather than urea since urea 5-year average costs not available.

Table 3.6: Nitrogen harvest index statistical outputs.

	Average	σ	n	Grain N [kg/ha]	N in the Total Aboveground Biomass [kg/ha]
All	0.79	0.075	458	89	114
Spring	0.81[a]	0.082	108	62	77
Winter	0.78[b]	0.071	350	97	126
Hard Red (HR)	0.78[1]	0.091	83	107	141
Soft White (SW)	0.79[1]	0.071	375	85	108
HR Spring	0.85[i]	0.047	24		
HR Winter	0.75[ii]	0.090	59		
SW Spring	0.82[iii]	0.083	72		
SW Winter	0.78[iv]	0.067	303		

Note: a, 1, ii represent different statistical testing groups

Table 3.7: Grain N and total nitrogen in total aboveground biomass prediction results.

Dependent Variables	Independent Variables	RMSE ([N kg/ha])
N_t	NDRE	47
N_t	NDRE, Season, Class, Farm, Year	39
N_g	NDRE	28
N_g	NDRE, Season, Class, Farm, Year	28
N_g	NDRE, Class	28

Table 3.8: Multi-linear regression factor results. Total number of times factors achieve top 5 factors for predicting grain N in multi-linear regression analysis.

Factors	Linear model uses
Fall EC	10
Spring EC	7
Land slope	6
Cross-sectional curvature	5
Topographic Wetness Index	5
Solar radiation	5
ET/Peq	4
Longitudinal curvature	3
Equivalent precipitation	3
Relative elevation	3
Soil depth	3
Transpiration	2
Percent clay	1
Average bulk density	1

Peq = equivalent precipitation, ET = evapotranspiration, EC = apparent electrical conductivity

Table 3.9: Percent of map area by nitrogen balance index metric.

	C12	C13*	C14*	C15	G12	G15	G16	L13	L14	L16	T13	T15	AVG
Crop	*HR WW*	*HR SW*	*HR SW*	*HR WW*	*HR SW*	*SW WW*	*HR SW*	*SW WW*	*SW SW*	*SW WW*	*HR WW*	*HR WW*	
NBI < 0.4	0.9%	13.0%	13.6%	5.6%	0.1%	0.6%	0.0%	0.1%	1.4%	0.4%	0.5%	0.3%	3.0%
0.4 ≤ NBI < 0.8	18.4%	65.9%	60.2%	23.4%	12.0%	38.2%	1.1%	6.7%	8.8%	53.3%	44.5%	24.6%	29.8%
0.8 ≤ NBI < 1.2	76.6%	21.1%	26.1%	61.1%	83.2%	59.9%	11.8%	92.9%	58.1%	45.6%	53.4%	74.7%	55.4%
NBI > 1.2	4.1%	0.0%	0.0%	10.0%	4.7%	1.3%	87.1%	0.4%	31.7%	0.7%	1.6%	0.5%	11.8%

C12 = Colfax 2012, G12 = Genesee 2012, L13 = Leland 2013, T13 = Troy 2013; *Does not include area from Tier III field due to cloud coverage issues.

Table 3.10: Percent of map per field area by class.

	G12	L13	L14	L16	T15	AVG
Crop	*HRSW*	*SWWW*	*SWSW*	*SWWW*	*HRWW*	
Class 1	73.7%	71.6%	19.3%	40.6%	53.6%	51.7%
Class 2	0.8%	3.1%	1.4%	44.4%	8.5%	11.6%
Class 3	25.1%	21.7%	70.5%	5.7%	19.1%	28.4%
Class 4	0.3%	3.6%	8.8%	9.4%	18.9%	8.2%

G12 = Genesee 2012, L13 = Leland 2013, T15 = Troy 2015

Table 3.11: Percent of map area per field for returns to risk metric [$/ha].

	G12	L13	L14	L16	T15	AVG
Crop	*HRSW*	*SWWW*	*SWSW*	*SWWW*	*HRWW*	
≤ -$200	2.6%	0.7%	15.6%	0.0%	1.3%	4.1%
-$200 - $0	5.0%	1.9%	47.9%	0.4%	4.2%	11.9%
$0 - $300	18.6%	16.3%	34.5%	9.4%	16.7%	19.1%
$300 - $600	46.2%	45.1%	1.7%	45.4%	26.6%	33.0%
> $600	27.5%	36.0%	0.4%	44.8%	51.2%	32.0%

G12 = Genesee 2012, L13 = Leland 2013, T15 = Troy 2015

Table 3.12: Returns to risk [$/ha] point data for Colfax.

	HRSW	HRWW
Average	$(274.08)	$431.00
SD	$424.16	$378.60
CV	-155%	88%
South Facing Slope	$(5.07)	$595.89
North Facing Slope	$(851.45)	$223.46
Draw or Flat	$(273.50)	$426.09
Ridge	$(441.08)	$362.61

CHAPTER 4: AGRICULTURAL EXTENTION APPLICATIONS AND CONCLUSIONS

SUMMARY

In the Palouse region, the majority of the fields struggled to meet crop quality standards as well as nitrogen efficiency goals. Even with three of the four locations implementing variable rate application strategies, N efficiency ranged broadly both temporally and spatially at each farm as well as between farms. Regional five-year average of N uptake efficiency (52%) was similar to N uptake estimates in current fertilizer guides (50%). Much of the variability in crop N use and crop performance is undoubtedly affected by variability in soil physical and biological characteristics from a long legacy of soil erosion in the region. Classification metrics indicated that at the point scale 43% of the sites struggled to meet grain protein and nitrogen efficiency goals. Spatial classification suggests that most growers did not struggle to achieve yield goals, with an average 67% of each field achieving county average yields. Regionally, spring wheat consistently underperformed winter wheat and were less profitable. This study demonstrates there can be extreme spatial and temporal variability in crop performance at the field scale and there are effective evaluation techniques. This data also demonstrates there are methods which identify and interpret some of the drivers behind spatial patterns and temporal stability. Effective evaluation methodologies will be a critical component for adaptive management strategies.

Adaptive management practices will be most effective through iterative and interdisciplinary evaluation strategies. The three evaluation metrics in this study (NBI, Classification and RR) have been effective at evaluating N efficiency, profitability and crop performance at both the field and point scale. The direct relationship between NBI and N uptake ($R^2 = 0.50$) allow spatially explicit nitrogen efficiency maps to be derived through remote sensing imagery. Inherent error in this relationship limits the absolute application of this metric alone, but when integrated with other metrics such as returns to risk and/or classification, it can provide insight into general field patterns. The direct relationship (R^2 ranging from 0.52 to 0.93) between RR and NBI at each farm suggests that there are direct returns in efficient nitrogen fertilizer management. The long rotation schedules and limitations of these metrics necessitate long term evaluation before making drastic management changes. The Colfax fields demonstrated the temporally stable crop responses to uniform fertilizer applications suggesting variable rate applications would prove profitable. Conversely, the Genesee farm consistently demonstrated effective N management strategies. Management strategies which can potentially increase soil organic matter may improve overall crop performance. Long term agricultural study (LTAR) sites will be central to quantifying consistent spatial and temporal patterns to changing climate, and evaluating long term suitability and stability agricultural production.

Remotely sensed imagery has great potential to make sampling and management practices more effective. Point scale topographic analysis demonstrates that even though this study attempted to select diverse point locations, satellite imagery can better identify areas of different crop productivity. For six metrics (yield, % organic matter, % clay, bulk density, NBI and RR) only the draw locations were significantly different from the flat locations while the north and south facing slopes were not statistically unique. This suggests that soil and plant sampling may be improved by satellite and/or drone imagery by better identifying the areas of success and struggle. Sampling these areas may tell a more comprehensive story about needed management adjustments. For example, remotely sensed imagery could indicate whether an area is consistently not reaching yield goals. Subsequent soil sampling could indicate the reasons for poor crop performance. If the soil sample reveals nutrient deficiencies, or poor physical or biological soil characteristics (e.g. low organic matter) it may be useful to either increase soil health in the area or lower yield goals. High acidity could indicate over application of N fertilizer and lowering rates may assist in matching N requirements. Alternatively, this could support lime application as a worthy long- term investment. Alternatively, if soil samples reveal good soil health, it could also indicate there was not enough available precipitation that season which would suggest no management adaptations. Point based sampling guided by field scale evaluation may help determine whether poor crop performance is based on management decisions or environmental factors.

Although there is great promise for satellite image applications, current availability and expense to process these images will make adoption of these methods difficult. Further research is needed to adapt and/or update current fertilizer guides to integrate effective evaluation metrics such as the ones described in this study. This would allow for adaptive management strategies to be currently evaluated. This study briefly investigated point based evaluation methods and updated current fertilizer guide worksheets in Appendix 3.A and Appendix 3.B. Because the average N uptake for the region is consistent with current fertilizer guide estimates, it may be useful for growers to not only use fertilizer guides to estimate how much N should be used, but to calculate how much nitrogen should have been applied for the actual yields achieved. The integrative assessment approach developed and applied in this study can be a powerful tool to explicitly reveal poorly managed regions within a field and could provide the convincing evidence to a grower that variable rate strategies can be a profitable and useful management approach. One major outcome of these spatial management methods may be increased adoption of site-specific precision agriculture strategies and overall improvement in sustainability of the agroecosystems in the region.

APPENDIX 1: SUPPLEMENTAL MATERIALS FOR CHAPTER 2

APPENDIX 1.A: NITROGEN HARVEST INDEX

Data included in these results include the Site-Specific Climate Friendly Farming (SCF) project and the Davenport and Pullman locations discussed in (Maaz et al., 2017). Previous research has suggested that the nitrogen harvest index (NHI) is a consistent ratio within the region of study for individual wheat classes. These data suggest that seasonal variability is statistically significant (two-tail ANOVA) between spring and winter wheat whereas wheat class (i.e. hard red vs soft white) was not statistically significant (two-tail ANOVA). ANOVA, F-tests and t-tests were conducted in Microsoft Excel 2013.

Winter wheat had higher N content in the total aboveground biomass than spring wheat. This may be due to physiological differences and longer growth periods allowing for more N uptake. However, spring wheat had a higher NHI than winter wheat. This may suggest that spring wheat are more efficient at allocating N to the grain or that winter wheat must allocate more to growth during the long growing season and is less efficient but ultimately obtains a greater N concentration in the total aboveground biomass. Hard red wheat had higher N contents than soft white. This is likely due to genetic selection for high protein in hard reds for wheat quality standards.

Table A1.A-1: Nitrogen Harvest Index statistical outputs. Superscripts a, 1, ii represent different statistical testing groups.

	Average	σ	n	Grain N [kg/ha]	N in the Total Aboveground Biomass [kg/ha]
All	0.79	0.075	458	89	114
Spring	0.81[a]	0.082	108	62	77
Winter	0.78[b]	0.071	350	97	126
Hard Red (HR)	0.78[1]	0.091	83	107	141
Soft White (SW)	0.79[1]	0.071	375	85	108
HR Spring	0.85[i]	0.047	24		
HR Winter	0.75[ii]	0.090	59		
SW Spring	0.82[iii]	0.083	72		
SW Winter	0.78[iv]	0.067	303		

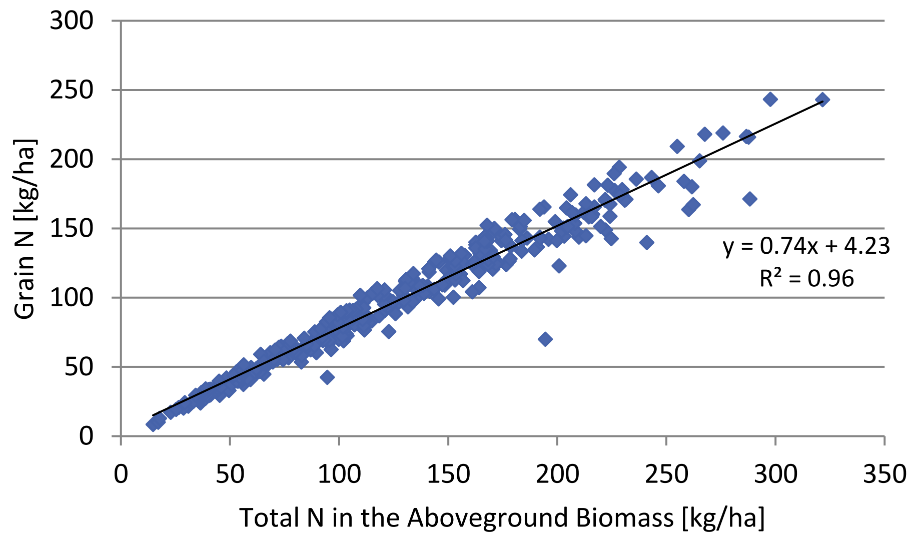

Figure A1.A-1: Nitrogen Harvest Index for mixed class winter wheat.

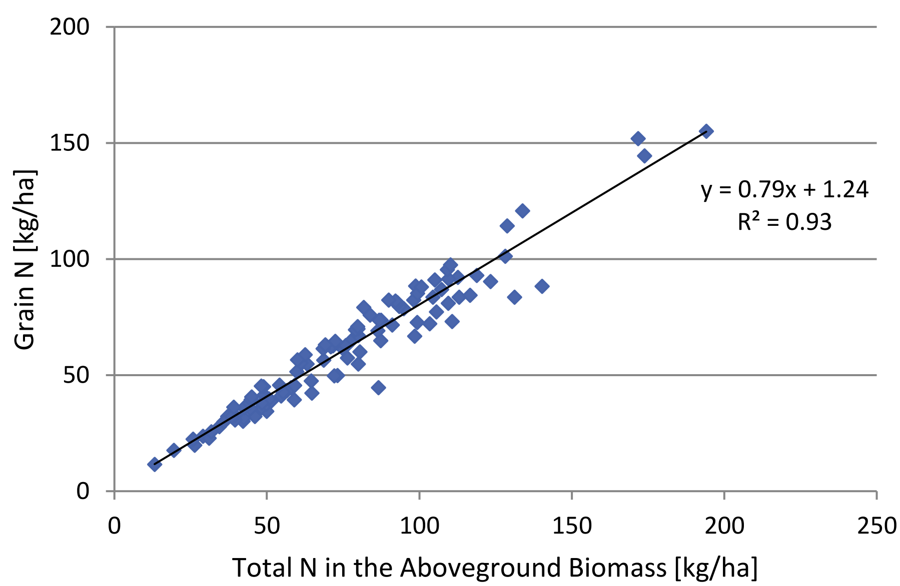

Figure A1.A-2: Nitrogen Harvest Index for mixed class spring wheat.

APPENDIX 1.B: REGIONAL SUMMARY TABLE PART

Table A1.B-1: Expanded crop performance summary.

	CROP	**PREC [MM]**	G_W [MG/HA]		PROTEIN [G/KG]		NUPTAKE [N_T/N_S]		NUE [KG G_W/KG N]		N RETENTION [N_{AV}/N_S]		NBI		N LOSSES [KG/HA]	
			$\bar{x}$	σ	$\bar{x}$	σ	$\bar{x}$	σ	$\bar{x}$	σ	$\bar{x}$	σ	$\bar{x}$	σ	$\bar{x}$	σ
C2012_T2	HRWW	4.6	4.6	1.4	111	12	NA	NA	NA	NA	NA	NA	0.76	0.22	NA	NA
C2013_T2	HRSW	3.2	3.2	1.3	171	8	0.42	0.14	12.6	4.26	0.65	0.03	0.67	0.29	84.6	30.1
C2014_T2	HRSW	2.0	2.0	0.8	165	4	0.23	0.09	7.0	2.65	0.67	0.02	0.45	0.18	113.1	82.1
C2015_T2	HRWW	5.3	5.3	1.4	127	14	0.50	0.14	18.7	5.45	0.93	0.03	0.99	0.29	78.3	121.4
C2015_T3	HRWW	5.6	5.6	1.2	134	10	NA	NA	NA	NA	NA	0.05	1.12	0.28	NA	NA
COLFAX			**4.2**	**1.8**	**142**	**25**	**0.38**	**0.17**	**12.8**	**6.4**	**0.75**	**0.22**	**0.80**	**0.35**	**65.6**	**93.0**
G2012_T2	HRSW	587	4.2	1.1	151	7	NA	NA	18.8	4.40	NA	NA	1.35	0.31	NA	NA
G2015_T2	SWWW	600	7.2	1.5	101	10	0.66	0.14	30.9	7.40	0.84	0.02	1.08	0.17	75.7	89.8
G2015_T3	SWWW	600	7.9	2.0	100	8	NA	NA	NA	NA	NA	0.03	1.23	0.26	NA	NA
G2016_T2	HRSW	625	5.0	1.3	147	5	NA	NA	NA	NA	NA	NA	1.65	0.50	NA	NA
G2016_T3	HRSW	625	5.2	1.4	147	5	NA	NA	NA	NA	NA	NA	1.77	0.60	NA	NA
GENESEE			**5.9**	**2.0**	**129**	**25**	**0.66**	**0.14**	**25.1**	**8.6**	**0.84**	**0.19**	**1.42**	**0.47**	**53.1**	**89.8**
L2013_T2	SWWW	631	5.7	1.0	97	9	0.49	0.07	25.2	4.50	0.62	0.02	0.84	0.13	87.5	29.3
L2014_T2	SWSW	541	2.8	0.4	161	14	0.60	0.10	17.3	2.70	0.90	0.03	0.95	0.14	31.1	27.1
L2016_T2	SWWW	608	5.8	1.5	86	5	NA	NA	NA	NA	NA	NA	0.78	0.22	NA	NA
L2016_T3	SWWW	608	5.6	0.6	90	5	NA	NA	NA	NA	NA	NA	0.76	0.09	NA	NA
LELAND			**4.9**	**1.6**	**110**	**33**	**0.55**	**0.10**	**21.2**	**5.4**	**0.76**	**0.20**	**0.84**	**0.17**	**53.5**	**44.4**
T2013_T2	HRWW	580	6.8	1.0	121	11	0.63	0.12	26.0	4.35	0.71	0.02	0.92	0.16	83.6	48.6
T2015_T2	HRWW	605	6.3	1.5	96	8	NA	NA	NA	NA	NA	0.04	0.67	0.16	NA	NA
T2015_T3	HRWW	605	5.3	1.2	100	16	NA	NA	NA	NA	NA	0.10	0.62	0.14	NA	NA
TROY			**6.1**	**1.3**	**105**	**16**	**0.63**	**0.12**	**26.0**	**4.4**	**0.71**	**0.13**	**0.74**	**0.20**	**83.6**	**48.5**
REGIONAL			5.2	1.9			0.50	0.18	19.6	8.55	0.76	0.22	0.98	0.44	62.4	75.8

C= Colfax, G =Genesee, L=Leland, T = Troy

APPENDIX 1.C: NBI ANOVA STATISTICS OUTPUTS

Table A1.C-1: Wheat class ANOVA test outputs.

ANOVA: SINGLE FACTOR

SUMMARY						
GROUPS	*COUNT*	*SUM*	*AVERAGE*	*VARIANCE*		
HARD RED	*131*	*130.49*	*1.00*	*0.26*		
SOFT WHITE	*68*	*64.62*	*0.95*	*0.06*		
ANOVA						
SOURCE OF VARIATION	*SS*	*DF*	*MS*	*F*	*P-VALUE*	*F CRIT*
BETWEEN GROUPS	*0.09*	*1*	*0.09*	*0.49*	*0.49*	*3.89*
WITHIN GROUPS	*38.3*	*197*	*0.19*			
TOTAL	*38.4*	*198*				

Table A1.C-2: Wheat season ANOVA test outputs.

ANOVA: SINGLE FACTOR

SUMMARY						
GROUPS	*COUNT*	*SUM*	*AVERAGE*	*VARIANCE*		
WINTER	*128*	*114.37*	*0.89*	*0.07*		
SPRING	*71*	*80.74*	*1.14*	*0.37*		
ANOVA						
SOURCE OF VARIATION	*SS*	*DF*	*MS*	*F*	*P-VALUE*	*F CRIT*
BETWEEN GROUPS	*2.7*	*1*	*2.71*	*14.99*	*0.00*	*3.89*
WITHIN GROUPS	*35.6*	*197*	*0.18*			
TOTAL	*38.4*	*198*				

Table A1.C-3: Hard red class ANOVA test outputs.

ANOVA: SINGLE FACTOR

SUMMARY						
GROUPS	*COUNT*	*SUM*	*AVERAGE*	*VARIANCE*		
HRWW	*72*	*61.16*	*0.85*	*0.08*		
HRSW	*59*	*69.33*	*1.18*	*0.44*		
ANOVA						
SOURCE OF VARIATION	*SS*	*DF*	*MS*	*F*	*P-VALUE*	*F CRIT*
BETWEEN GROUPS	*3.44*	*1*	*3.44*	*14.39*	*0.00*	*3.91*
WITHIN GROUPS	*30.8*	*129*	*0.24*			
TOTAL	*34.3*	*130*				

Table A1.C-4: Soft white class ANOVA test outputs.

ANOVA: SINGLE FACTOR

SUMMARY						
GROUPS	*COUNT*	*SUM*	*AVERAGE*	*VARIANCE*		
SWWW	*56*	*53.21*	*0.95*	*0.07*		
SWSW	*12*	*11.41*	*0.95*	*0.02*		
ANOVA						
SOURCE OF VARIATION	*SS*	*DF*	*MS*	*F*	*P-VALUE*	*F CRIT*
BETWEEN GROUPS	*2E-06*	*1*	*2E-06*	*3E-05*	*1E+00*	*4E+00*
WITHIN GROUPS	*4E+00*	*66*	*6E-02*			
TOTAL	*4E+00*	*67*				

APPENDIX 1.D: FARM NBI SITE SUMMARIES

Table A1.D-1: Colfax relative yield by sample site summary.

	POSITION	2012	2013	2014	2015	REL_AVG	SD
COLFAX_1_T2	SFS	1.00	0.83	1.05	0.94	0.95	0.09
COLFAX_2_T2	SFS	1.62	1.04	1.21	0.96	1.21	0.29
COLFAX_3_T2	Draw	1.05	0.73	1.09	1.25	1.03	0.22
COLFAX_4_T2	SFS	0.58	0.34	0.41	0.55	0.47	0.11
COLFAX_5_T2	Draw	1.08	1.38	1.39	1.24	1.28	0.14
COLFAX_6_T2	Draw	0.54	1.48	1.51	1.24	1.19	0.45
COLFAX_7_T2	NFS	0.92	1.17	0.95	0.93	0.99	0.12
COLFAX_8_T2	Flat	0.75	0.29	0.29	0.50	0.46	0.22
COLFAX_9_T2	NFS	1.15	0.95	0.71	0.85	0.92	0.19
COLFAX_10_T2	NFS	1.24	0.96	0.78	0.94	0.98	0.19
COLFAX_11_T2	NFS		1.23	1.05	0.94	1.07	0.15
COLFAX_12_T2	Draw	1.08	1.60	1.56	1.23	1.37	0.25
COLFAX_1_T3	NFS				1.24		
COLFAX_2_T3	NFS				1.25		
COLFAX_3_T3	Flat				0.84		
COLFAX_4_T3	SFS				1.14		
COLFAX_5_T3	Draw				1.11		
COLFAX_6_T3	NFS				0.62		
COLFAX_7_T3	NFS				0.59		
COLFAX_8_T3	NFS				1.26		
COLFAX_9_T3	Draw				1.26		
COLFAX_10_T3	NFS				0.94		
COLFAX_11_T3	SFS				1.01		
COLFAX_12_T3	Flat				1.07		
COLFAX_13_T3	Flat				1.11		

Table A1.D-2: Colfax relative nitrogen balance index by sample site summary.

	POSITION	2012	2013	2014	2015	REL_AVG	SD
COLFAX_1_T2	SFS	0.83	0.81	1.05	0.69	0.85	0.15
COLFAX_2_T2	SFS	1.39	0.97	1.22	0.80	1.10	0.26
COLFAX_3_T2	Draw	1.16	0.75	1.07	1.36	1.09	0.25
COLFAX_4_T2	SFS	0.54	0.33	0.40	0.48	0.44	0.09
COLFAX_5_T2	Draw	1.19	1.48	1.43	1.24	1.33	0.14
COLFAX_6_T2	Draw	0.62	1.58	1.48	1.18	1.22	0.43
COLFAX_7_T2	NFS	0.81	1.17	0.94	0.98	0.97	0.15
COLFAX_8_T2	Flat	0.82	0.28	0.30	0.50	0.48	0.25
COLFAX_9_T2	NFS	1.20	0.93	0.71	0.96	0.95	0.20
COLFAX_10_T2	NFS	1.35	0.90	0.74	0.96	0.99	0.26
COLFAX_11_T2	NFS		1.23	1.07	0.93	1.08	0.15
COLFAX_12_T2	Draw	1.09	1.55	1.57	1.15	1.34	0.26
COLFAX_1_T3	NFS				1.27		
COLFAX_2_T3	NFS				1.37		
COLFAX_3_T3	Flat				0.74		
COLFAX_4_T3	SFS				1.15		
COLFAX_5_T3	Draw				1.13		
COLFAX_6_T3	NFS				0.69		
COLFAX_7_T3	NFS				0.54		
COLFAX_8_T3	NFS				1.31		
COLFAX_9_T3	Draw				1.33		
COLFAX_10_T3	NFS				0.98		
COLFAX_11_T3	SFS				1.12		
COLFAX_12_T3	Flat				1.14		
COLFAX_13_T3	Flat				1.01		

Table A1.D-3: Colfax relative returns to risk by sample site summary.

	POSITION	2012	2013	2014	2015	REL_AVG	SD
COLFAX_1_T2	SFS	0.90	0.29	-0.11	0.96	0.51	0.51
COLFAX_2_T2	SFS	2.13	0.78	0.48	0.99	1.10	0.72
COLFAX_3_T2	Draw	1.00	0.06	0.03	1.57	0.67	0.75
COLFAX_4_T2	SFS	0.06	-0.83	-2.43	0.18	-0.75	1.20
COLFAX_5_T2	Draw	1.07	1.55	1.16	1.56	1.34	0.26
COLFAX_6_T2	Draw	-0.01	1.78	1.59	1.54	1.23	0.83
COLFAX_7_T2	NFS	0.75	1.08	-0.47	0.92	0.57	0.71
COLFAX_8_T2	Flat	0.41	-0.94	-2.87	0.07	-0.83	1.47
COLFAX_9_T2	NFS	1.21	0.57	-1.33	0.77	0.31	1.13
COLFAX_10_T2	NFS	1.38	0.61	-1.11	0.95	0.46	1.09
COLFAX_11_T2	NFS		1.22	-0.09	0.95	0.69	0.69
COLFAX_12_T2	Draw	1.06	2.05	1.75	1.53	1.60	0.41
COLFAX_1_T3	NFS				0.77		
COLFAX_2_T3	NFS				0.95		
COLFAX_3_T3	Flat				0.95		
COLFAX_4_T3	SFS				1.53		
COLFAX_5_T3	Draw				1.35		
COLFAX_6_T3	NFS				1.38		
COLFAX_7_T3	NFS				0.67		
COLFAX_8_T3	NFS				1.18		
COLFAX_9_T3	Draw				1.13		
COLFAX_10_T3	NFS				0.28		
COLFAX_11_T3	SFS				0.23		
COLFAX_12_T3	Flat				1.39		
COLFAX_13_T3	Flat				1.40		

Table A1.D-4: Genesee relative yield by sample site summary.

	POSITION	2012	2013	2014	2015	2016	REL_AVG	SD
GENESEE_1_T2	Draw				1.03	0.82	0.93	0.15
GENESEE_2_T2	SFS	0.87			0.85	0.77	0.83	0.06
GENESEE_3_T2	SFS	1.43			1.27	1.21	1.30	0.11
GENESEE_4_T2	SFS	1.02			0.93	0.84	0.93	0.09
GENESEE_5_T2	SFS	0.80			0.73	0.78	0.77	0.03
GENESEE_6_T2	Flat	1.22			1.15	1.10	1.16	0.06
GENESEE_7_T2	SFS	1.20			1.12	1.76	1.36	0.35
GENESEE_8_T2	Flat	1.03			0.88	0.81	0.91	0.11
GENESEE_9_T2	SFS	0.88			0.82	0.68	0.79	0.10
GENESEE_10_T2	NFS	0.59			0.69	0.89	0.72	0.15
GENESEE_11_T2	Draw	1.32			1.18	1.04	1.18	0.14
GENESEE_12_T2	NFS	0.63			0.74	0.86	0.74	0.11
GENESEE_1_T3	Flat				0.75	0.76	0.76	0.01
GENESEE_2_T3	SFS				0.97	1.31	1.14	0.24
GENESEE_3_T3	Draw				1.55	1.07	1.31	0.34
GENESEE_4_T3	NFS				1.25	1.09	1.17	0.11
GENESEE_5_T3	NFS				0.74	1.75	1.24	0.72
GENESEE_6_T3	NFS				1.00	0.76	0.88	0.17
GENESEE_7_T3	NFS				0.71	0.79	0.75	0.06
GENESEE_8_T3	NFS				1.21	1.61	1.41	0.28
GENESEE_9_T3	NFS				1.24	1.02	1.13	0.16
GENESEE_10_T3	SFS				1.28	0.69	0.98	0.42
GENESEE_11_T3	SFS				1.13	0.81	0.97	0.23
GENESEE_12_T3	SFS				0.80	0.80	0.80	0.00

Table A1.D-5: Genesee relative nitrogen balance index by sample site summary.

	POSITION	2012	2013	2014	2015	2016	REL_AVG	SD
GENESEE_1_T2	Draw				0.92	0.82	0.87	0.07
GENESEE_2_T2	SFS	1.01			1.13	0.77	0.97	0.18
GENESEE_3_T2	SFS	1.28			1.15	1.21	1.21	0.07
GENESEE_4_T2	SFS	0.92			0.73	0.84	0.83	0.09
GENESEE_5_T2	SFS	1.04			0.95	0.78	0.93	0.13
GENESEE_6_T2	Flat	1.40			1.16	1.10	1.22	0.16
GENESEE_7_T2	SFS	0.98			0.85	1.76	1.20	0.49
GENESEE_8_T2	Flat	0.93			0.74	0.81	0.82	0.10
GENESEE_9_T2	SFS	0.79			0.84	0.68	0.77	0.08
GENESEE_10_T2	NFS	0.69			0.90	0.89	0.83	0.12
GENESEE_11_T2	Draw	1.23			0.91	1.04	1.06	0.16
GENESEE_12_T2	NFS	0.72			0.96	0.86	0.85	0.12
GENESEE_1_T3	Flat				0.69	0.76	0.73	0.05
GENESEE_2_T3	SFS				1.13	1.31	1.22	0.12
GENESEE_3_T3	Draw				1.11	1.07	1.09	0.03
GENESEE_4_T3	NFS				1.21	1.09	1.15	0.09
GENESEE_5_T3	NFS				1.50	1.75	1.62	0.17
GENESEE_6_T3	NFS				0.78	0.76	0.77	0.01
GENESEE_7_T3	NFS				0.88	0.79	0.84	0.06
GENESEE_8_T3	NFS				1.30	1.61	1.45	0.22
GENESEE_9_T3	NFS				0.97	1.02	0.99	0.03
GENESEE_10_T3	SFS				1.11	0.69	0.90	0.30
GENESEE_11_T3	SFS				1.01	0.81	0.91	0.14
GENESEE_12_T3	SFS				1.06	0.80	0.93	0.19

Table A1.D-6: Genesee relative returns to risk by sample site summary.

	POSITION	2012	2013	2014	2015	2016	REL_AVG	SD
GENESEE_1_T2	Draw				1.11	0.98	1.05	0.09
GENESEE_2_T2	SFS	0.80			0.88	0.57	0.75	0.16
GENESEE_3_T2	SFS	1.75			1.46	1.58	1.60	0.15
GENESEE_4_T2	SFS	1.02			0.95	1.06	1.01	0.05
GENESEE_5_T2	SFS	0.66			0.70	0.56	0.64	0.07
GENESEE_6_T2	Flat	1.43			1.33	1.09	1.28	0.17
GENESEE_7_T2	SFS	1.31			1.21	1.79	1.44	0.31
GENESEE_8_T2	Flat	1.04			0.89	0.94	0.96	0.08
GENESEE_9_T2	SFS	0.78			0.79	0.70	0.76	0.05
GENESEE_10_T2	NFS	0.29			0.64	0.72	0.55	0.23
GENESEE_11_T2	Draw	1.56			1.33	1.30	1.40	0.14
GENESEE_12_T2	NFS	0.36			0.71	0.70	0.59	0.20
GENESEE_1_T3	Flat				0.60	0.76	0.68	0.12
GENESEE_2_T3	SFS				0.91	1.24	1.08	0.24
GENESEE_3_T3	Draw				1.60	1.64	1.62	0.03
GENESEE_4_T3	NFS				1.24	1.41	1.32	0.12
GENESEE_5_T3	NFS				0.65	0.65	0.65	0.00
GENESEE_6_T3	NFS				0.92	0.78	0.85	0.10
GENESEE_7_T3	NFS				0.58	0.56	0.57	0.01
GENESEE_8_T3	NFS				1.22	1.53	1.38	0.22
GENESEE_9_T3	NFS				1.23	1.36	1.29	0.09
GENESEE_10_T3	SFS				1.28	0.65	0.96	0.44
GENESEE_11_T3	SFS				1.08	0.91	1.00	0.12
GENESEE_12_T3	SFS				0.69	0.51	0.60	0.13

Table A1.D-7: Leland relative yield by sample site summary.

	POSITION	2012	2013	2014	2015	2016	REL_AVG	SD
LELAND_1_T2	NFS		0.88	1.19		0.63	0.90	0.28
LELAND_2_T2	NFS		1.20	1.14		1.49	1.27	0.19
LELAND_3_T2	Flat		0.75	0.91		0.79	0.82	0.08
LELAND_4_T2	Draw		1.12	1.17		1.14	1.14	0.03
LELAND_5_T2	Flat		0.97	0.93		1.53	1.15	0.34
LELAND_6_T2	Flat		1.04	0.92		1.03	1.00	0.07
LELAND_7_T2	Flat		0.85	0.77		0.79	0.80	0.04
LELAND_8_T2	Draw		1.06	0.99		1.11	1.06	0.06
LELAND_9_T2	Flat		1.10	1.13		1.00	1.08	0.07
LELAND_10_T2	SFS		1.26	0.94		0.80	1.00	0.24
LELAND_11_T2	SFS		0.70	0.98		1.03	0.90	0.18
LELAND_12_T2	NFS		1.07	0.92		0.75	0.91	0.16
LELAND_1_T3	Flat					1.09		
LELAND_2_T3	Flat					0.92		
LELAND_3_T3	Draw					0.85		
LELAND_4_T3	Draw					0.88		
LELAND_5_T3	Flat					1.05		
LELAND_6_T3	Flat					0.90		
LELAND_7_T3	Draw							
LELAND_8_T3	Draw							
LELAND_9_T3	Draw					1.07		
LELAND_10_T3	Draw							
LELAND_11_T3	Draw							
LELAND_12_T3	Draw					1.14		

Table A1.D-8: Leland relative nitrogen balance index by sample site summary.

	POSITION	2012	2013	2014	2015	2016	REL_AVG	SD
LELAND_1_T2	NFS		1.04	1.14		0.63	0.94	0.27
LELAND_2_T2	NFS		1.22	1.08		1.49	1.26	0.21
LELAND_3_T2	Flat		0.69	1.00		0.79	0.83	0.16
LELAND_4_T2	Draw		1.16	1.17		1.14	1.16	0.02
LELAND_5_T2	Flat		0.91	0.74		1.53	1.06	0.42
LELAND_6_T2	Flat		0.94	0.95		1.03	0.97	0.05
LELAND_7_T2	Flat		0.93	0.86		0.79	0.86	0.07
LELAND_8_T2	Draw		1.19	1.05		1.11	1.12	0.07
LELAND_9_T2	Flat		1.03	1.20		1.00	1.08	0.11
LELAND_10_T2	SFS		1.06	0.78		0.80	0.88	0.16
LELAND_11_T2	SFS		0.80	1.08		1.03	0.97	0.15
LELAND_12_T2	NFS		1.05	0.93		0.75	0.91	0.15
LELAND_1_T3	Flat					1.09		
LELAND_2_T3	Flat					0.92		
LELAND_3_T3	Draw					0.85		
LELAND_4_T3	Draw					0.88		
LELAND_5_T3	Flat					1.05		
LELAND_6_T3	Flat					0.90		
LELAND_7_T3	Draw							
LELAND_8_T3	Draw							
LELAND_9_T3	Draw					1.07		
LELAND_10_T3	Draw							
LELAND_11_T3	Draw							
LELAND_12_T3	Draw					1.14		

Table A1.D-9: Leland relative returns to risk by sample site summary.

	POSITION	2012	2013	2014	2015	2016	REL_AVG	SD
LELAND_1_T2	NFS		0.81	1.70		0.37	0.96	0.68
LELAND_2_T2	NFS		1.32	1.50		1.53	1.45	0.11
LELAND_3_T2	Flat		0.59	0.70		0.68	0.66	0.06
LELAND_4_T2	Draw		1.20	1.64		1.12	1.32	0.28
LELAND_5_T2	Flat		0.96	0.78		1.89	1.21	0.59
LELAND_6_T2	Flat		1.07	0.71		1.05	0.94	0.20
LELAND_7_T2	Flat		0.76	0.19		0.70	0.55	0.31
LELAND_8_T2	Draw		1.11	0.99		0.95	1.02	0.08
LELAND_9_T2	Flat		1.17	1.47		1.01	1.22	0.24
LELAND_10_T2	SFS		1.38	0.64		0.99	1.00	0.37
LELAND_11_T2	SFS		0.51	0.94		1.09	0.85	0.30
LELAND_12_T2	NFS		1.11	0.73		0.64	0.83	0.25
LELAND_1_T3	Flat					1.05		
LELAND_2_T3	Flat					0.74		
LELAND_3_T3	Draw					0.82		
LELAND_4_T3	Draw					1.10		
LELAND_5_T3	Flat					1.10		
LELAND_6_T3	Flat					1.08		
LELAND_7_T3	Draw							
LELAND_8_T3	Draw							
LELAND_9_T3	Draw					0.94		
LELAND_10_T3	Draw							
LELAND_11_T3	Draw							
LELAND_12_T3	Draw					1.17		

Table A1.D-10: Troy relative yield by sample site summary.

	POSITION	2012	2013	2014	2015	2016	REL_AVG	SD
TROY_1_T2	Flat		1.22		1.20		1.21	0.01
TROY_2_T2	Flat		0.83		1.29		1.06	0.32
TROY_3_T2	Draw		1.01		1.07		1.04	0.04
TROY_4_T2	NFS		0.90		0.59		0.75	0.22
TROY_5_T2	NFS		0.85		0.73		0.79	0.08
TROY_6_T2	Draw		0.96		1.20		1.08	0.17
TROY_7_T2	SFS		0.85		1.40		1.13	0.39
TROY_8_T2	SFS		1.07		1.24		1.15	0.11
TROY_9_T2	SFS		0.95		0.94		0.95	0.00
TROY_10_T2	SFS		1.24		1.40		1.32	0.11
TROY_11_T2	Draw		1.15		1.01		1.08	0.10
TROY_12_T2	NFS		0.97		0.96		0.96	0.00
TROY_1_T3	SFS				0.77			
TROY_2_T3	NFS				0.98			
TROY_3_T3	Draw				0.85			
TROY_4_T3	Flat				0.64			
TROY_5_T3	NFS				1.08			
TROY_6_T3	Flat				0.96			
TROY_7_T3	NFS				0.71			
TROY_8_T3	Flat				1.02			
TROY_9_T3	SFS				1.06			
TROY_10_T3	Draw				1.32			
TROY_11_T3	SFS				0.63			
TROY_12_T3	Draw				0.96			

Table A1.D-11: Troy relative nitrogen balance index by sample site summary.

	POSITION	2012	2013	2014	2015	2016	REL_AVG	SD
TROY_1_T2	Flat		0.88		1.23		1.06	0.25
TROY_2_T2	Flat		0.85		1.22		1.04	0.26
TROY_3_T2	Draw		1.03		0.91		0.97	0.09
TROY_4_T2	NFS		0.72		0.60		0.66	0.08
TROY_5_T2	NFS		1.00		0.70		0.85	0.21
TROY_6_T2	Draw		1.06		1.29		1.17	0.16
TROY_7_T2	SFS		1.10		1.36		1.23	0.19
TROY_8_T2	SFS		0.90		1.13		1.02	0.16
TROY_9_T2	SFS		1.12		0.86		0.99	0.18
TROY_10_T2	SFS		1.07		1.28		1.17	0.15
TROY_11_T2	Draw		1.38		1.02		1.20	0.25
TROY_12_T2	NFS		0.89		0.80		0.84	0.06
TROY_1_T3	SFS				0.75			
TROY_2_T3	NFS				0.92			
TROY_3_T3	Draw				0.82			
TROY_4_T3	Flat				0.90			
TROY_5_T3	NFS				1.10			
TROY_6_T3	Flat				1.09			
TROY_7_T3	NFS				0.95			
TROY_8_T3	Flat				1.08			
TROY_9_T3	SFS				1.09			
TROY_10_T3	Draw				1.43			
TROY_11_T3	SFS				0.57			
TROY_12_T3	Draw				0.89			

Table A1.D-12: Troy relative returns to risk by sample site summary.

	POSITION	2012	2013	2014	2015	2016	REL_AVG	SD
TROY_1_T2	Flat		1.27		1.23		1.25	0.03
TROY_2_T2	Flat		0.75		1.33		1.04	0.41
TROY_3_T2	Draw		1.05		0.97		1.01	0.06
TROY_4_T2	NFS		0.75		0.23		0.49	0.37
TROY_5_T2	NFS		0.78		0.43		0.60	0.25
TROY_6_T2	Draw		0.96		1.19		1.07	0.16
TROY_7_T2	SFS		0.78		1.52		1.15	0.52
TROY_8_T2	SFS		1.09		1.21		1.15	0.08
TROY_9_T2	SFS		0.95		0.77		0.86	0.13
TROY_10_T2	SFS		1.37		1.47		1.42	0.07
TROY_11_T2	Draw		1.28		0.88		1.08	0.28
TROY_12_T2	NFS		0.97		0.79		0.88	0.13
TROY_1_T3	SFS				0.69			
TROY_2_T3	NFS				1.14			
TROY_3_T3	Draw				0.84			
TROY_4_T3	Flat				0.39			
TROY_5_T3	NFS				1.34			
TROY_6_T3	Flat				1.10			
TROY_7_T3	NFS				0.54			
TROY_8_T3	Flat				1.24			
TROY_9_T3	SFS				1.33			
TROY_10_T3	Draw				1.92			
TROY_11_T3	SFS				0.37			
TROY_12_T3	Draw				1.11			

APPENDIX 1.E: PROTIEN RELATIONSHIPS BY CLASS

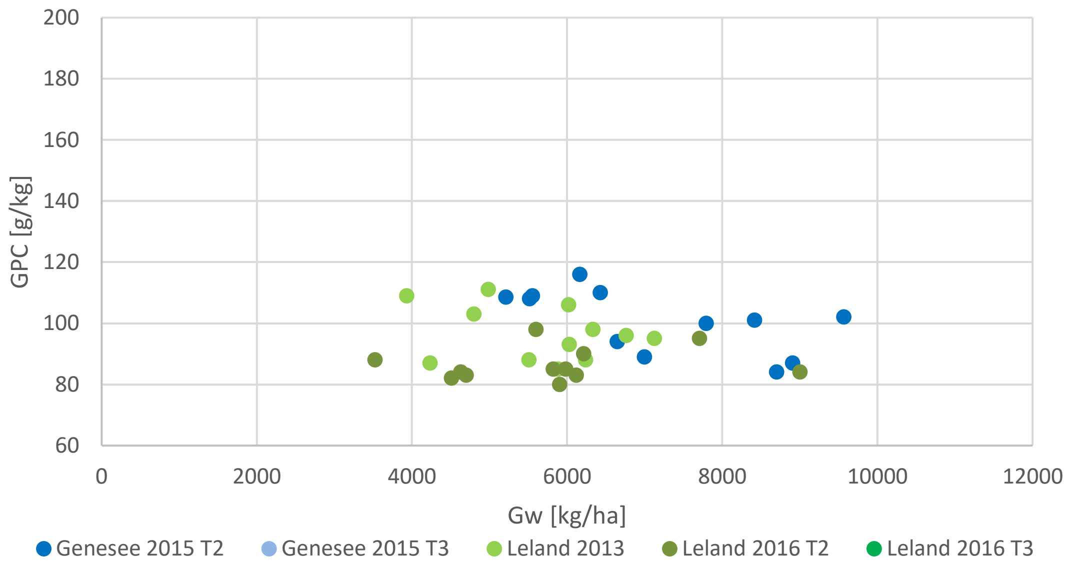

Figure A1.E-1: Soft white winter wheat grain protein concentration [g/kg] and yield [kg/ha] relationship.

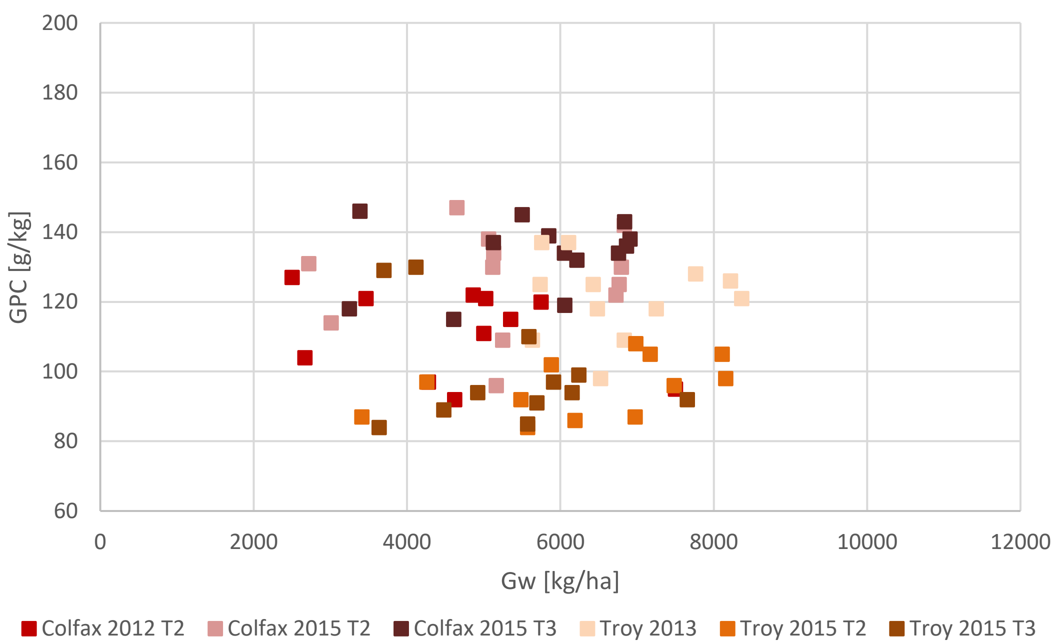

Figure A1.E-2: Hard red winter wheat grain protein concentration [g/kg] and yield [kg/ha] relationship.

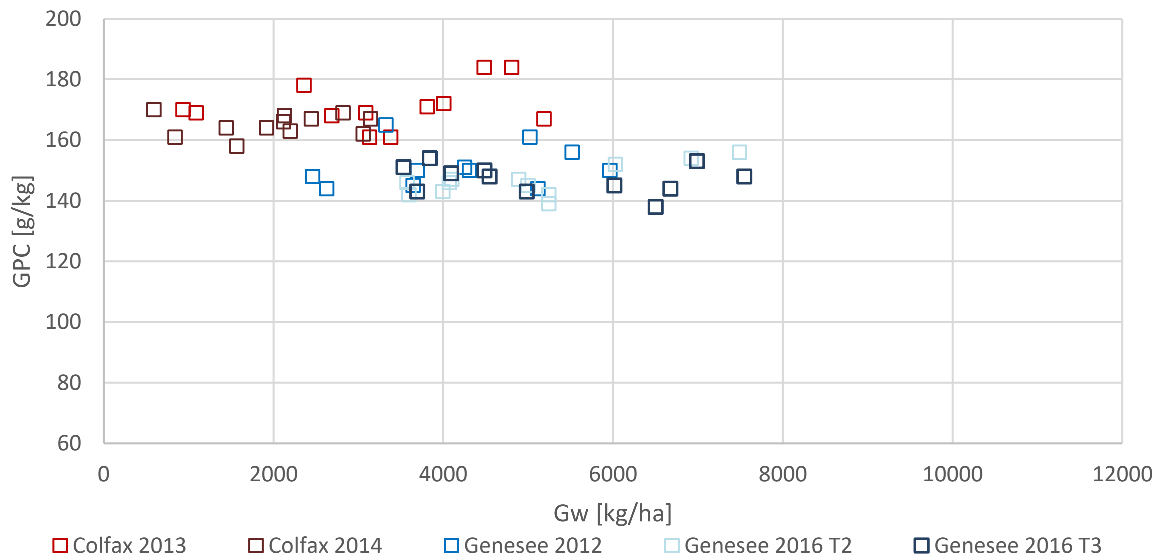

Figure A1.E-3: Hard red spring wheat grain protein concentration [g/kg] and yield [kg/ha] relationship.

APPENDIX 2: SUPPLEMENTAL MATERIALS FOR CHAPTER 3

APPENDIX 2.A: GROWING DEGREE DAY VS NDRE ANALYSIS FOR GRAIN N

Satellite image selection for this study was derived from the predictive power of the normalized difference red edge vegetative index (NDRE) to at harvest grain nitrogen concentration. For each summer image (up to five per growing season), NDRE was calculated for each sample site and evaluated based on its prediction power (R^2/RMSE) for grain N content at each location (Colfax, Genesee, Leland and Troy). The growing degree day (GDD) was calculated for each image to determine whether there were consistent trends for image acquisition. Growing degree day (GDD) calculations began at planting dates provided by the growers. Optimal GDD dates for spring wheat were between 1300-1500 GDD and winter wheat between 800-1000 GDD. Final dates chosen for this study can be seen in Table 2A-1. Prediction power of each summer image over a growing season for each location can be seen in Figures 3.A-1 to 2A-4. Prediction power of summer images by wheat class can be seen in Figures 2A-5 and 2A-6.

Table A2.A-1: Satellite image date selection for each farm by site average normalized difference red edge index (NDRE) and growing degree day (GDD) with RapidEye tile id (TID).

	Crop	Average NDRE	GDD
COLFAX (TID 1160613)			
6.25.2012 T2	HRWW	0.524	1482
7.8.2013 T2	HRSW	0.495	1039
6.19.2014 T2	HRSW	0.432	701
6.5.2015 T2	HRWW	0.538	1576
6.5.2015 T3	HRWW	0.559	1576
GENESEE (TID 1160515)			
7.10.2012 T2	HRSW	0.533	874
6.8.2015 T2	SWWW	0.609	1117
6.8.2015 T3	SWWW	0.618	1117
6.30.2016 T2	HRSW	0.581	828
6.30.2016 T3	HRSW	0.609	828
LELAND (TID 160516)			
6.6.2013 T2	SWWW	0.620	880
7.11.2014 T2	SWSW	0.559	882
6.6.2016 T2	SWWW	0.554	1270
6.6.2016 T3	SWWW	0.460	1270
TROY (TID 1160615)			
6.6.2013 T2	HRWW	0.582	718
6.8.2015 T2	HRWW	0.586	935
6.8.2015 T3	HRWW	0.562	935

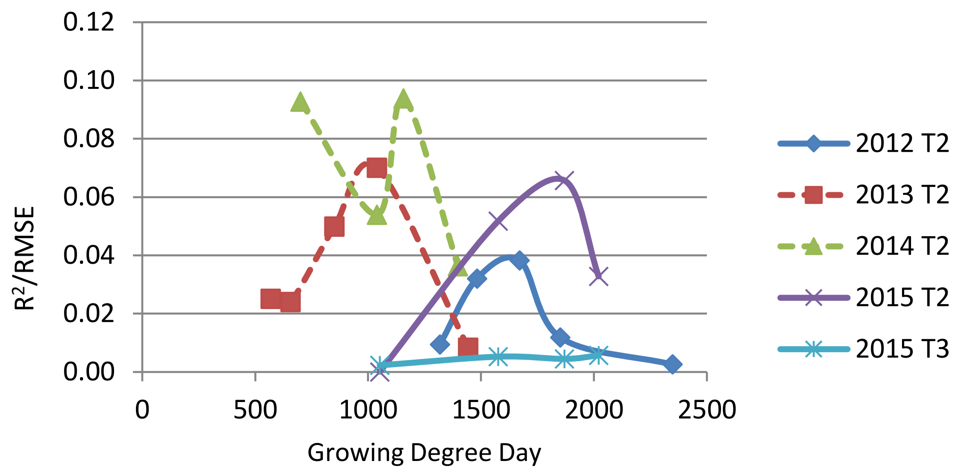

Figure A2.A-1: Summer satellite images in predicting grain N [kg/ha] at Colfax sample sites.

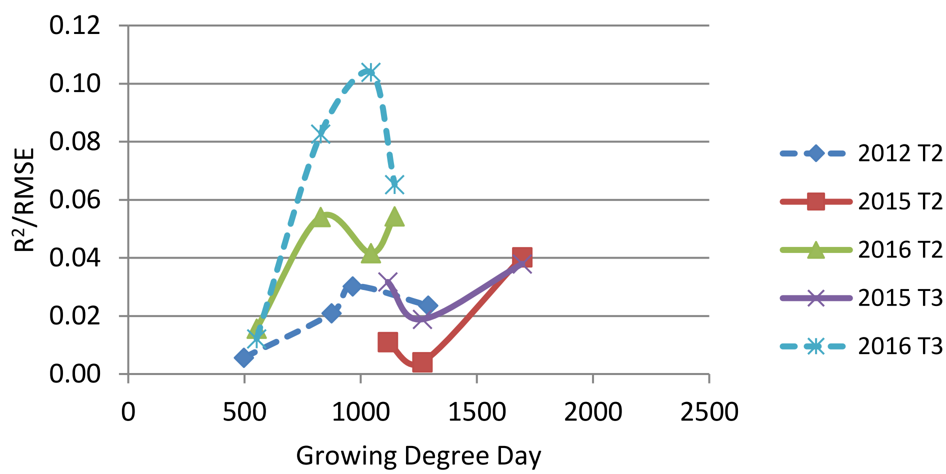

Figure A2.A-2: Summer satellite images in predicting grain N [kg/ha] at Genesee sample sites.

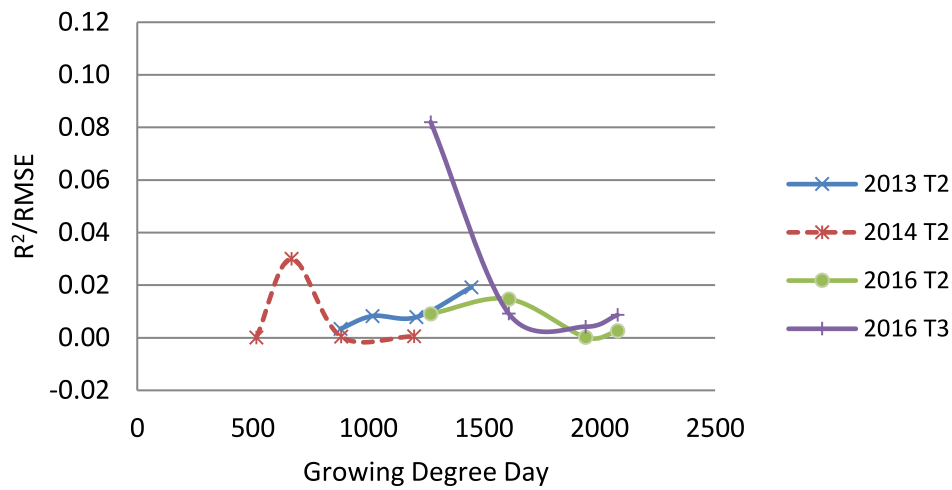

Figure A2.A-3: Summer satellite images in predicting grain N [kg/ha] at Leland sample sites.

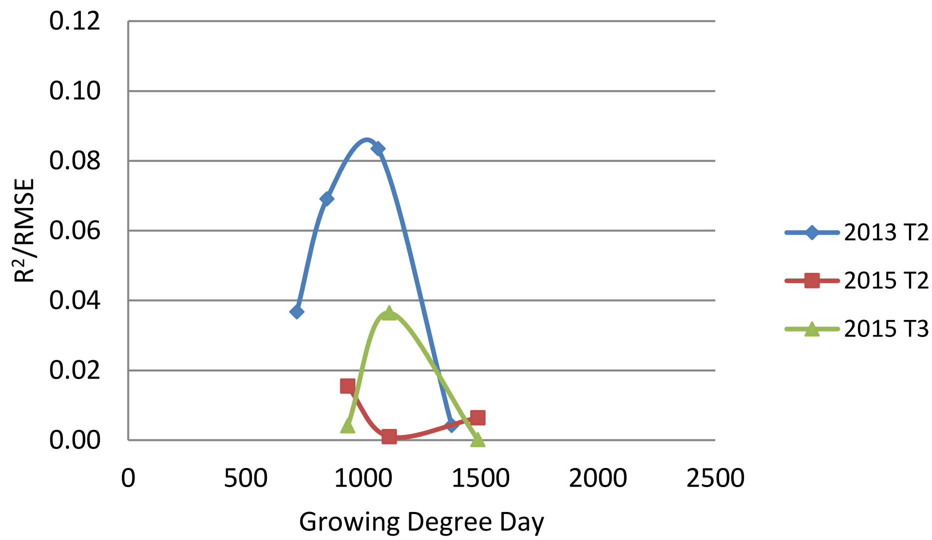

Figure A2.A-4: Summer satellite images in predicting grain N [kg/ha] at Colfax sample sites.

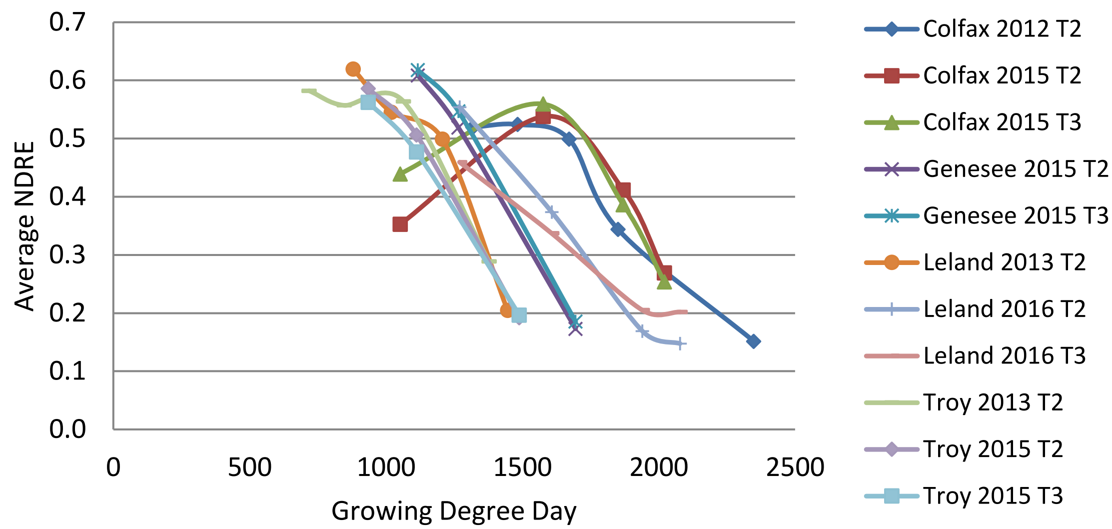

Figure A2.A-5: Summer satellite images in predicting grain N [kg/ha] at winter wheat sample sites.

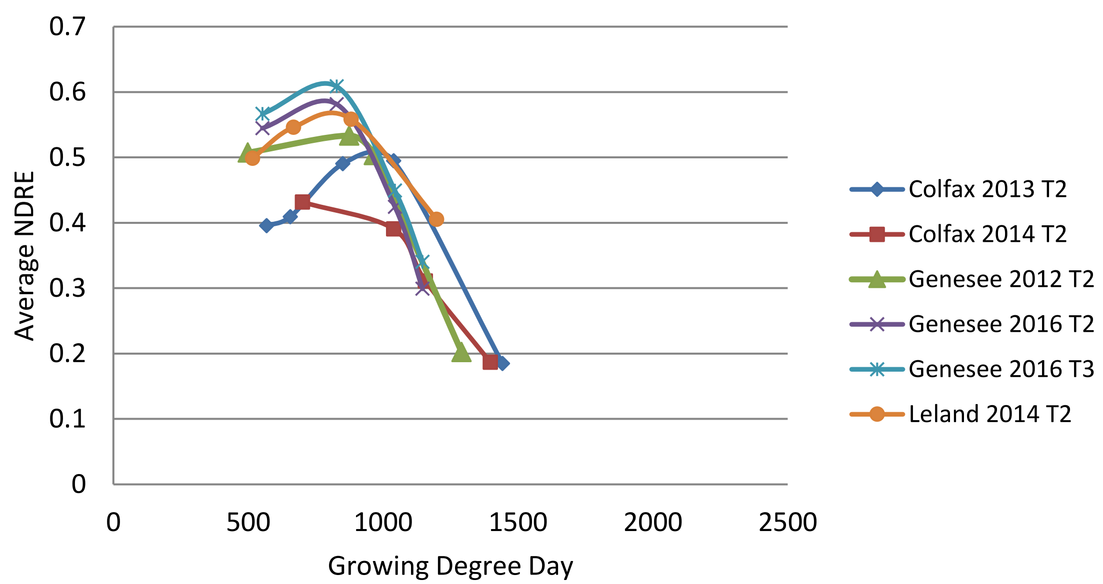

Figure A2.A-6: Summer satellite images in predicting grain N [kg/ha] at spring wheat sample sites.

APPENDIX 2.B: NITROGEN HARVEST INDEX TABLES AND FIGURES

Previous research has suggested that the nitrogen harvest index (NHI) is a consistent ratio within the region of study for individual wheat classes. These data suggest that seasonal variability is statistically significant (ANOVA, Table 3.B-1) between spring and winter wheat whereas wheat class (i.e. hard red vs soft white) was not statistically significant (ANOVA, Table 3.B-2). Within each seasonal group (i.e. winter wheat and spring wheat) wheat class was significantly different (ANOVA Tables 3.B-3, 3.B-4). ANOVA, F-tests and t-tests were conducted in Microsoft Excel 2013. Data included in these results include the Site-Specific Climate Friendly Farming (SCF) project and the Davenport and Pullman locations discussed in (Maaz et al., 2017).

Winter wheat had higher total N content in the total aboveground biomass than spring wheat. This may be due to physiological differences and longer growth periods allowing for more N uptake. However, spring wheat had a higher NHI than winter wheat. This may suggest that spring wheat are more efficient at allocating N to the grain or that winter wheat must allocate more to growth during the long growing season and is less efficient but ultimately obtains a greater N concentration in the total aboveground biomass. Hard red wheat had higher N contents than soft white. This is likely due to genetic selection for high protein in hard reds for wheat quality standards.

Table A2.B-1: ANOVA nitrogen harvest index summary statistics for winter and spring wheat.

ANOVA: Single Factor

SUMMARY						
Groups	*Count*	*Sum*	*Average*	*Variance*	*σ*	
Spring	108	88	0.81	0.0068	0.082	
Winter	350	272	0.78	0.0051	0.071	
ANOVA						
Source of Variation	*SS*	*df*	*MS*	*F*	*P-value*	*F crit*
Between Groups	0.10	1	0.096	17.6	3.3E-05	3.9
Within Groups	2.5	456	0.0055			
Total	2.6	457				

Table A2.B-2: ANOVA nitrogen harvest index summary statistics for hard red and soft white wheat.

ANOVA: Single Factor

SUMMARY						
Groups	*Count*	*Sum*	*Average*	*Variance*	*σ*	
Hard Red	83	64	0.78	0.008	0.091	
Soft White	375	295	0.79	0.005	0.071	
ANOVA						
Source of Variation	*SS*	*df*	*MS*	*F*	*P-value*	*F crit*
Between Groups	0.0	1	0.0087	1.5	0.2	3.9
Within Groups	2.6	456	0.0057			
Total	2.6	457				

Table A2.B-3: ANOVA nitrogen harvest index summary statistics for class differences in spring wheat.

ANOVA: Single Factor

SUMMARY						
Groups	*Count*	*Sum*	*Average*	*Variance*	*σ*	
HRSW	24	20.3	0.85	0.0022	0.047	
SWSW	84	67.3	0.80	0.0076	0.087	
ANOVA						
Source of Variation	*SS*	*df*	*MS*	*F*	*P-value*	*F crit*
Between Groups	0.04	1	0.038	5.8	0.0	3.9
Within Groups	0.69	106	0.0065			
Total	0.72	107				

Table A2.B-4: ANOVA nitrogen harvest index summary statistics for class differences in winter wheat.

ANOVA: Single Factor

SUMMARY						
Groups	*Count*	*Sum*	*Average*	*Variance*	*σ*	
HRWW	59	44	0.75	0.008	0.089	
SWWW	291	228	0.78	0.004	0.066	
ANOVA						
Source of Variation	*SS*	*df*	*MS*	*F*	*P-value*	*F crit*
Between Groups	0.063	1	0.063	12.9	0.00038	3.9
Within Groups	1.7	348	0.0049			
Total	1.8	349				

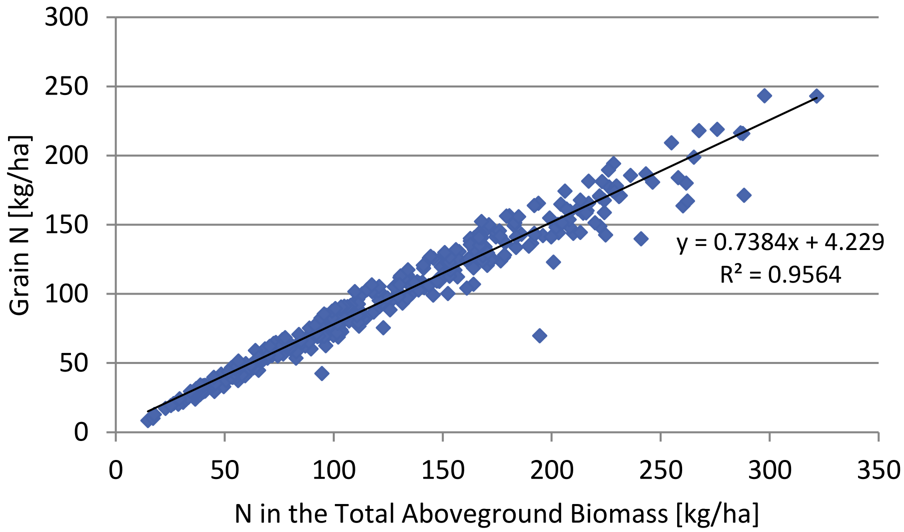

Figure A2.B-1: Nitrogen Harvest Index for mixed class winter wheat.

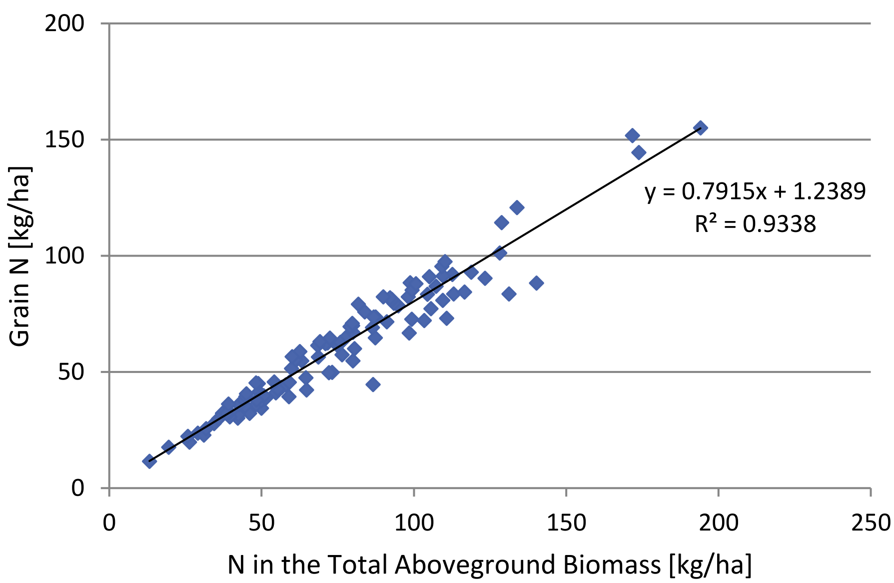

Figure A2.B-2: Nitrogen Harvest Index for mixed class spring wheat.

APPENDIX 2.C: LINEAR REGRESSION NG VS NDRE

lm(formula = Ng_kgpha~ NDRE + Class, data = T2, na.action = na.exclude)

Coefficients:	Estimate	Std. Error	t value	Pr(>|t|)
(Intercept)	-51.4	11.6	-4.4	1.86e-05 ***
NDRE	312.9	22.5	13.9	< 2e-16 ***
ClassSoft White	-35.0	4.4	-7.9	6.24e-13 ***

Signif. codes: 0 ‘***’ 0.001 ‘**’ 0.01 ‘*’ 0.05 ‘.’ 0.1 ‘ ’ 1

Residual standard error: 22.8 on 139 degrees of freedom

Multiple R-squared: 0.59, Adjusted R-squared: 0.58

F-statistic: 100.2 on 2 and 139 DF, p-value: < 2.2e-16

RMSE = 28.1 kg/ha

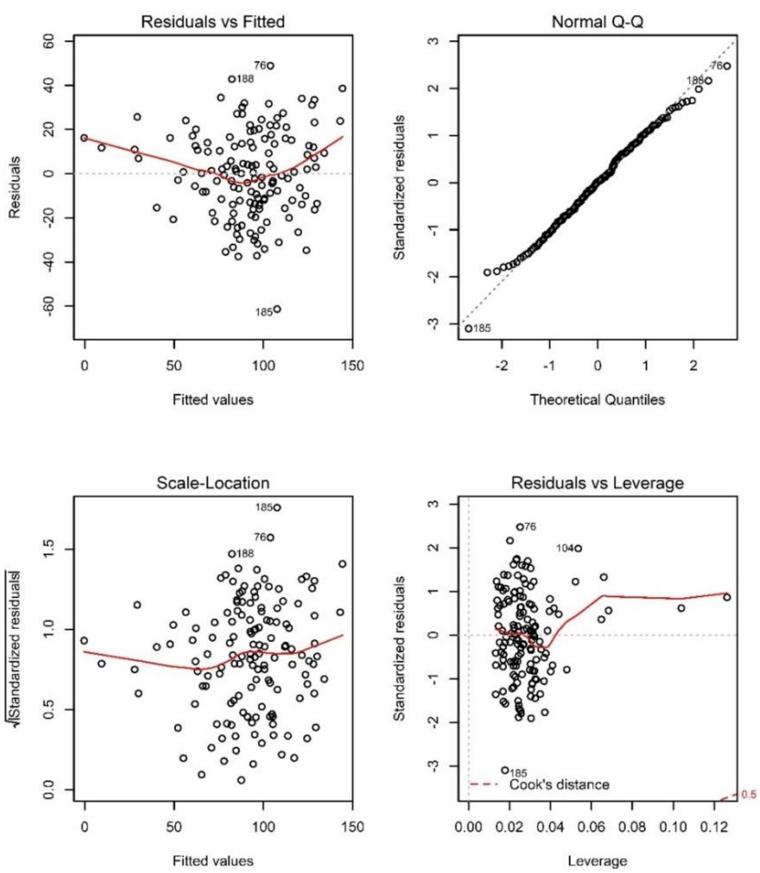

Figure A2.C-1: Residual graphical outputs for grain N and NDRE linear regression.

Table A2.C-1: Linear regression summary for N content in the total aboveground biomass and normalized difference red-edge index.

	Summary Outputs	RMSE [kg/ha]
Nt ~ NDRE	Residual standard error: 29.34 on 140 DF Multiple R-squared: 0.4473, Adjusted R-squared: 0.4433 F-statistic: 113.3 on 1 and 140 DF, p-value: < 2.2e-16	46.6
Nt ~ NDRE + Season + precip_in + Year + Season*NDRE	Residual standard error: 28.77 on 136 DF Multiple R-squared: 0.4835, Adjusted R-squared: 0.4646 F-statistic: 25.47 on 5 and 136 DF, p-value: < 2.2e-16	41.1
Nt ~ NDRE + Season	Residual standard error: 29.43 on 139 DF Multiple R-squared: 0.4479, Adjusted R-squared: 0.44 F-statistic: 56.39 on 2 and 139 DF, p-value: < 2.2e-16	46.4
Nt~ NDRE + Class + precip_in + Year	Residual standard error: 24.97 on 137 DF Multiple R-squared: 0.6082, Adjusted R-squared: 0.5968 F-statistic: 53.17 on 4 and 137 DF, p-value: < 2.2e-16	40.3
Nt ~ NDRE + Class + precip_in + Year + Class*NDRE	Residual standard error: 25.06 on 136 DF Multiple R-squared: 0.6084, Adjusted R-squared: 0.594 F-statistic: 42.25 on 5 and 136 DF, p-value: < 2.2e-16	40.4
Nt~ NDRE + Class	Residual standard error: 25.91 on 139 DF Multiple R-squared: 0.5721, Adjusted R-squared: 0.5659 F-statistic: 92.91 on 2 and 139 DF, p-value: < 2.2e-16	43.0

Table A2.C-2: Linear regression summary for N content in the grain and normalized difference red-edge index.

	Summary Outputs	RMSE[kg/ha]
Ng~ NDRE + Season + precip_in + Year	Residual standard error: 24.25 on 137 DF Multiple R-squared: 0.4255, Adjusted R-squared: 0.4087 F-statistic: 25.37 on 4 and 137 DF, p-value: 9.805e-16	26.7
Ng ~ NDRE + Season + precip_in + Year + Season*NDRE	Residual standard error: 24.29 on 136 DF Multiple R-squared: 0.428, Adjusted R-squared: 0.4069 F-statistic: 20.35 on 5 and 136 DF, p-value: 3.988e-15	26.3
Ng~ NDRE + Season	Residual standard error: 24.5 on 139 DF Multiple R-squared: 0.4051, Adjusted R-squared: 0.3965 F-statistic: 47.32 on 2 and 139 DF, p-value: < 2.2e-16	28.2
Ng~ NDRE + Class	Residual standard error: 20 on 137 DF Multiple R-squared: 0.5905, Adjusted R-squared: 0.5846 F-statistic: 100.2 on 2 and 139 DF, p-value: < 2.2e-16	28.1
Ng~ NDRE + Class + precip_in + Year	Residual standard error: 20 on 137 DF Multiple R-squared: 0.6092, Adjusted R-squared: 0.5978 F-statistic: 53.4 on 4 and 137 DF, p-value: < 2.2e-16	28.2
Ng ~ NDRE + Class + precip_in + Year + Class*NDRE	Residual standard error: 20.07 on 136 DF Multiple R-squared: 0.6093, Adjusted R-squared: 0.5949 F-statistic: 42.41 on 5 and 136 DF, p-value: < 2.2e-16	28.2

APPENDIX 2.D: LINEAR REGRESSION YIELD VS NDRE

lm(formula = Yield [kg/ha] ~ NDRE + Season, data = T2, na.action = na.exclude)

Coefficients:

	Estimate	Std.Error	t value	Pr(>|t|)
(Intercept)	-1594.6	588.8	-2.708	0.00761 **
NDRE	10145.4	1146.1	8.852	3.57e-15 ***
SeasonWinter	1873.4	216.2	8.667	1.02e-14 ***

Signif. codes: 0 ‘***’ 0.001 ‘**’ 0.01 ‘*’ 0.05 ‘.’ 0.1 ‘ ’ 1

Residual standard error: 1067 on 139 degrees of freedom

Multiple R-squared: 0.63, Adjusted R-squared: 0.62

F-statistic: 115.9 on 2 and 139 DF, p-value: < 2.2e-16

RMSE [Mg/ha]: 1.4

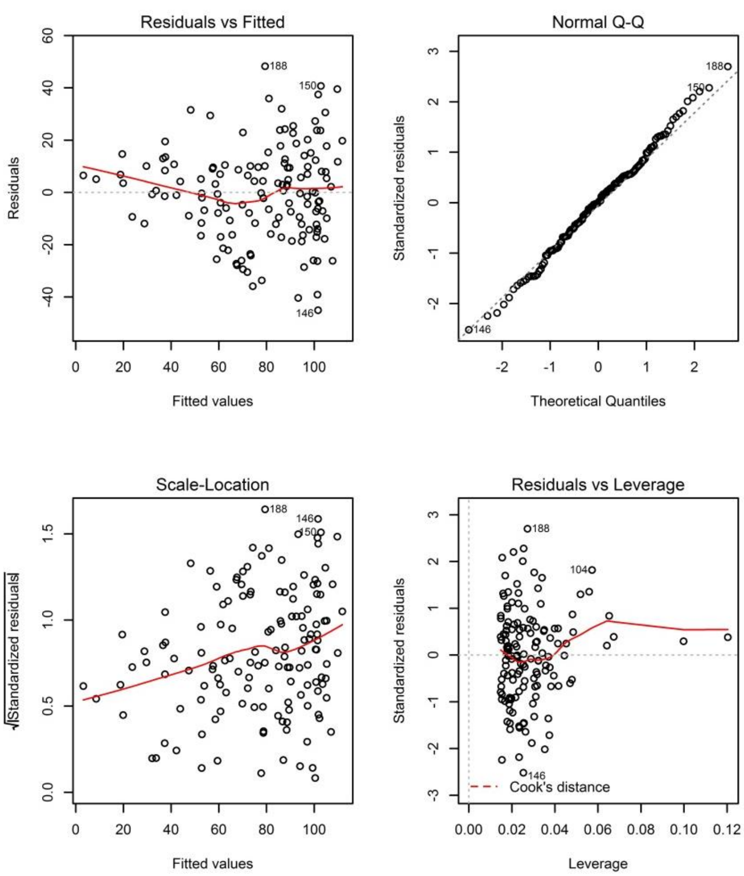

Figure A2.D-1: Residual graphical outputs for yield [kg/ha] and NDRE linear regression.

APPENDIX 2.E: LINEAR REGRESSION GPC VS NDRE

Two models were investigated in predicting grain protein concentration (GPC). The direct model investigated the direct relationship between NDRE and GPC and the indirect model used the NDRE based yield (G_w)and grain N concentration (N_g) models to predict GPC. GPC was not found to be significantly related in either case (Appendix E). The range of error for the linear models (direct model RMSE = 168 [g/kg], indirect model = 190 [g/kg]) was generally too large to detect the relatively small variability in GPC (farm and class population standard deviation GPC ranging 46.9 [g/kg] – 350 [g/kg]). Other factors such as crop season, class, year and location were more significant coefficients than NDRE in the model and therefore suggest NDRE not to be directly related to GPC. This is also supported by the lack of correlation seen between N_g and GPC in Chapter 2 and the strong linear relationship with minimal variability seen between N_g and G_w seen in Chapter 2.

lm(formula = GPC [g/kg] ~ NDRE + Variety + Season + Year, data = T2, na.action = na.exclude)

Coefficients:

	Estimate Std.	Error	t value	Pr(>|t|)
(Intercept)	53896.0	18013.3	2.992	0.003288 **
NDRE	-44.7	141.6	-0.316	0.752650
ClassSoft White	-101.4	27.7	-3.662	0.000356 ***
SeasonWinter	-502.9	25.2	-19.927	< 2e-16 ***
Year	-26.0	8.9	-2.901	0.004329 **

Signif. codes: 0 ‘***’ 0.001 ‘**’ 0.01 ‘*’ 0.05 ‘.’ 0.1 ‘ ’ 1

Residual standard error: 138.1 on 137 degrees of freedom

Multiple R-squared: 0.802,   Adjusted R-squared: 0.7962

F-statistic: 138.7 on 4 and 137 DF, p-value: < 2.2e-16

RMSE[g/kg] 168.1

APPENDIX 2.F: NDRE VARIABLE FARM CORRELATION MATRICES

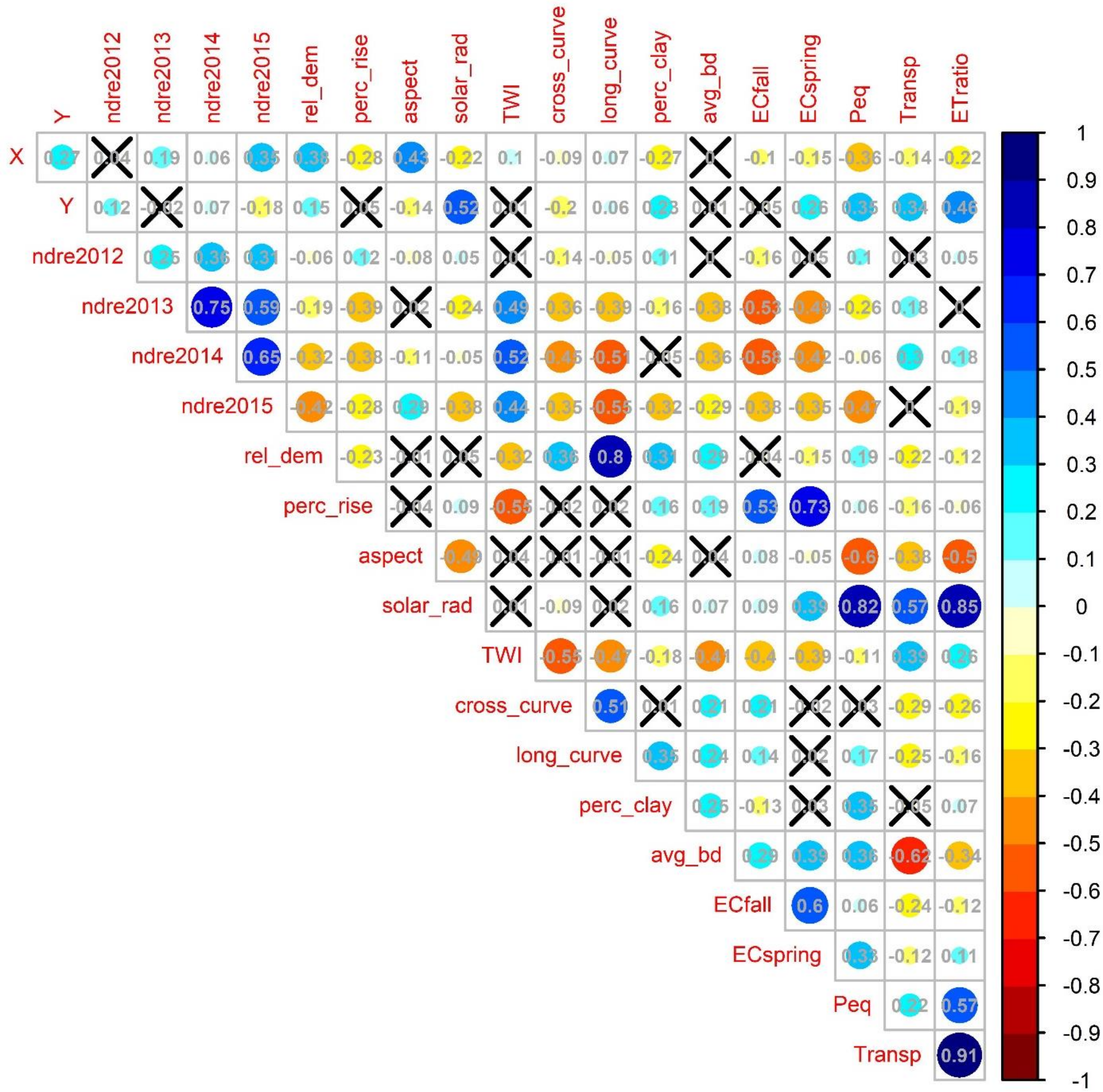

Figure A2.F-1: Colfax correlation matrix for spatial predictors of normalized difference red edge index variability.

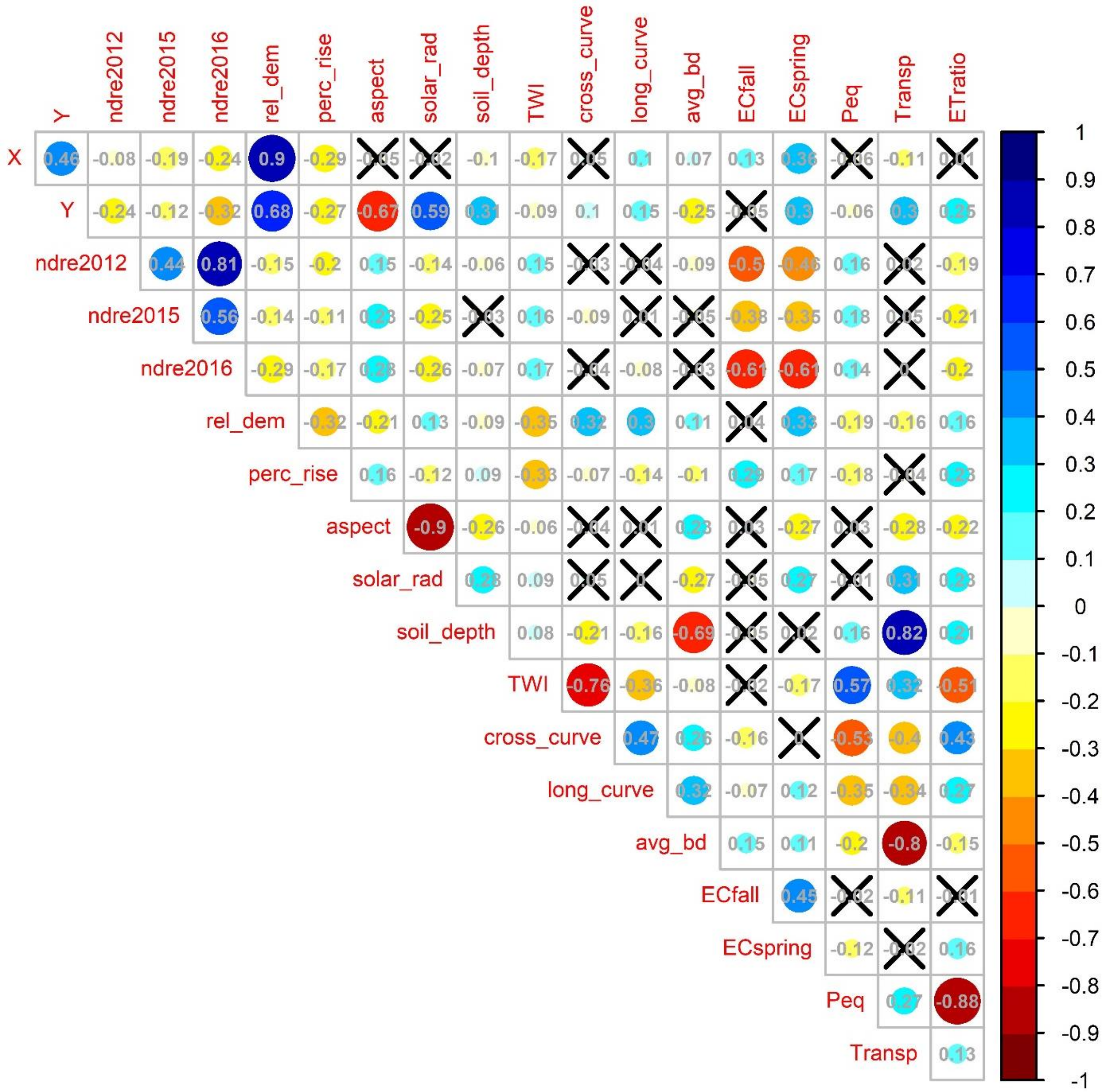

Figure A2.F-2: Genesee correlation matrix for spatial predictors of normalized difference red edge index variability.

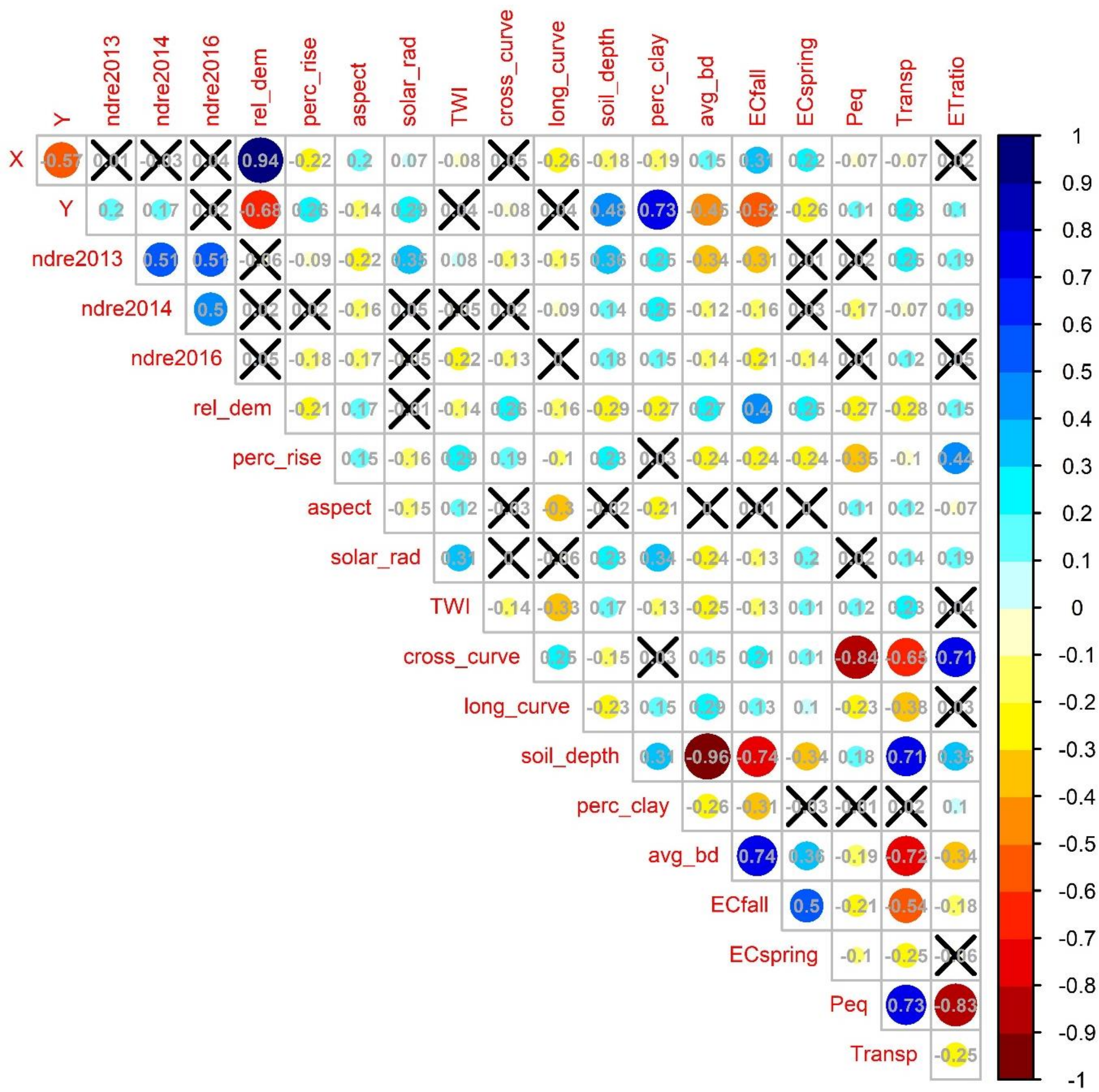

Figure A2.F-3: Leland correlation matrix for spatial predictors of normalized difference red edge index variability.

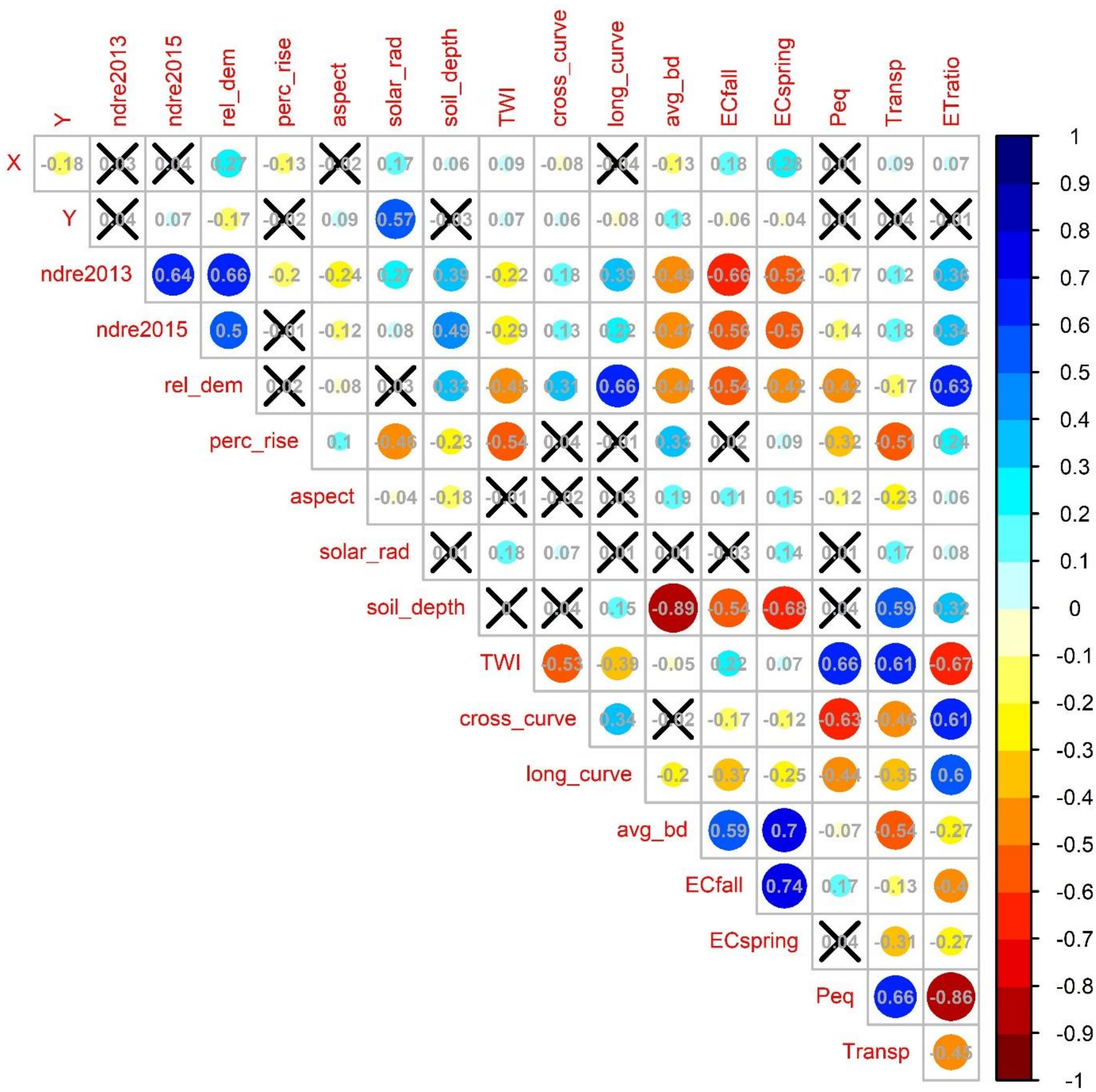

Figure A2.F-4: Troy correlation matrix for spatial predictors of normalized difference red edge index variability.

APPENDIX 2.G: NITROGEN BALANCE INDEX FARM YEARLY COMPARATIVE MAPS

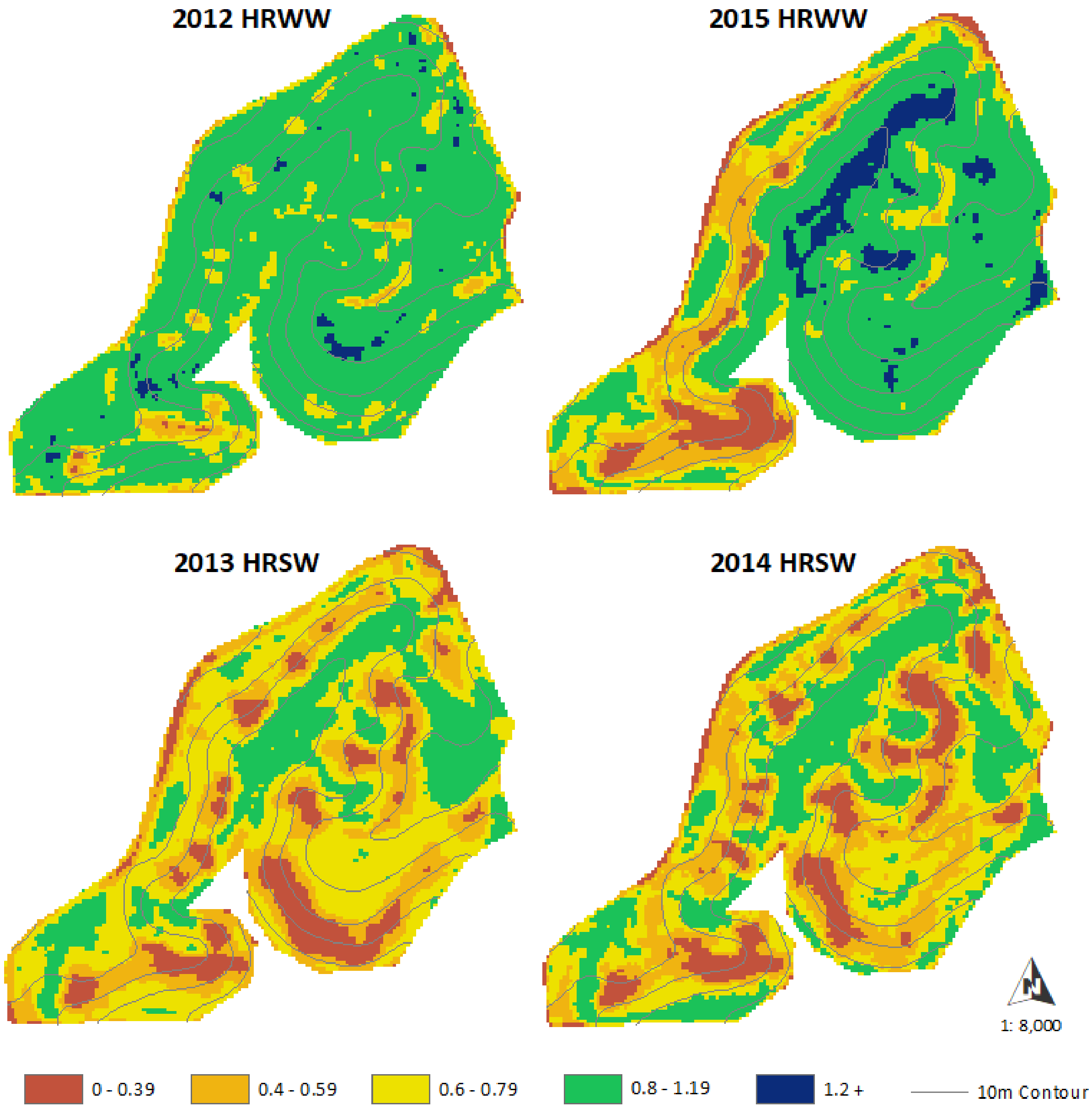

Figure A2.G -1: Nitrogen balance index temporal variability at Colfax.

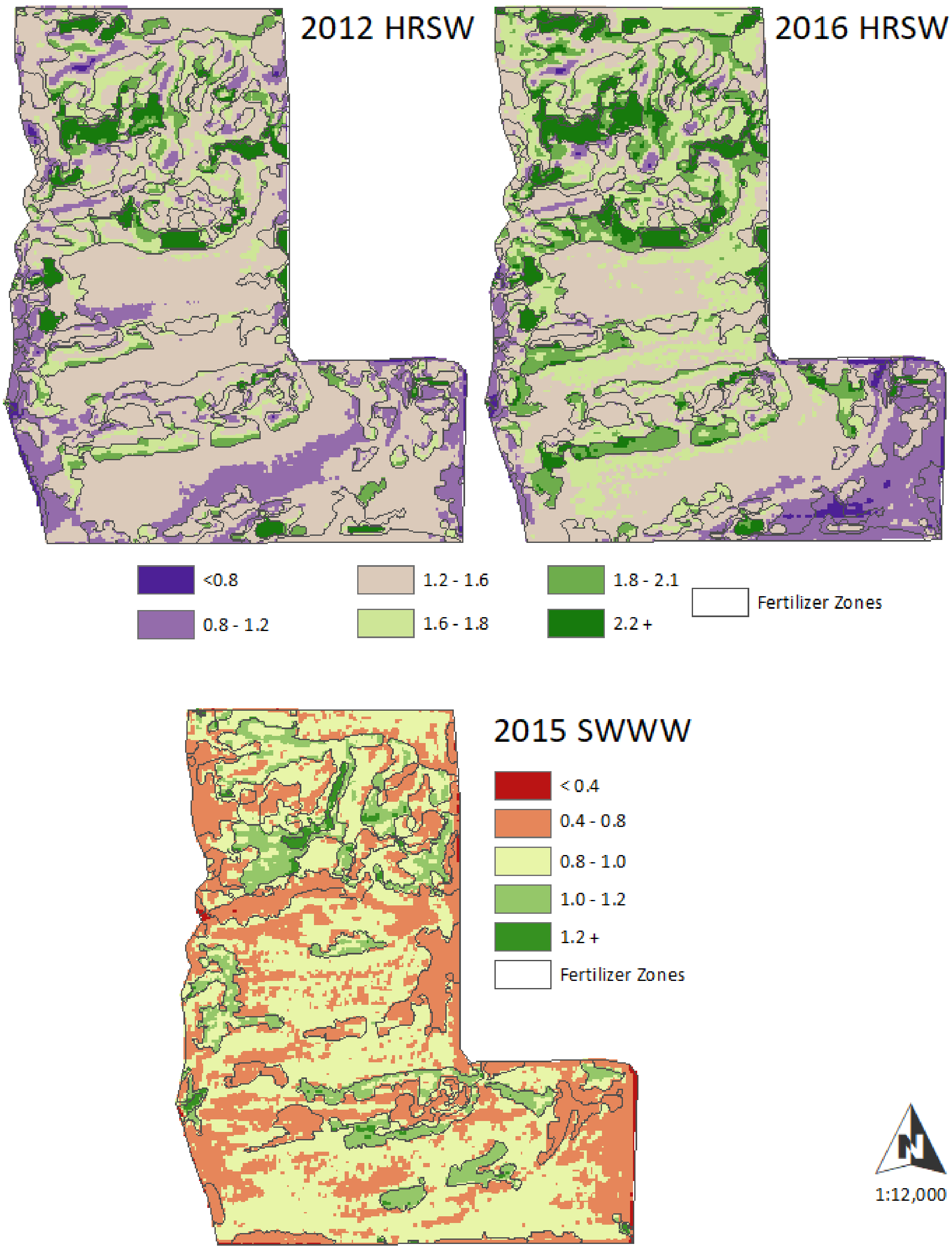

Figure A2.G -2: Nitrogen balance index temporal variability at Genesee.

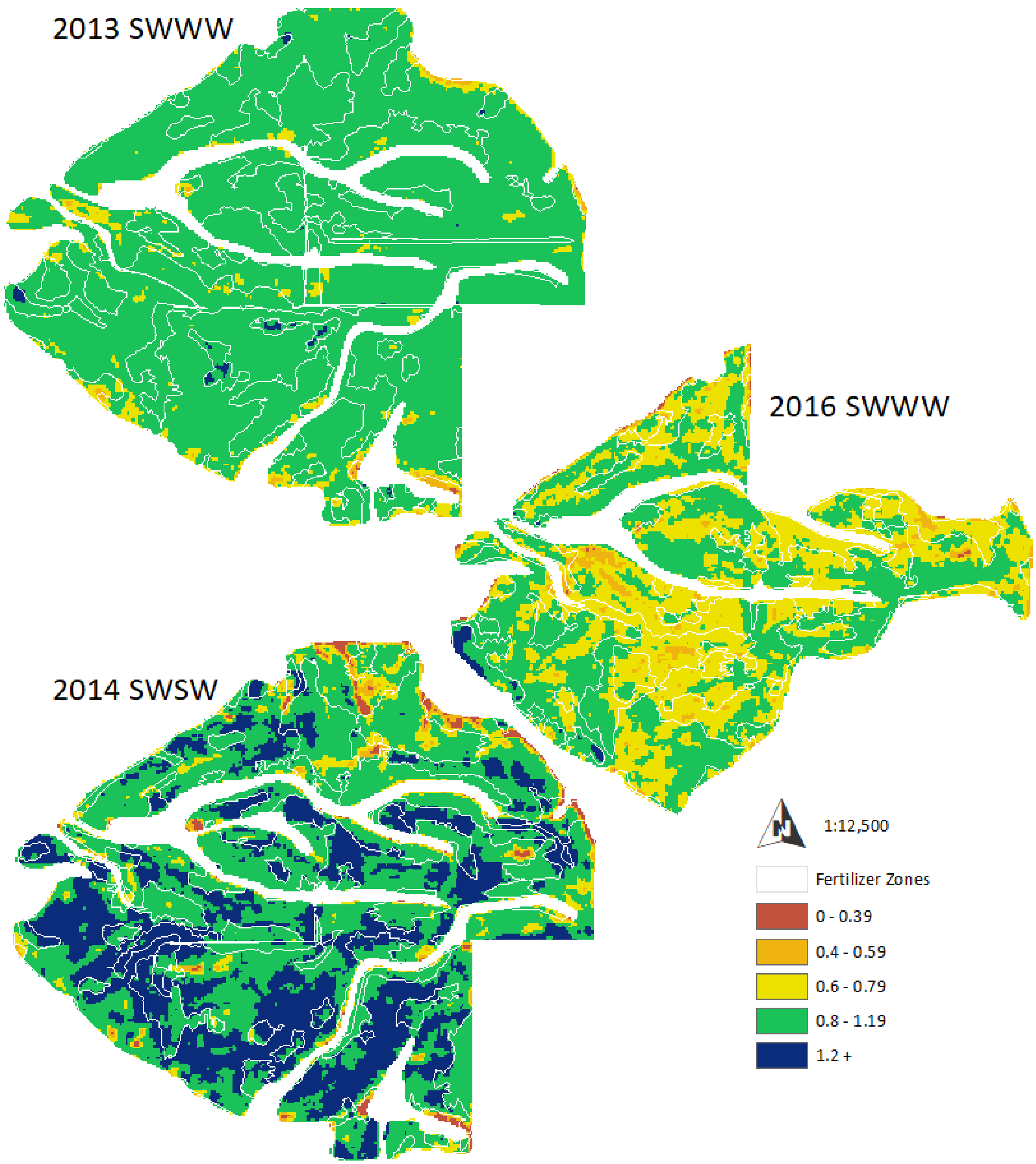

Figure A2.G -3: Nitrogen balance index temporal variability at Leland.

APPENDIX 2.H: N EFFICIENCY MAPPING APPLICATIONS

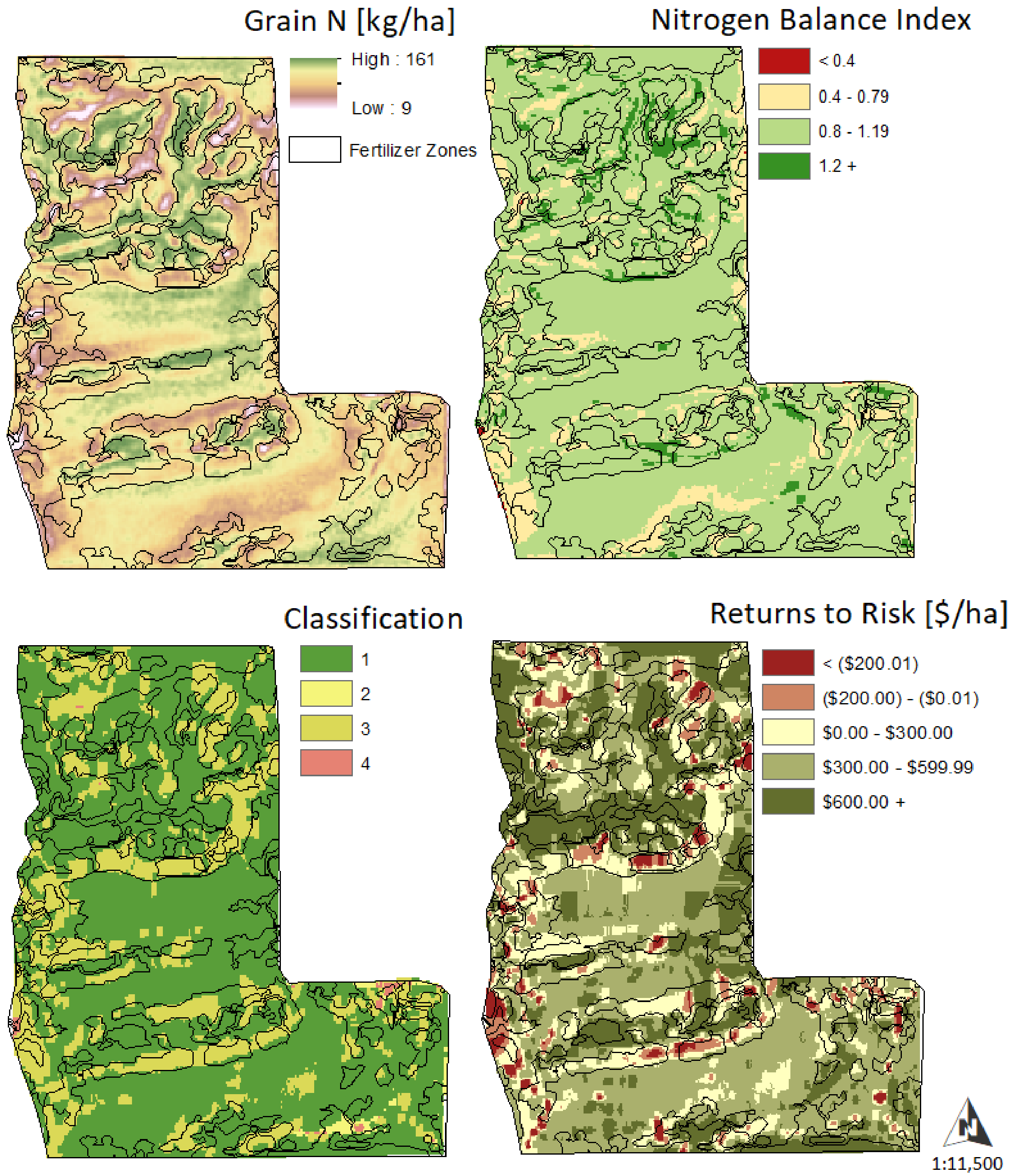

Figure A2.H-1: 2012 crop performance at Genesee.

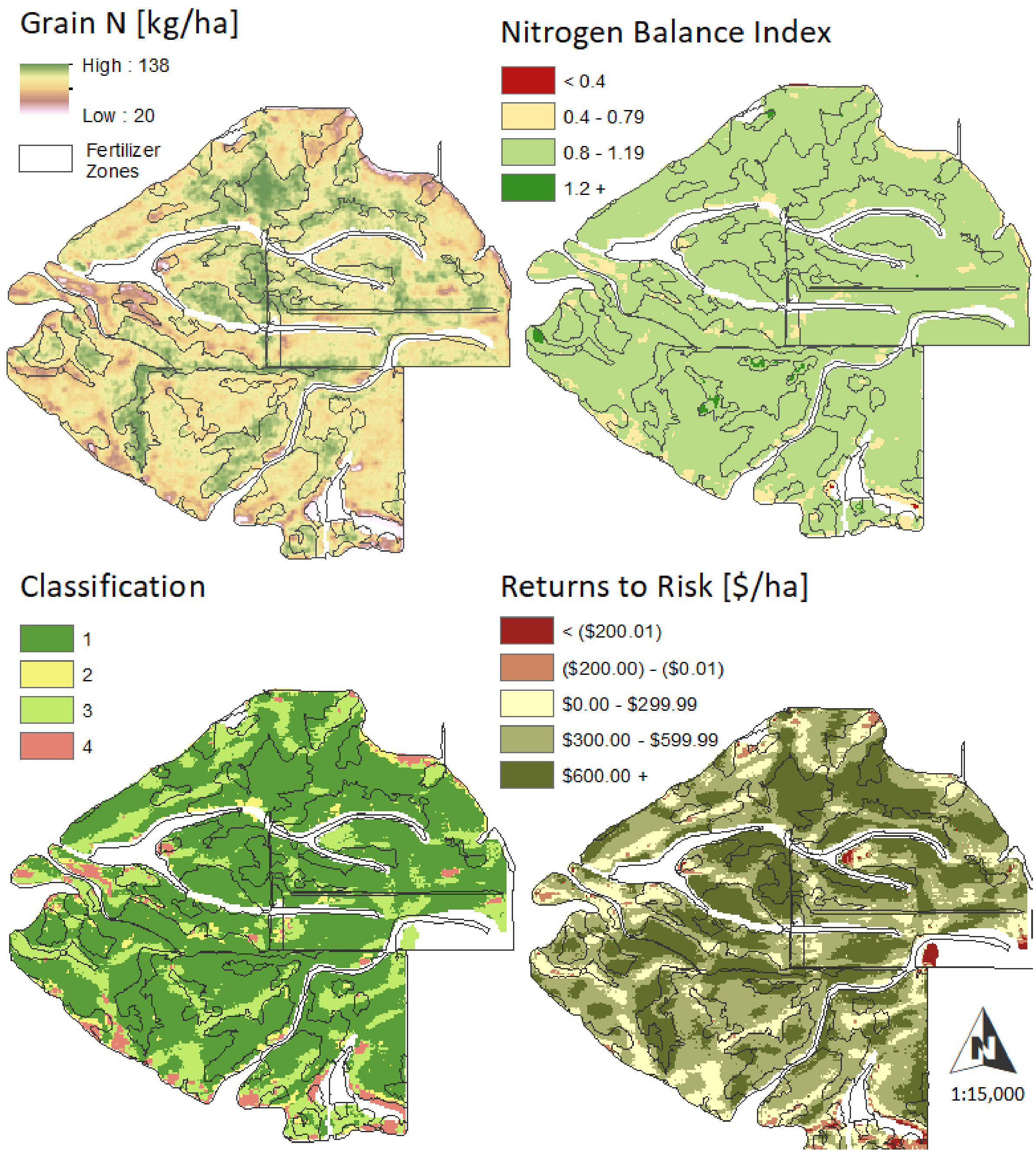

Figure A2.H-2: 2013 crop performance at Leland.

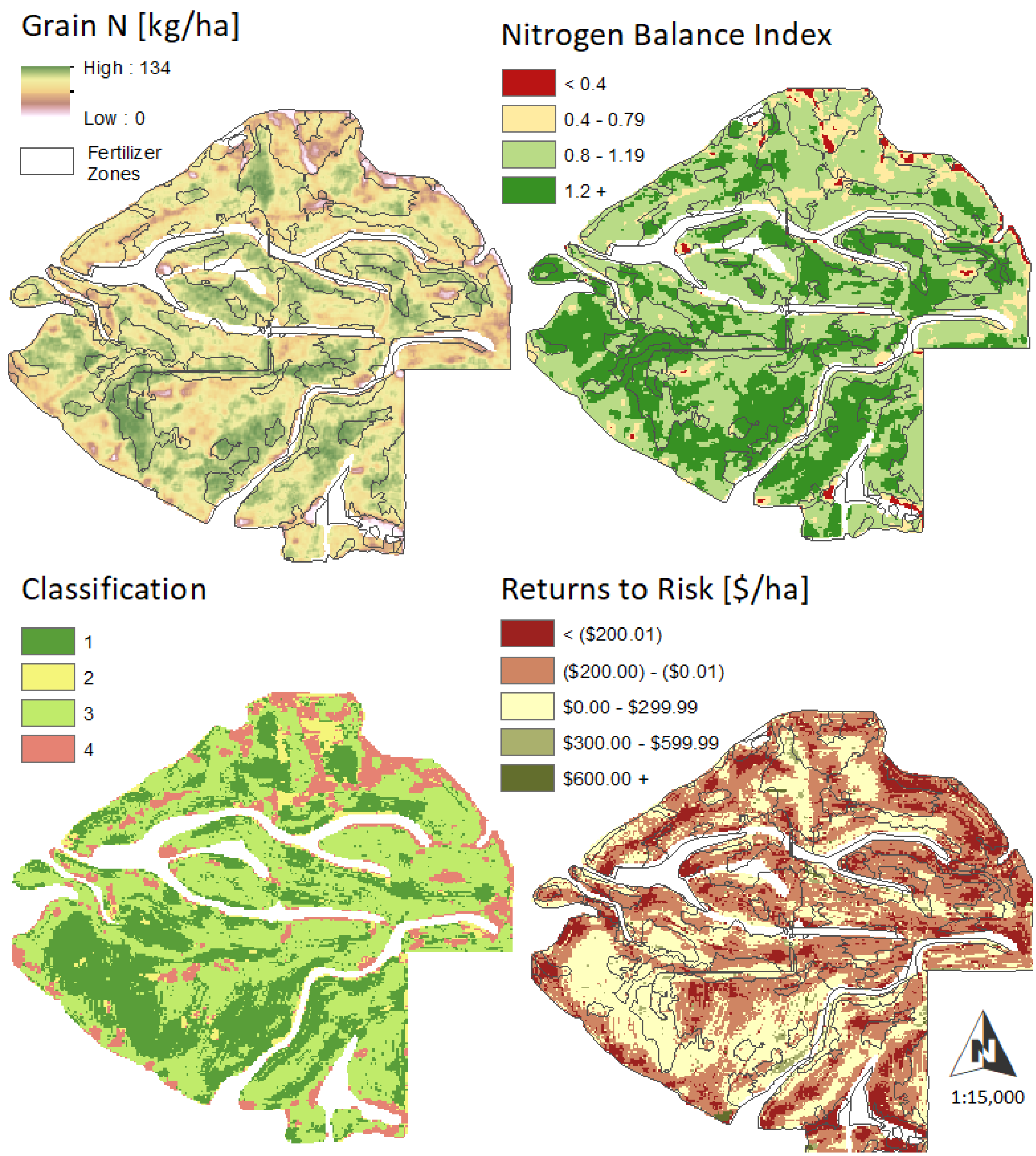

Figure A2.H-3: 2014 crop performance at Leland.

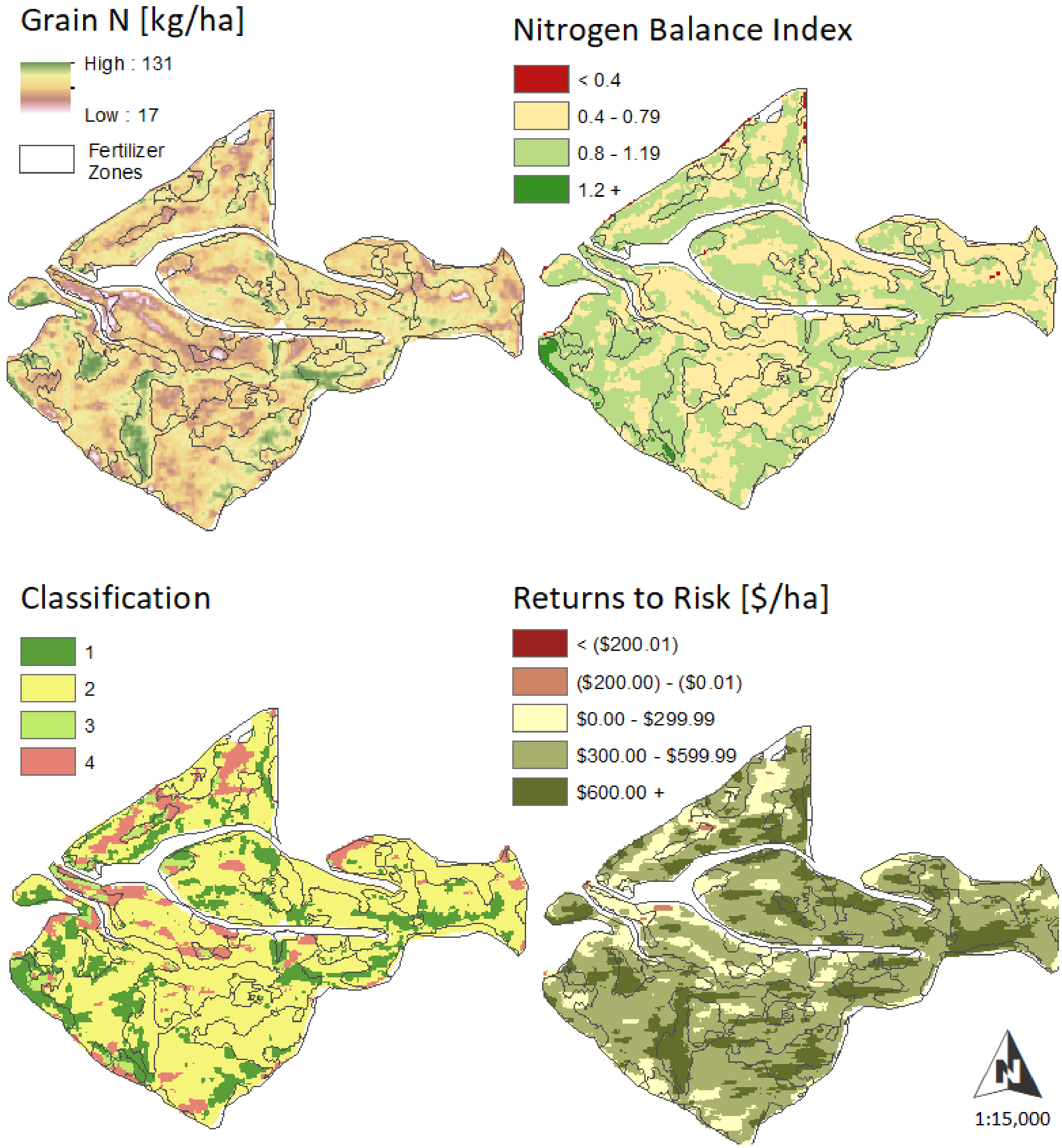

Figure A2.H-4: 2016 crop performance at Leland.

APPENDIX 3: SUPPLEMENTAL MATERIALS FOR CHAPTER 4

APPENDIX 3.A: POST-HARVEST NITROGEN MANAGEMENT EVALUATION POINT BASED WORKSHEET

FERTILIZER ZONE EVALUATION

Results from these methods are best evaluated and compared over several years and looking at general crop response patterns. This method can be completed at the farm or field scale depending on your available data.

NEEDED MATERIALS:

Best results come from samples being from various topographic positions and locations:

- Fertilizer guides for your different wheat class as a reference.
- Calculate the average yield for each fertilizer zone for the current year and the season before (including garbs and non-wheat crops)
- Precipitation amount for the growing season (Oct1 year before– Sept30 current year)
- Average organic matter samples for each fertilizer zone.
- Average total soil inorganic nitrogen samples for each fertilizer zone. Use fertilizer guides for conversion tables for ppm to lb/ac.
- Verify the following charts are representative of farm costs. Use farm specific values where possible.
- 5-year averages (2011-2015) of crop prices can be found in Table 5.

METHOD:

1. Organize and average your results first by class and then by fertilizer zone. Use table in Appendix 4A as a guide as needed.
2. Use fertilizer guides to determine look-up values for each variable for each fertilizer zone, using the tables found in your class specific fertilizer guides.
3. Complete all non-colored cells on page 1 of the calculations table with information from “Needed Materials” section
4. Using values from step 3, look up all green cells from attached tables.

5. Calculate the values in the gray cells using the line values in the equation.

INTERPRETATION

Any negative values in lines 12, 13, 15, 17 should be seen as losses. These are estimates of losses. The more representative the samples are from these zones, the more representative these numbers are for the field. These values are estimates and should be compared to other years to determine general patterns. For example, does Zone 1 always lose money? How much? Does Zone 3 always make money? Should fertilizer amounts be adjusted? These data can provide some insight into how each zone is doing and can compare crops

		Wheat Class 1		Wheat Class 2	
		Zone 1	Zone 2	Zone 1	Zone 2
1	Nitrogen Fertilizer [lb/ac] (**Nitrogen ONLY** not composite #)				
	Average Precipitation [in/yr]				
2	**Unit Nitrogen Requirement** (Table 1)				
3	G_w goal or potential G_w [bu/ac]				
4	Average G_w [bu/ac]				
	Prior Year G_w[bu/ac] or [lb/ac]				
5	**Straw Breakdown N Requirement** (Table 2 if prior crop was pulse)				
6	**Legume Credit** (Table 3 if prior crop was legume)				
	Average OM [%]				
7	**Nitrogen Mineralization [lb/ac]** (Table 4)				
8	Average total Inorganic Nitrogen [lb/ac]				
9	Crop Price [$/bu] (5 year averages Table 5)				
10	Fertilizer Price [$/lb]				
11	G_w based on fertilizer [bu/ac] Calculate: (1-5+6+7+8)/2				
12	Average G_w difference [bu/ac] Calculate: 11-4				
	Cost: 12*9				
13	G_w goal difference [bu/ac] Calculate: 11-3				
	Cost: 13*9				
14	N_f needed for G_w average [lb/ac] Calculate: (2*4)+5-8-6-7				
15	N_f difference (needed -applied) [lb/ac] Calculate: 14-1				
	Cost:15*10				
16	N_f needed for G_w goal [lb/ac] Calculate: (2*3)+5-8-6-7				
17	N_f difference (goal – applied) [lb/ac] Calculate: 16-1				
	Cost: 17*10				

		Wheat Class 1		Wheat Class 2	
		Zone 1	Zone 2	Zone 1	Zone 2
18	Returns to Risk Step 1 Calculate: 4*9				
19	Cost of Production [$/ac] (Estimates Table 6)				
20	Returns to Risk Step 2 Calculate:1*10				
	Returns to Risk [$/ac] Calculate: (18-(19+20))				

Table 1: Unit N Requirement by Precipitation Zone

Precipitation [in]	WW	SWSW	HRSW
20	2.5	2.3	3.7
21	2.5	2.3	3.7
22	2.7	2.4	3.7
23	2.7	2.4	3.7
24	2.7	2.4	3.7
25	2.8	2.5	3.7

Table 2: Straw Breakdown

Previous Season Yield [bu/ac]	Residue tons/ac	N Needed lb/ac
10-19	0.5	7.5
20-39	1	15
40-49	2	30
50-59	2.5	37.5
60-69	3	45
70+	3.5	50

Table 3: Legume Credit

Yield [lb/ac]	Residue [tons]	N credit [lb/ac]
0	0	0
500	0.5	3
1000	1	6
1500	1.5	9
2000	2	12
3000	3	18
4000	4	24

*One ton of legume residue is produced from 1,000 pounds of lentil or pea grain produce

Table 4: Organic Matter

OM%	lb N/ac/year	
	Conventional	Reduced
0.9	20	17
1	20	17
1.1	22	19
1.2	24	20
1.3	26	22
1.4	28	24
1.5	30	26
1.6	32	27
1.7	34	29
1.8	36	31
1.9	38	32
2	40	34
2.1	42	36
2.2	44	37
2.3	46	39
2.4	48	41
2.5	50	43
2.6	52	44
2.7	54	46
2.8	56	48
2.9	58	49
3	60	51

Table 5: Crop Price

	Crop Price [$/bu]
HRWW	$ 8.41
HRSW	$ 8.41
SWWW	$ 6.44
SWSW	$ 6.44

Table 6: Estimated Production Costs

	Cost of Production w/o fertilizer [$/ac]
HRWW	$ 394.92
HRSW	$ 345.80
SWWW	$ 294.01
SWSW	$ 296.40

APPENDIX 3.B: POST-HARVEST NITROGEN MANAGEMENT EVALUATION SATELLITE IMAGERY WORKSHEET

SATELLITE IMAGE FERTILIZER ZONE EVALUATION

Results from these methods are best evaluated and compared over several years and looking at general crop response patterns.

NEEDED MATERIALS:

Best results come from farm specific values if possible

- Fertilizer maps [lb/ac] for nitrogen only
- Yield maps
- Satellite image
- Spatial Software program

METHOD:

This methodology can be completed at the farm or field scale depending on your available data.

1. Ensure current fertilizer maps are accurate
2. Make sure yield monitors are working and measuring fields during harvest
3. Obtain atmospherically corrected, satellite images for fields, use table below for estimating best date for image
    a. If possible running a growing season analysis of growing degree day (GDD) vs. normalized difference red edge index (NDRE) would provide best approximate dates for different crops. Table values represent regional averages. Drier regions may find optimum GDD values to be later than regional averages.

	GDD
Spring Wheat	800-1000
Winter Wheat	1000-1200

4. Load yield, fertilizer and satellite images into spatial software.
5. Verify satellite image and farm data are in the same projection. Convert if necessary.

6. Convert fertilizer maps to raster files (if necessary) and add foliar application totals for a total nitrogen fertilizer amount for the growing season. Ensure fertilizer maps are for *nitrogen values ONLY* in lb/ac not for the whole fertilizer applied.
7. Verify yield maps have correctly calculated for moisture content (verify dry yield and wet yield are different). If not, use the following equation to correct for moisture and calculate accurate bu/ac measurement.

$$Gw\ \left[\frac{bu}{ac}\right] = \frac{\left(\frac{Crop_{flow\left[\frac{lb}{s}\right]}}{Prod\ \left[\frac{ac}{hr}\right]} * 3600\ \left[\frac{s}{hr}\right]\right)\left(\frac{\frac{1 - \%\ Moisture}{100}}{\frac{1 - 13.5\%}{100}}\right)}{60\ \left[\frac{lb}{bu}\right]}$$

8. Interpolate yield map using kriging with max distance of 30m.
9. Using the following equations, separately calculate grain N [lb/ac] for spring wheat and winter wheat fields.

   Hard Red: $N_{g_{lb/ac}} = 279.4 * NDRE - 45.9$

   Soft White $N_{g_{lb/ac}} = 279.4 * NDRE - 77.2$
10. Calculate the nitrogen balance index (grain N/fertilizer N applied)
11. Using the following logic statement, calculate classification if desired.

    =IF(Yield >= **Yield goal**, IF(NBI >= 0.8,1,2),IF(NBI >=0.8,3,4))

12. Using the following equation and Tables 5& 6 (if necessary), calculate returns to risk (RR) values. Values in the tables are *generalized* estimates for management types and fertilizer choices. Farm specific values are best if possible.

$$RR = (P_c * G_w) - (P_p + (P_n * N_f))$$

P_c is the price of the crop [$/bu], G_w is the yield [bu/ac], P_p is the Price of production [$/ac], P_n is the price of N [$/lb] and N_f is the fertilizer application [lb/ac].

INTERPRETATION

Values in the NBI map that are less than 0.88 should be considered areas of low efficiency (n uptake < 50%).Classes 1 or 2 achieve yield goals, class 3 and 4 do not. Classes 1 and 3 achieve nitrogen efficiency goals. RR maps negative values are areas of monetary losses from yield and positive values are where yield is sufficient to cover N fertilizer and generalized production costs. These maps are estimates and should be compared to other years to determine general patterns. For example, does Zone 1 always lose money? How much? Does Zone 3 always make money? Should fertilizer amounts be adjusted? These data can provide some insight into how each zone is doing and can compare crops.